Spring 1-1-2011

Design and Experimental Evaluation of a Single Incision Laparoscopic Surgery Camera System for Minimally Invasive Surgery

Zachary Mills
University of Colorado at Boulder, zachary.mills@colorado.edu

DESIGN AND EXPERIMENTAL EVALUATION OF A SINGLE INCISION LAPAROSCOPIC SPECIFIC CAMERA SYTEM FOR MINIMALLY INVASIVE SURGERY

by

ZACHARY MILLS

B.S., New Mexico State University, 2009

A thesis submitted to the
Faculty of the Graduate School of the
University of Colorado in partial fulfillment
of the requirement for the degree of
Master of Science
Department of Mechanical Engineering 2011

This thesis entitled:

Design and Experimental Evaluation of a Single Incision Laparoscopic Surgery Camera System for Minimally Invasive Surgery

Written by Zachary Mills

has been approved for the Department of Mechanical Engineering

_____

Mark Rentschler, Ph.D.

_____

Derek Reamon, Ph.D.

Date April 19, 2011

The final copy of this thesis has been examined by the signatories, and we find that both the content and the form meet acceptable presentation standards of scholarly work in the above mentioned discipline

Zachary Mills (M.S., Mechanical Engineering)

Design and Experimental Evaluation of a Single Incision Laparoscopic Surgery Camera System for Minimally Invasive Surgery

Thesis Directed by Professor Mark Rentschler, Ph.D.
Surgical Collaborator Professor Jonathan Schoen, M.D.

Single incision laparoscopic surgery (SILS) offers many benefits over traditional open surgery. SILS is a type of minimally invasive surgery (MIS) which aims to reduce patient trauma by decreasing the number of incisions required for a surgical operation down to one located at the belly button (umbilicus). This offers patient benefits including reduced trauma, risk of infection, post-operative pain, scaring, and a shorter recovery time. SILS remains surgically challenging due to limited surgical tool motion and positioning of the traditional laparoscope through the SILS entry incision.

The SILS-specific camera systems presented here integrates all the features of a laparoscopic vision system into a small, inexpensive, portable package that enables point-of-care applications, does not compete for space with the surgical tools, and removes the need for a dedicated laparoscope port. Two different design approaches were taken by initially incorporating a camera and viewing system directly into the SILS port (SILS Port Camera) and then by completely decoupling the camera and viewing system from the SILS port (SILS Magnet Camera).

Each approach was developed into a prototype and experimentally tested in order to prove initial feasibility and functionality of the device as compared to the traditional industry SILS laparoscopic setup. The first functionality test was performed using an *ex vivo* participant study pitting the SILS camera against a traditional laparoscopic set up over two different surgical tasks, ball drop and cutting tasks. The participant study indicated the SILS Port Camera performs similarly to a typical

SILS setup. However the SILS Magnet Camera approach showed a significant improvement in functionality when compared with the traditional SILS setup.

Both devices were tested in an *in vivo* porcine model by a practicing surgeon. The SILS Port Camera resulted in a premature termination of a cholecystectomy due to tool interference and poor view of the surgical site. The SILS Magnet Camera allowed for successful cystic duct resection and liver biopsy. The surgeon noted increased viewing capacity from the cameras pan/tilt system, enhanced camera system mobility offered by the magnets, the increased range and movement for his hands, and the ability to use the extra port for a third tool for liver retraction.

Acknowledgments

I would like to give a special thanks to Professor Mark Rentschler for his incredible direction and guidance, Dr. Derek Reamon for serving on my committee, Ben Terry for his collaboration and insight, Austin Ruppert for his initial Port Camera design and work, Dr Jonathan Schoen for his extremely generous time and effort commitments and serving on my committee, and the entire Advanced Medical Technologies Laboratory group for providing resources and advice.

Table of Contents

Acknowledgments v

Glossary xiv

Chapter 1 - Introduction 1

1.1 Minimally Invasive Surgery (MIS) 1

1.2 MIS Drawbacks 3

1.3 Related Work 4

1.3.1 Incision Types 4

1.3.2 Entry Techniques 4

1.3.3 Trocars 5

1.3.4 Single Incision Platforms: SILS Ports 6

1.3.4 Flexible Surgical Instruments 9

1.3.5 Laparoscopes 10

1.3.6 Future Technologies 11

Chapter 2 - SILS Camera Concept and Design 16

2.1 Port Camera Introduction 16

2.2 Magnet Camera Introduction 17

2.3 Device Design: SILS Port Camera 19

2.3.1 Device Design: Port Camera 19

2.3.2 Port Camera: Prototype 1 19

2.3.3 Port Camera: Prototype 2 23

2.3.4 Prototype 2: Deployment Procedure 25
2.4 Device Design: SILS Magnet Camera 25
2.4.1 Device Design: SILS Magnet Camera 26
2.4.2 SILS Magnet Camera: Prototype 3 26
2.5 Video System Evaluation 49
Chapter 3 - Participant Study 51
3.1 IRB Test Protocol 51
3.2 Participant Criteria 51
3.3 Surgical Simulation Cavity: MIS Environment 51
3.4 Configurations 52
3.5 Trainer and LCD Placement 54
3.6 Task and Configuration Order 55
3.7 Participant Time Allocation 56
3.8 Ball Drop Task: Tissue Identification 57
3.9 Ball Drop Task: Evaluation and Scoring 58
3.10 Participant Instructions 58
3.10.1 Background Info 58
3.10.2 Ball Drop Task: Participant Instructions 59
3.10.3 Cut Task 61
3.11 Cut Task: Evaluation and Scoring 62
3.11.1 Cut Task: Participant Instructions 62

3.12 Task Set Up: Test Dimensions 64
3.13 Penalty and Task Difficulty Reasoning 65
3.14 Questionnaire 66
3.15 Participant Results 69
3.15.1 Port Camera 70
3.15.2 SILS Magnet Camera 72
3.16 Questionnaire Results 74
3.16.1 Port Camera 74
3.16.2 SILS Magnet Camera 76
Chapter 4 - Porcine Study 78
4.1 Port Camera 78
4.1.1 Discussion 82
4.2 SILS Magnet Camera 82
4.2.1 Discussion 89
Chapter 5 - Conclusion 91
Chapter 6 – Future Work 94
Chapter 7 - Bibliography 96

Tables

Table 1: P-values indicating significant interactions between test parameters and configurations. ……71

Table 2 Power and sample size interactions between test parameters and configurations. 72

Table 3: P-values indicating significant interactions between test parameters and configurations. ……73

Table 4: Power and sample size interactions between test parameters and configurations......74

Figures

Figure 1: Minimally Invasive Surgery (MIS) setup (left). 1

Figure 2: SILS Setup with the Tri Port (left) and GelPOINT (right) [9, 10]. 2

Figure 3: Veress Needle [18]. 5

Figure 4: Bladed Trocar[21]. 5

Figure 5: Bladeless Trocar [23]. 6

Figure 6: Blunt Trocar [26]. 6

Figure 7: Tri-Port (Advanced Surgical) [29]. 7

Figure 8: SILS Port (Covidien)[31]. 8

Figure 9: GelPort (Applied Medical)[33]. 8

Figure 10: The Tri-Port in case A-B uses straight tools and case C uses articulated tools [34]. ..9

Figure 11: RealHand Articulating Laparoscopic Tool [37]. 10

Figure 12: Roticulator Articulating Laparoscopic Tool [39]. 10

Figure 13: EndoEye Laparoscope [42]. 11

Figure 14: Version 1.5 of the PortCamera [44]. 12

Figure 15: MAGS System [45]. 13

Figure 16: Novel MAGS Camera System [46]. 13

Figure 17: Novel MAGS Camera System [47]. 14

Figure 18: da Vinci Surgical System [49]. 15

Figure 19: SILS Port Camera Deployed in SILS Port left and in vivo right (all units are in mm)...

…..16

Figure 20: SILS Magnet Camera deployed in vivo. 18

Figure 21:Cross-section of the SILS Port Camera CAD model (left) and Prototype 1 (right). 20

Figure 22: Cross-section of the SILS Port Camera camera module, seals, and mount. 20

Figure 23: SILS Port Camera camera module. 21

Figure 24: SILS Port Camera deployed (top-left), un-deployed (bottom-left), and activation mechanism (right). 21

Figure 25: RS4018-55 Analog Video Camera [51] 22

Figure 26: SILS Port Camera tilt activation. 23

Figure 27: SILS Port Camera with 7" (17.8 cm) LCD screen. 23

Figure 28: SILS Port Camera Prototype 2. 24

Figure 29: SILS Port Camera activation knob. 25

Figure 30: Typical SILS surgical tool and laparoscope operation [52]. 27

Figure 31: Coviden SILS Port. Vertical tool operation (left). Horizontal tool operation (right) [53]. 27

Figure 32: SILS Magnet Camera deployed in vivo. 28

Figure 33: 6 Volt DC Micro-Mo 6 mm motor[54]. 29

Figure 34: Gimbal degrees of freedom [55]. 29

Figure 35: SILS Magnet Camera motor mounting and operation. 30

Figure 36: SILS Magnet Camera camera module mounting mechanism. 30

Figure 37: SILS Magnet Camera pan mechanism. 31

Figure 38: SILS Magnet Camera tilt mechanism 32

Figure 39: SILS Magnet Camera un-translated state (top) and Translated state (bottom). 33

Figure 40 36

Figure 41: SILS Magnet Camera housing layout. 37

Figure 42: SILS Magnet Camera camera mount assembly. 38

Figure 43: SILS Magnet Camera camera module assembly. 39

Figure 44: SILS Magnet Camera gimbal motor locations. 40

Figure 45: SILS Magnet Camera linear actuator mounting bracket. 40

Figure 46: SILS Magnet Camera inner motor housing assembly. 41

Figure 47: SILS Magnet Camera outer motor housing. 42

Figure 48: SILS Magnet Camera hook & ring mounting system. 42

Figure 49: SILS Magnet Camera magnet mounting system. 43

Figure 50: One inch N52 cylindrical magnet pull force [57]. 44

Figure 51: Size 8 Linear actuator force vs. speed curves [61]. 47

Figure 52: SILS Magnet Camera control box (left) and linear actuator circuit (right). 47

Figure 53: SILS Magnet Camera power supply hook up. 48

Figure 54: Contrast vs. feature size comparison of the Stryker 1188HD, Analog RS-5018, and Digital OV7690 video systems [50] 49

Figure 55: Color quality comparison of the Stryker 1188HD, Analog RS-5018, and Digital OV7690 video systems [50]. 50

Figure 56: 3-Dmed's minimally invasive training system [62]. 52

Figure 57: SILS Port Camera ball drop and cut task test configurations. 53

Figure 58: SILS Magnet Camera ball drop and cut task test configurations. 54

Figure 59: Monitor and LCD locations SILS Port Camera (left) and SILS Magnet Camera (right). 55

Figure 60: Ball drop task (left) and cut task (right). 55

Figure 61: Ball drop task setup. 57

Figure 62: Cut task setup. 61

Figure 63: Test setup inner dimensions. 65

Figure 64: SILS Port Camera participant questionnaire. 67

Figure 65: SILS Magnet Camera participant questionnaire. 68

Figure 66: Mean normalized ball and cut task times (left) and errors (right). 70

Figure 67: Mean normalized ball and cut task times (left) and errors (right). 73

Figure 68: SILS Port Camera participant questionnaire average answer. 75

Figure 69: SILS Port Camera participant questionnaire average answer. 77

Figure 70: SILS Port insertion (left) and SILS Port Camera insertion (right). 78

Figure 71: SILS Port Camera undeployed (left) and deployed (right)......79

Figure 72: Tool triangulation of a straight and articulated grasping tool. 79

Figure 73: Clipping the cystic duct of the gallbladder......80

Figure 74: SILS Port Camera Operation. 81

Figure 75: SILS Magnet Camera insertion. 83

Figure 76: SILS Port and laparoscope port insertion......83

Figure 77: SILS Port Camera surgical setup. 84

Figure 78: SILS Port Camera underneath the liver (left.) Blood being cleaned off the camera lens (right)......85

Figure 79: Magnet handle suspending SILS Magnet Camera (left). Initial suspension of the gallbladder (right). 85

Figure 80: SILS Magnet Camera magnet system (left). Deployed SILS Magnet Camera (right). 86

Figure 81: Grasper tool triangulation used to dissect tissue surronding the cystic duct......87

Figure 82: *Clipping the cystic duct of the gallbladder (left).Cutting the cystic duct (right).* 87

Figure 83: Liver biopsy (left) and small bowel biopsy (right). 88

Figure 84: SILS Magnet Camera surgical tool positioning during cholecystectomy. 89

Glossary

Ball Drop Task

The Ball Drop Task simulates tissue identification, and requires the participants to use a grasper tool to move four different colored balls to their corresponding bin.

Cut Task

The Cut Task simulates a tissue biopsy procedure, and requires the participants to simultaneously use a cutter and grasper tool to grab, stretch, and cut along marked lines on three clipped rubber bands.

Laparoscope

A laparoscope is a type of endoscope used to provide visual information on the abdominal and pelvic organs in order to perform minimally invasive surgery.

MIS

Refers to “minimally invasive surgery”.

Participant Study

A study was performed in which volunteers with no surgical experience were to complete the ball drop and cut tasks with the SILS Port Camera, SILS Magnet Camera, and a traditional laparoscopic setup. The goal of the study is to determine if the SILS devices perform similarly or better than the traditional laparoscopic setup.

Pneumoperitoneum

Pneumoperitoneum is air or gas in the peritoneal cavity. In the case of MIS gas is injected into the abdominal cavity to insufflate it, providing working room for the surgery.

Porcine Study

The SILS devices were tested in a live porcine model at the University of Colorado Anschutz Medical Campus by an experienced MIS surgeon. The surgeon performed exploratory surgery of the peritoneal cavity, a cystic duct dissection and division, and a liver biopsy.

Prototype 1-2

SILS Port Camera, which integrates the camera and display systems onto a cannula.

Prototype 3

SILS Magnet Camera System, which decouples the camera system away from the SILS port.

SILS

Refers to “single incision laparoscopic surgery”.

SILS Port Camera

The SILS Port Camera integrates all components of a laparoscopic vision system into an inexpensive, portable cannula port. During use, the device is inserted into a 12 mm incision (similar to a standard cannula) and then activated, which deploys a small camera module *in vivo* at the distal end of the device. An on-patient LCD display at the proximal end of the device provides the view of the surgical site.

SILS Magnet Camera

The SILS Magnet Camera System incorporates all of the features of a laparoscopic vision system into a small, inexpensive, portable package that is attached entirely inside the abdominal cavity, thereby avoiding competition for space between the surgical tools. This SILS Magnet Camera includes three degrees-of-freedom: one translational motion and two rotations. During use, the device is inserted through a 26 mm incision in the umbilicus, followed by a SILS port, which is used to support the insertion of additional tools. The camera, now *in vivo*, remains separate from the SILS port, thereby removing the need a dedicated laparoscope, and thus allowing for an overall reduction in SILS port size or the use of a third tool through the insertion port regularly reserved for the laparoscope. The SILS Magnet Camera is mounted to the abdominal ceiling using one of two methods, fixation to the SILS port through the use of a rigid ring and cantilever bar, or through the use of an external magnetic handle.

Chapter 1 - Introduction

1.1 Minimally Invasive Surgery (MIS)

Laparoscopic surgery is a modern minimally invasive surgical technique in which the surgeon makes multiple small incisions in the abdominal and pelvic regions (0.5-1.5 cm) in order to view and perform operations in the abdominal cavity [1]. A trocar is used to make the small incisions in the abdominal wall and is combined with a cannula port to allow for the insufflation of the peritoneal cavity providing a region large enough to work in and view the surgical site [2]. Cannula ports provide sealed access points used for the insertion of a wide range of surgical tools. Typically at least three incisions are required for laparoscopic operations. Where one incision is occupied by the laparoscope (viewing system), and the other two incisions allow for various grasping, cutting, and sealing tools, see Figure 1 [3, 4].

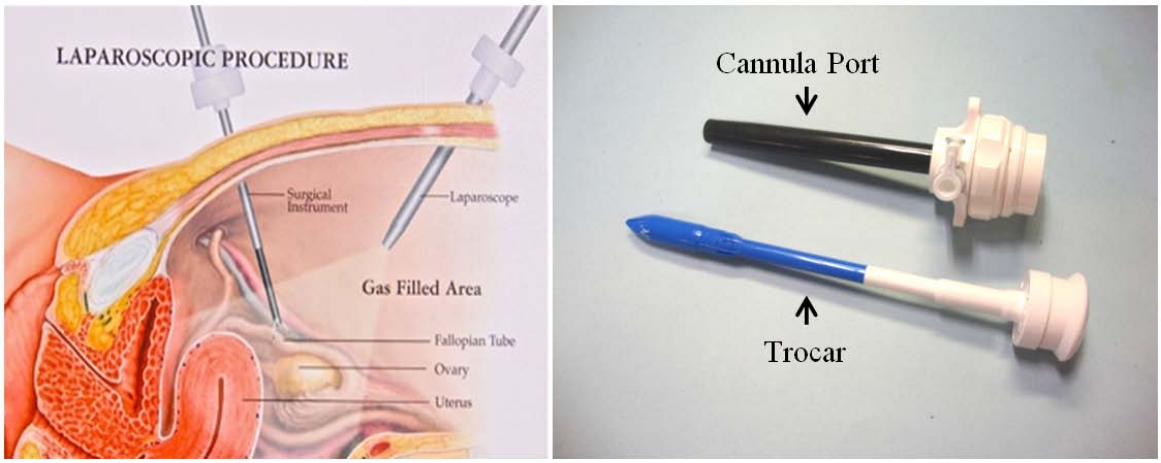

Figure 1: Minimally Invasive Surgery (MIS) setup (left). Cannula (right top) and trocar (right bottom)[4].

Surgeons may use one of two different types of laparoscopes in a laparoscopic surgery: 1) a telescopic rod lens system connected to a video camera located *ex vivo* at the distal end of the laparoscope, and 2) a digital video system located *in vivo* at the proximal end of the laparoscope. Both types of laparoscopes make use of a fiber optic cable and a halogen or xenon light source to provide illumination inside the abdominal cavity [5].

A wide range of MIS include appendectomy, cholecystecotmy, nephrectomy, hysterectomy, oophorectomy, adrenalectomy, gastric bypass, Nissen fundoplication, hernia repair, splenecromy, colon resection, liver resection, cryoblation, and much more [6]. Some of the benefits of MIS over laparotmy include reducing the invasiveness, trauma, pain scarring, and recovery time of patients [7].

As the popularity of MIS increases new surgical techniques have been adapted to further minimize the invasiveness, trauma, pain, scarring, and recovering time of surgery by reducing the size and number of access ports. Single Incision Laparoscopic Surgery (SILS) is a relatively new surgical technique that can be performed entirely through the umbilicus by passing multiple tools through a single incision point, see Figure 2 [8].

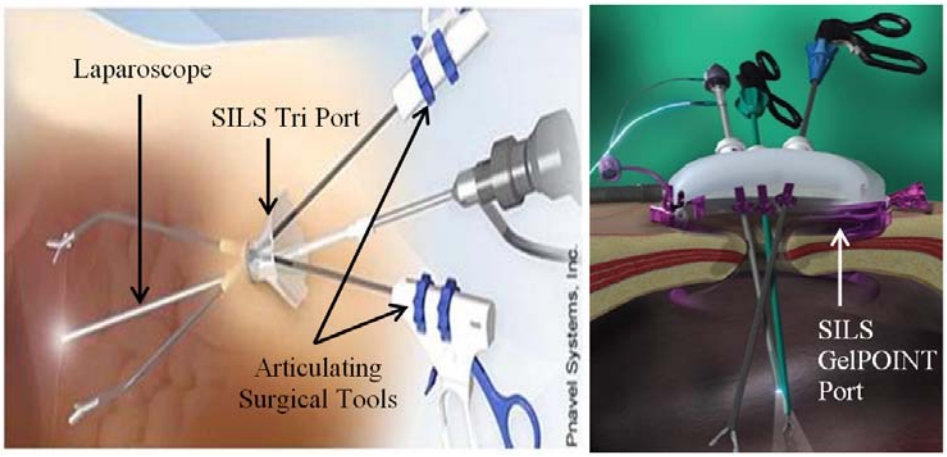

Figure 2: SILS Setup with the Tri Port (left) and GelPOINT (right) [9, 10].

The equipment for SILS falls into two categories: 1) SILS access ports, and 2) SILS laparoscopic tools. There are a number of SILS access ports which provide a sealed access point to the abdominal cavity, insufflation of the abdominal cavity, and the insertion of surgical tools. These ports can be made of rigid plastics, elastomers, hydro-gels, and a combination of all three. Depending on the surgical procedure both standard in-line or articulating surgical tools can be used. There are a number of different articulating designs, ranging from cable to simple angle locking systems. Choosing a port and tool system depends largely on the surgeons skill, ergonomics, and price of the SILS systems [11].

1.2 MIS Drawbacks

Even though MIS offers many advantages over open surgery, it is not without drawbacks. MIS remains surgically challenging due to: 1) limited tool and cannula port motion, 2) restricted and disorienting views of the abdominal cavity, 3) non-intuitive surgical tool control, 4) reduced tactile feedback, 5) reduced depth perception, and 6) long distance to the surgical site [12]. SILS further compounds these issues by passing multiple tools and the laparoscope through a single incision leading to collisions and dexterity challenges for the surgeon.

During open surgery the surgeon has a direct line of sight inside the abdominal cavity and can easily track hand and surgical tool movement. In MIS a laparoscope provides a two dimensional representation of the abdominal cavity and surgical tools. The field of view is limited by the range and mobility of the laparoscope, and its insertion point into the abdominal cavity [13]. The video images from the laparoscope are displayed in two dimensions on an off patient monitor. The limited field of view and two dimensional representation of the surgical site reduces a surgeons depth perception and can make tool manipulation non intuitive and difficult [14]. In traditional laparoscopic surgery the limited field of view can be improved by locating the dedicated laparoscopic port away from the tool ports in order to inspect the tool ports and the tools themselves during use. However, SILS dictates that the laparoscope must share the same port as the surgical tools reducing visual information to an inline path with the tools.

The cannula ports in which laparoscopic tools are inserted through directly interact with the abdominal wall during tool use creating resistance and restrict tool motion. This restriction in tool motion and the removal of a direct line of site to the surgical tools (open surgery) removes the tactile feedback provided by the end of the tool and instead focuses more on cannula motion. This reduction in tactile feedback causes the surgeon to rely heavily on visual information provided by the laparoscope to determine tool location and tissue interaction. SILS further reduces tactile feedback

and tool control. The positioning of multiple tools and the laparoscope at the entry incision causes collisions and dexterity challenges.

1.3 Related Work

To improve the vision system used in SILS procedures SILS insertion techniques, ports, surgical tools, laparoscopes, and similar systems were reviewed. Fully understanding the insertion technique and securing system for each SILS port design, and the maximum tool motion offered by each SILS Port is critical in developing an improved vision system.

1.3.1 Incision Types

Different incisions are made depending on the use of a SILS specific port or multiple laparoscopic ports. Before SILS ports, which allowing for multiple tools to be passed through channels, were developed surgeons would make a 2-3 cm vertical incision in the umbilicus and use dissected subcutaneous flaps to allow for multiple ports to be inserted and secured [15]. Over developing the subcutaneous flap can lead to seroma formation near the incision site [16]. Single incision ports do not require skin flaps to maintain a tight seal in the abdominal wall but require a larger single incision.

1.3.2 Entry Techniques

Two different entry techniques are commonly used to provide access to the abdominal cavity, the Veress needle and cut down techniques, see Figure 3. The Veress needle is inserted into a small incision located at the base of the umbilicus, and used to insufflate the peritoneum cavity with carbon dioxide. A trocar and cannula are then inserted through the incision in the umbilicus, once the cannula is secured and connected to a insufflation line the trocar and Veress needle is removed [17]. This process is repeated until enough ports are available for the surgical procedure.

Figure 3: Veress Needle [18].

The open laparoscopic entry technique is used to support the insertion of SILS ports. A small incision is made in the umbilicus down to the fascia, followed by the palpation of the peritoneal cavity and insertion of a trocar. The abdominal cavity is palpated to protect the bowel during the insertion of the trocar [19]. The trocar is removed and the SILS port is inserted into the incision, and used to insufflate the abdominal cavity with carbon dioxide.

1.3.3 Trocars

Trocars are sharp mechanical instruments that provide the introduction of a cannula into the abdominal wall by separating or cutting through tissue fibers. There are three basic categories of trocars: bladed, bladeless, and blunt. Bladed or conventional trocars use a shield to dilate the tissue and a spring loaded blade to cut through the tissue, see Figure 4. As the trocar is being pressed into the abdominal wall the spring is compressed as the shield is pushed back, exposing the blade, once the trocar passes into the abdominal cavity the spring is uncompressed, as the shield meets no resistance, retracting the blade. The shield helps prevent abdominal damage from occurring by reducing organ exposure to an exposed blade [20].

Figure 4: Bladed Trocar[21].

Bladeless trocars utilize a pointed plastic tip to separate tissue fibers, see Figure 5. During insertion the trocar creates a smaller fascial defect in the abdominal wall, followed with low insertion force provided by the surgeon to separating tissue fibers allowing for a cannula to be secured in the abdominal wall. For most insertion sites the bladeless trocar allows for the tissue to be repositioned without using closure techniques once the trocar and cannula are removed [22].

Figure 5: Bladeless Trocar [23].

In order to reduce the risk of causing internal damage during trocar insertion, surgeons can use a scalpel to cut through most of the abdominal wall followed by the insertion of a blunt trocar to push through last bit of abdominal tissue and into the peritoneal cavity, see Figure 6 [24]. Normally sutures are applied around the incision site to provide stability to the cannula during use and to maintain insufflation (prevent leaking of pneumoperitoneum around the cannula) [25].

Figure 6: Blunt Trocar [26].

1.3.4 Single Incision Platforms: SILS Ports

SILS utilizes multiple tools operating in the same incision site, often times this leads to collisions between the tools, ports, and surgeons hands making the surgical procedure technically difficult. Special ports and modified cannulas have been developed for SILS to reduce crowding at the incision site. Modified cannulas consists of a reduced cross sectional profile, created by decreasing the

insufflation housing and seal size [27]. The reduction in overall size allows for greater tool motion and improves surgeon dexterity.

SILS ports have been developed to provide multiple tool access through either multilumen channels, gel quadrants, or cannula filled channels. Often times the SILS ports have a designated channel used for insufflation of the abdominal cavity.

The Tri-Port is a SILS port designed by Advanced Surgical Concepts that utilizes two 5 mm gel ports and a 12 mm gel port to allow for surgical tool access. The ports sit inside of a cylindrical plastic sheet, which uses an expandable diaphragm on the distal end of the SILS port to provide a seal between the port and the abdominal wall, see Figure 7. A 1.5 to 2 cm incision up to the fascia is made in the umbilicus to allow for the inflatable diaphragm to be inserted into the abdominal cavity with the use of a flat 12 mm trocar. Once the diaphragm has expanded the port is moved down the length of the plastic cylinder and secured to the abdominal wall via the diaphragm in *ex vivo* [28].

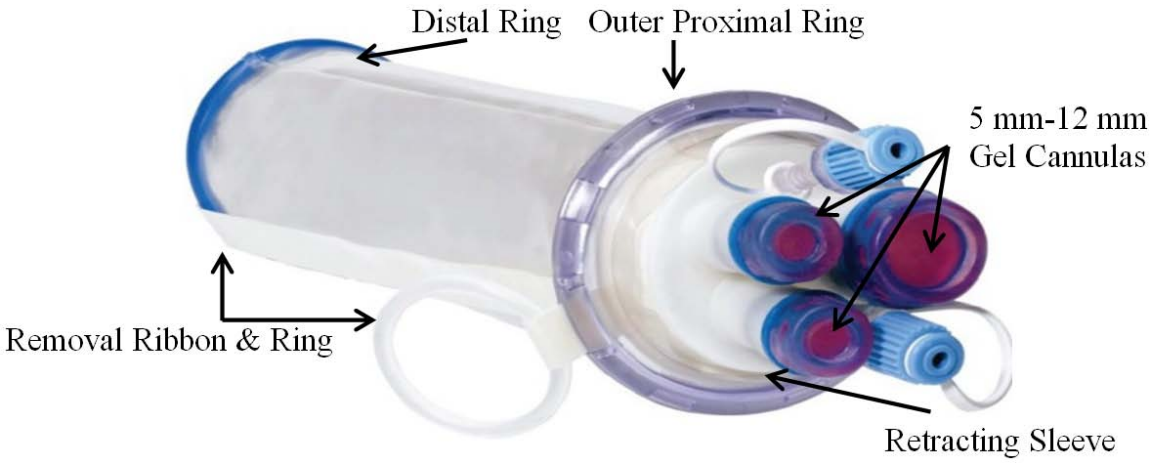

Figure 7: Tri-Port (Advanced Surgical) [29].

Covidien's SILS port uses three 5mm channels to accommodate two 5 mm cannulas and one 5-12 mm cannual for tool insertion, see Figure 8. The port utilizes an hour glass shape made out of a flexible elastomer, in which the larger flange sections are used to seal the port to the abdominal wall as well as stabilize it during use. The SILS port is inserted using the laparoscopic entry technique

through a 2 cm incision made in the umbilicus. Once inserted the port can provide insufflation and smoke evacuation through a dedicated port [30].

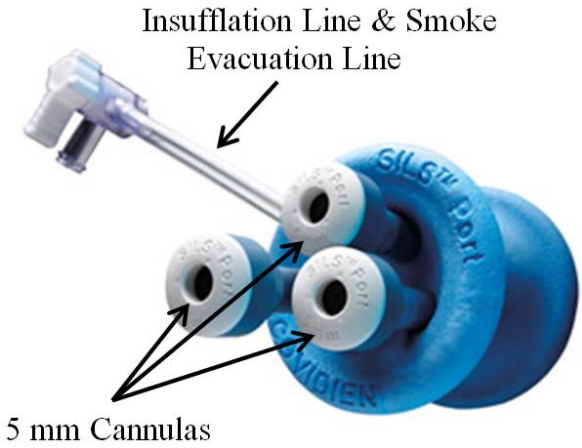

Figure 8: SILS Port (Covidien)[31].

Applied Medicals GelPort uses an expandable diaphragm inserted through a 3 cm incision in the umbilicus. Once the diaphragm is in place a gel cover is attached to the abdominal wall by clamping on to the diaphragms *ex vivo* rigid ring, see Figure 9. Three to four 5 mm cannulas can be inserted into different quadrants in the gel dome to allow or tool access. The gel also allows for tools to be inserted without the use of cannulas, further improving the range of motion for each tool [32].

Figure 9: GelPort (Applied Medical)[33].

The above SILS ports represent the three general types of single incision ports that are commercially available: either through an expandable diaphragm used to open the incision and

provide sealed access through either 1) built in multilumenal channels or 2) a gel dome, or 3) a flexible elastomer used to open and seal the incision while providing abdominal cavity access through cannulas inserted into channels in the port.

1.3.4 Flexible Surgical Instruments

Insertion of traditional in-line laparoscopic tools through a SILS port only supports an in-line approach angle to the surgical site, causing tool clashing and obstructs the laparoscopes view of the distal ends of each tool, see case B in *Figure 10*. To improve SILS success rate and procedure safety a wide range of steerable tools have been developed to allow the surgeon to triangulate the distal ends of the tools at the surgical site, see case C in *Figure 1Figure 10* [34]. Triangulation often times requires crossing each tool, making tool control non-intuitive. Most SILS operations can be performed with one in-line tool and one articulated tool. Often time's surgical tool length is varied to offset the surgeons hands during tool use, reducing handle and hand clashing [35].

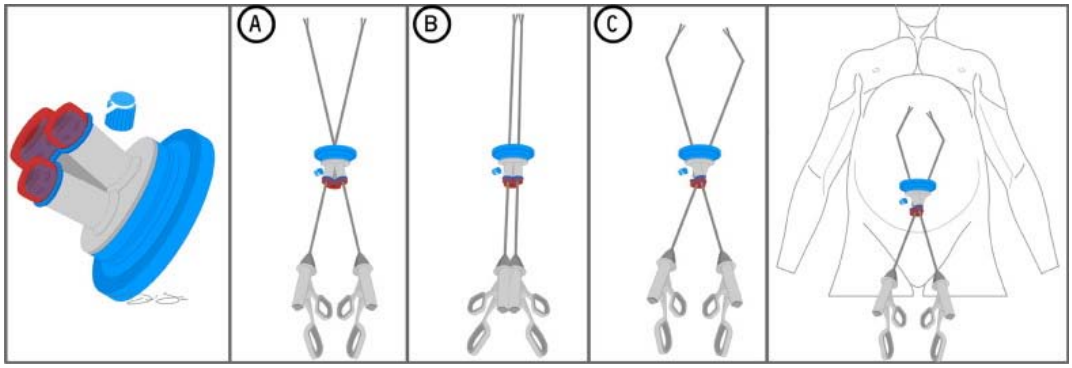

Figure 10: The Tri-Port in case A-B uses straight tools and case C uses articulated tools [34].

Novare Surgical Systems articulating RealHand surgical tool line uses a cable system to link the tool tip and tool handle allowing the tool tip to mimic the movements of the surgeon's hands, see Figure 11. A mechanical locking system can be used to fix the tool in an in-line straight position or at 90 degrees in any direction [36].

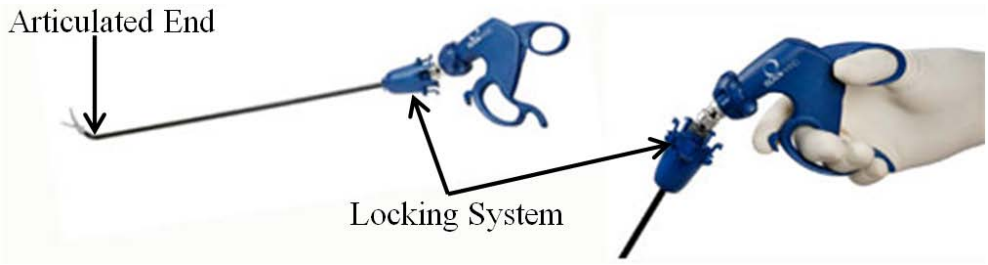

Figure 11: RealHand Articulating Laparoscopic Tool [37].

Covidein's Roticulator surgical too line provides articulation up to 80 degrees through the use of a rotating activation sheath, see Figure 12. As the activation sheath is rotated the tool tip is extended away from the handle. The rod connecting the tool tip to the handle is pre bent near the jaws at 80 degrees, so as it pushed out of the tool housing it returns to its pre bent state [38].

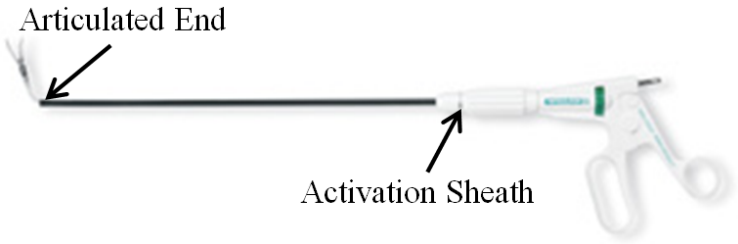

Figure 12: Roticulator Articulating Laparoscopic Tool [39].

The above SILS tools represent two general types of single incision articulating surgical instruments that are commercially available. Typically the tools can articulate either through a cable system that can be locked, or a pre bent tool end that can be released from an outer retaining housing.

1.3.5 Laparoscopes

Traditional laparoscopes provide an in-line view of the surgical site during SILS procedures, reducing the surgeon's field of view, and creating blind spots behind the surgical tools. Often times a 5 mm, 30 degree laparoscope provides a sufficient field of view to perform most SILS operations, such as a cholecystectomy (gallbladder removal). For some surgical procedures, such as applying a gastric band, the laparoscope may not be able to cover the distance between the distal end to the surgical site due to length limitations and being operated from the umbilicus [40] . Standard

laparoscopes contain a relatively large handle of outer diameters close to 40mm, taking up valuable workspace shared with the laparoscopic tools. SILS specific laparoscopes have been developed to provide different viewing angles, through the use of articulating optics and flexible endoscopes for complicated SILS procedures and to increase tool range of motion by reducing handle diameters. Olympus Surgical and Industrial Americas EndoEye laparoscope offers a 100 degree flexible tip that can be rotated 360 degrees around the length of the laparoscope, see Figure 13. The EndoEye can articulate and lock the camera end with minimal handle movement, increasing the working tools range of motion [41].

Figure 13: EndoEye Laparoscope [42].

1.3.6 Future Technologies

PortCamera Surgical System

Austin Ruppert, a previous Advanced Medical Technologies Laboratory research student, proposed the idea of integrating a vision and display system directly onto a typical 12 mm cannula to be used in traditional laparoscopic surgery. This integration removes the need of a dedicated laparoscope port, brings the surgeons focus back to the patient (on-patient monitor), and couples the camera with tool motion thus making tool control more intuitive and reducing the trauma associated with MIS procedures, see Figure 14. To prove the feasibility of the camera system, called the "PortCamera", a participant and porcine study were completed to evaluate the effectiveness of the Port Camera versus a traditional laparoscopic setup. Overall the device performed similarly to a traditional laparoscope and was successfully used to perform a gallbladder resection as well as a liver biopsy [43]. Many of the design features of the PortCamera system were used in making an analog SILS specific design, as discussed latter.

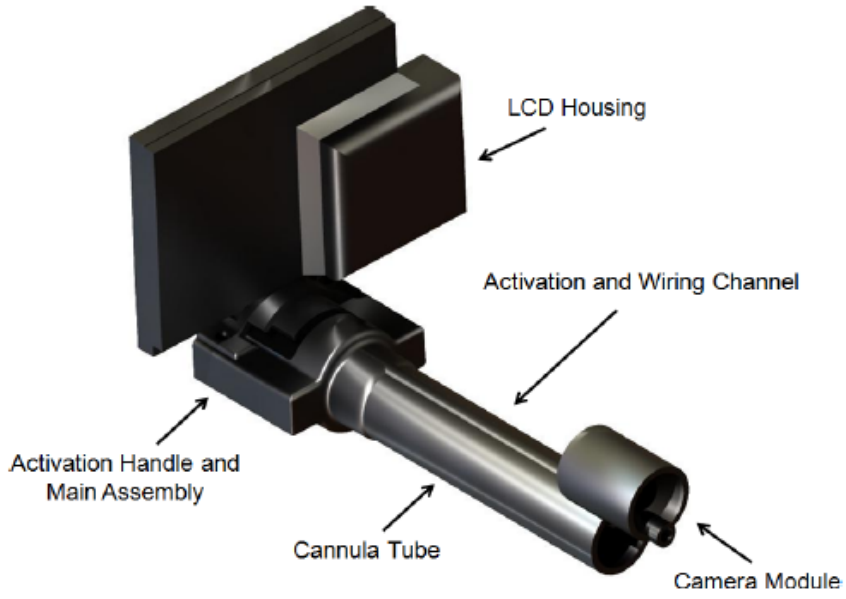

Figure 14: Version 1.5 of the PortCamera [44].

MAGS Surgical Systems

Transabdominal magnetic anchoring and guidance systems (MAGS) are being developed to suspend and move imaging systems and surgical tools inside the abdominal cavity. Initially the intra-abdominal instruments are inserted into the peritoneal cavity and then anchored to the abdominal wall using *ex vivo* magnetic handles, see Figure 15. These intra-abdominal instruments can be used to view, grasp, retract, suspend, and cauterize abdominal contents (tissue and organs) during MIS procedures. For instance, the magnetic graspers (passive tissue retractors) are held and moved along the abdominal wall with the use of *ex vivo* magnetic handles, and can be attached to organs, such as the gallbladder, using laparoscopic grasper tools in order to retract the organ during MIS procedures [45].

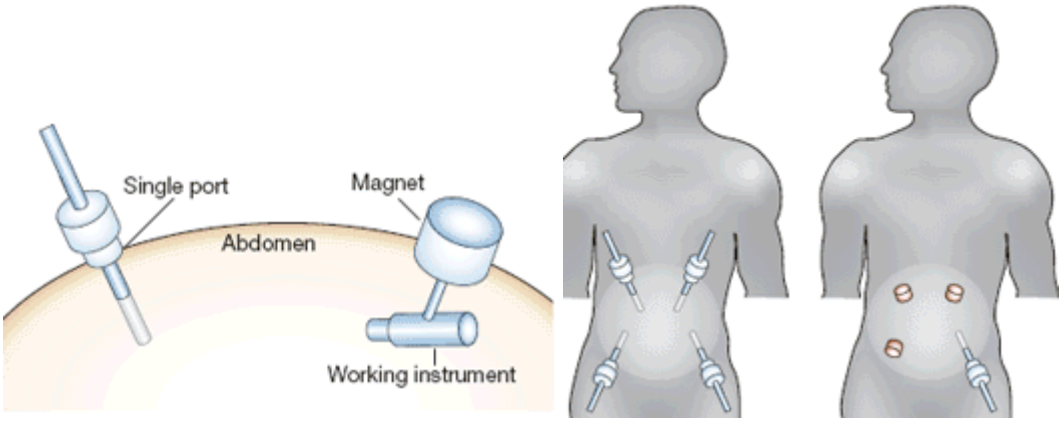

Figure 15: MAGS System [45].

A novel MAGS intra-abdominal camera was developed by a group at the University of Texas Southwestern Medical Center to facilitate SILS. The camera consists of a digital imaging system, on board LED, and magnets contained in a biocompatible sealed plastic housing, see Figure 16. The MAGS camera system was inserted into the abdominal cavity to be attached and moved along the abdominal wall through the use of a magnetic handle. The onboard camera system is fixed latterly in the housing and can be angled through the manipulation of the magnetic handle. The group successfully used the device to perform a nephrectomy and appendectomy in two human participants. Ultimately the MAGS camera system reduced surgical tool collision, improved the range of surgical tool motion by eliminating the laparoscope, and provided a comparable image to a traditional laparoscopic setup [46].

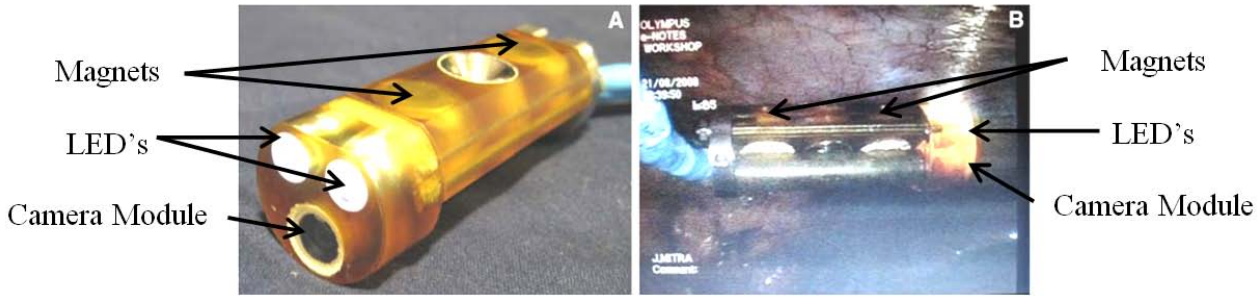

Figure 16: Novel MAGS Camera System [46].

MAGS systems help reduce trauma to the patient by reducing the number of abdominal incisions required, they increase the mobility of intra-abdominal instruments, and increase the surgical working space. The MAGS system is not without drawbacks however. As the abdominal wall thickness increases the magnetic force between the handle and the instrument decreases, requiring stronger magnets depending on the body mass index (BMI) of the patient. Strong magnets are dangerous in an operating room full of ferrous tools, and can cause inadvertent damage to either the patient or the surgeon as surgical tools are drawn to the magnets.

Robotic Surgical Systems

A novel robotic laparoscope is being developed by the Department of Computer Science at Columbia University in New York to improve MIS. The laparoscope contains an onboard imaging, lighting, and control system allowing for the camera module to pan 120 degrees and tilt up to 90 degrees while illuminating and providing visual feedback on the intra-abdominal cavity, see Figure 17. The overall device is 110 mm long and 20 mm in diameter and is inserted through an incision in the umbilicus and sutured to the abdominal wall to hold it in place. Once secured the camera module is controlled remotely using a standard joy stick allowing for repositioning of the camera during the surgical procedure. The group has successfully performed an intra-abdominal exploration of the device in a porcine model and is working on the next iteration of the device [47].

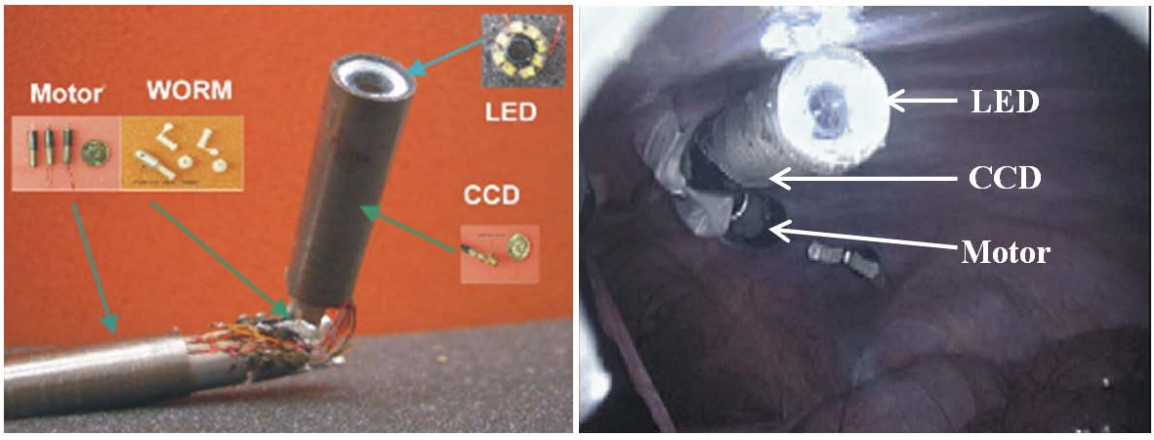

Figure 17: Novel MAGS Camera System [47].

Motorized laparoscopes help to improve the surgeon's field of view of the surgical site, free up valuable surgical tool real-estate, and improve the safety of MIS procedures.

Robotic SILS systems, such as the da Vinci surgical system, allow for the surgeon to remotely control intra-abdominal instruments that are motorized, offering additional degrees of freedom as well as improved triangulation that is not offered with traditional articulating surgical hand tools, see Figure 18. By removing the need for external tool leveraging, tool clashing is reduced and surgical working space is greatly increased. Due to quicker patient recovery times when compared to traditional MIS, patients pay 33% less by leaving the hospital earlier [48]. The upfront capital cost for robotic surgical systems like the da Vinici is roughly 1 million dollars, with continual costs in the form of maintenance and disposable tools make the system unviable for purchase for some hospitals [48].

Figure 18: da Vinci Surgical System [49].

Chapter 2 - SILS Camera Concept and Design

2.1 Port Camera Introduction

This paper addresses two design versions based on the basic design concept of a Port Camera system originally developed by the University of Colorado's Advanced Medical Technology Laboratory (AMTL) for traditional laparoscopic use [50]. First, this paper discusses the modified version of a previous design, then this paper will focus on a new design.

The first version is a modified design, called a SILS Port Camera that I designed, built, and tested for single incision laparoscopic surgery (SILS). The port camera system (SILS Port Camera) integrates all components of a laparoscopic vision system into an inexpensive, portable cannula port that enables point-of-care applications. The device can be incorporated with different commercially available ports, such as Coviden's SILS Port. The SILS Port camera uses one of the SILS ports open channels, followed by the insertion of the SILS port into a 1-2 cm incision through the belly button (umbilicus). During use a camera module and LED system located on the distal end of the SILS Port Camera is deployed by rotating the module 180 degrees and locking it in place at the top of the cannula. An on-patient liquid crystal display (LCD) screen located at the distal end of the SILS Port Camera device displays the video images of the surgical site, see Figure 19.

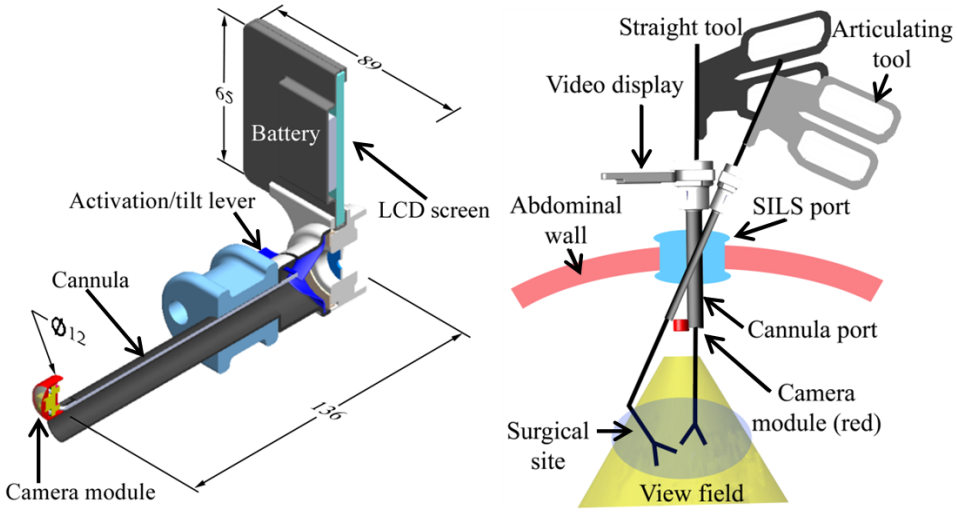

Figure 19: SILS Port Camera Deployed in SILS Port left and in vivo right (all units are in mm).

The device's camera module and on-patient LCD screen remove the need for an off-patient monitor and light source, bringing the surgeons attention back to the patient. Once the camera module is activated a surgical tool can be inserted into the cannula. This eliminates the need for a dedicated laparoscope channel in the SILS port and the surgical assistant who operates the laparoscope independently of the surgeon. By mechanically coupling the camera, surgical tools, and LCD display, tool control becomes more intuitive and less disorienting.

The SILS Port Camera design improves SILS in several ways:

1) By eliminating the dedicated laparoscope channel, the design reduces the size of SILS ports or allowing for an extra tool to be used.
2) By incorporating an inexpensive CMOS camera sensor, light emitting diode (LED), and eliminating the surgical assistant who controls the laparoscope, the design reduces surgical cost.
3) By decreasing the required incision and SILS port size to complete the procedure, the design helps to reduce the likelihood of patient trauma.
4) By removing the interference caused by a laparoscope, this design makes SILS more intuitive, providing an on-patient view of the surgical site, increase the flexibility in the cameras field of view and surgical tool control.

2.2 Magnet Camera Introduction

Since the SILS Magnet Camera design was designed, built, and tested after significant testing of the SILS Port Camera, this paper focuses on completely removing the camera system away from the SILS port thus increasing range and dexterity for the surgeon's hands, see Figure 20.

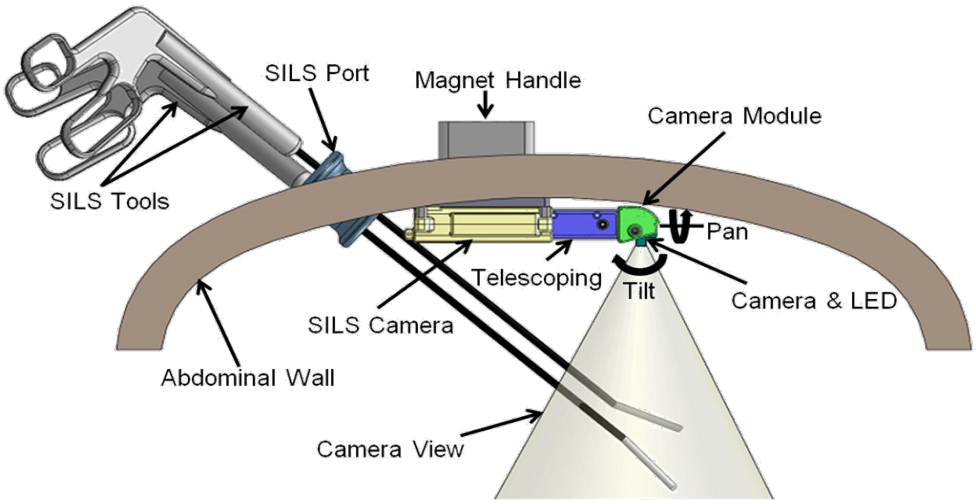

Figure 20: SILS Magnet Camera deployed in vivo.

This device integrates all the features of a laparoscopic vision system into a small, inexpensive, portable package that enables point-of-care applications and does not compete for space with the surgical tools. During use, the device is inserted into a 26 mm incision in the umbilicus, followed by the SILS port, which is used to support the insertion of additional tools. The camera, now *in vivo*, remains separate from the SILS port, thereby removing the need for a dedicated laparoscope, and thus allowing for an overall reduction in SILS port size or the use of a third tool through the insertion port regularly reserved for the laparoscope. The SILS Magnet Camera is mounted to the abdominal ceiling using one of two methods: fixation to the SILS port through the use of a rigid ring and cantilever bar, or through the use of an external magnetic handle.

The SILS Magnet Camera system is designed to improve SILS by:

1) By eliminating the dedicated laparoscope channel, this system reduces interference between the camera system and surgical tools.
2) By enhancing camera system mobility, i.e. offering pan, tilt, and telescope camera degrees of freedom, this system increases the surgeon's field of view.
3) By increasing procedure safety (improved field of view and tool control), this system enhances SILS.

2.3 Device Design: SILS Port Camera

The SILS Port Camera design requirements were developed after careful review of the PortCamera device created by the AMTL and assessment of SILS port limitations. The design specifications for the SILS Port Camera includes sealable housings which are Gamma Sterilization compatible [AS-400 polymer check]; electronics with low heat dissipation [LED and Camera] that can be coated to prevent shorting; camera tilt that can be controlled with one hand; Device and SILS port interaction that does not inhibit tool motion; a robust design that withstands heavy use; an ergonomic design that keeps surgeon posture upright, elbows in and wrists straight, a cannula cross-section no more than 14 mm and length no more than 150 mm; a maximum total unit cost of 500 dollars; and a design to mass produce custom parts.

2.3.1 Device Design: Port Camera

The development and testing effort of the SILS Port Camera device consisted of three phases: development of a prototype of the device, an experimental evaluation of the device using surgical residents, and a test of the device in a live porcine model. The prototype has the following features: 1) rapid prototyped using AS-400 polymer, 2) 88.9 mm (3.5”) diagonal LCD screen from Accelevision, 3) a RS4018A-55 analog video camera utilizing a CMOS video imager with an NTSC output, 4) A single, low-power, high efficiency 5 mm, 15 degree white LED, and 5) An activation knob for deployment and tilt. Future prototypes will be battery powered; this version uses an external power supply.

2.3.2 Port Camera: Prototype 1

Prototype 1.0 represents the integration of an imaging system, display system, lighting system, and sealable access to the abdominal cavity offered by a traditional cannula into one complete package. The design focuses around using a cannula like housing to serve as a backbone for the camera module and the on-patient LCD. Prototype 1 was developed using SolidWorks, a computer aided drafting program, see Figure 21.

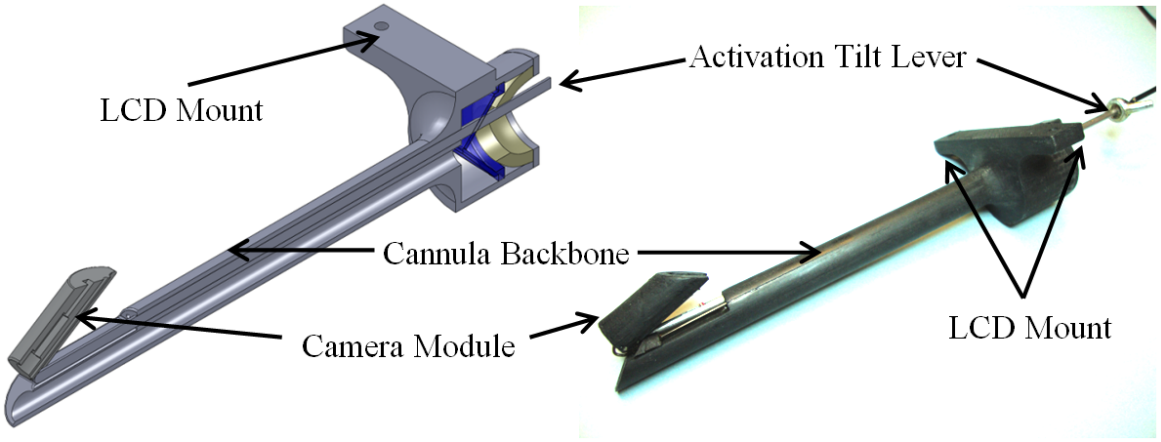

Figure 21:Cross-section of the SILS Port Camera CAD model (left) and Prototype 1 (right).

The cannula, camera module, and LCD display housings were printed using a Stratys Prodigy Plus 3D-Printer Rapid Prototyping System. The cannula, camera module, and LCD housings were made out of AS-400 polymer through fused deposition modeling. The Stratys Prodigy Plus provides a resolution of 1.27 mm (0.05”) for face features and 0.254 mm (0.1”) for chamfers and fillets.

An inner ridge was created inside of the cannula housing to hold two seals used to retain insufflation at all times, whether a tool is in use or not. A mounting feature was placed above the seals to allow for the LCD attachment to the device, see Figure 22.

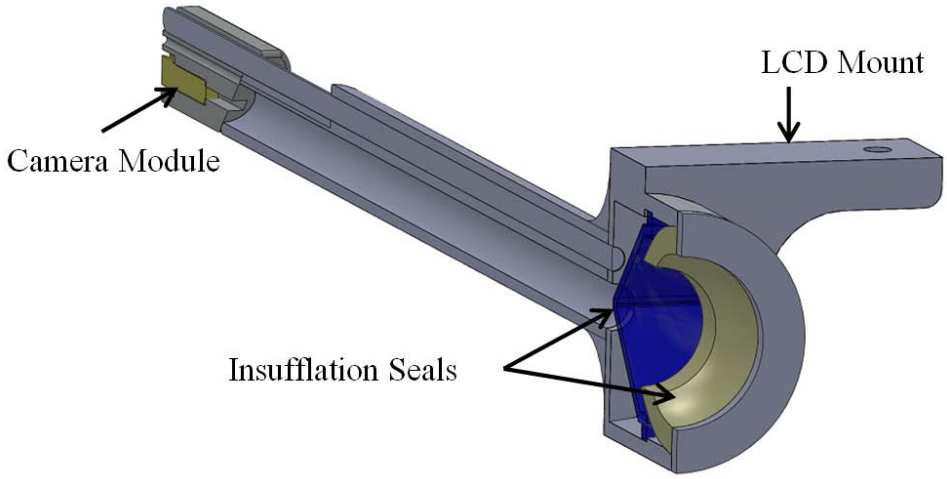

Figure 22: Cross-section of the SILS Port Camera camera module, seals, and mount.

A recessed pocket was used to tightly secure the camera package and LED inside the camera module, see Figure 23.

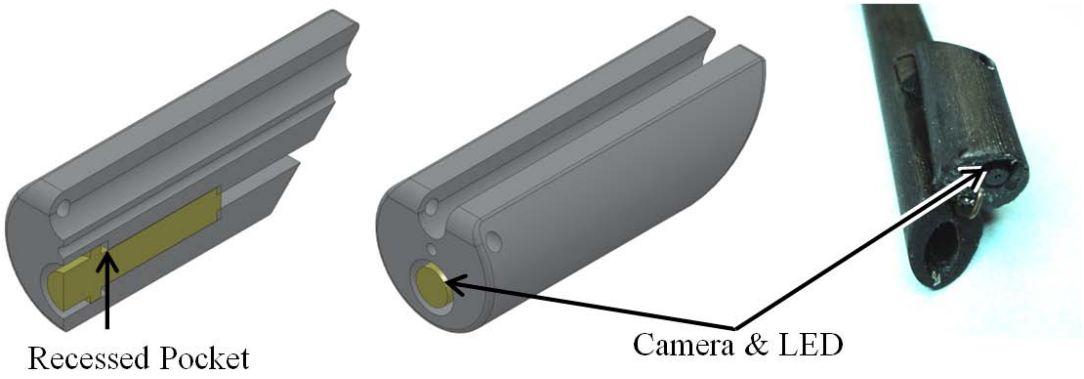

Figure 23: SILS Port Camera camera module.

The Camera module has two positions, deployed and un-deployed. The un-deployed mode is used during insertion and retraction of the Port Camera device. Then through the use of a 3.175 mm (0.125”) hollow stainless steel tube, that spans the length of the cannula, the camera module is rotated 180 degrees and pulled back into a grove representing its activated mode. The 28 gauge camera and LED wires are run through the stainless steel tube and out the end of the activation knob, see Figure 24.

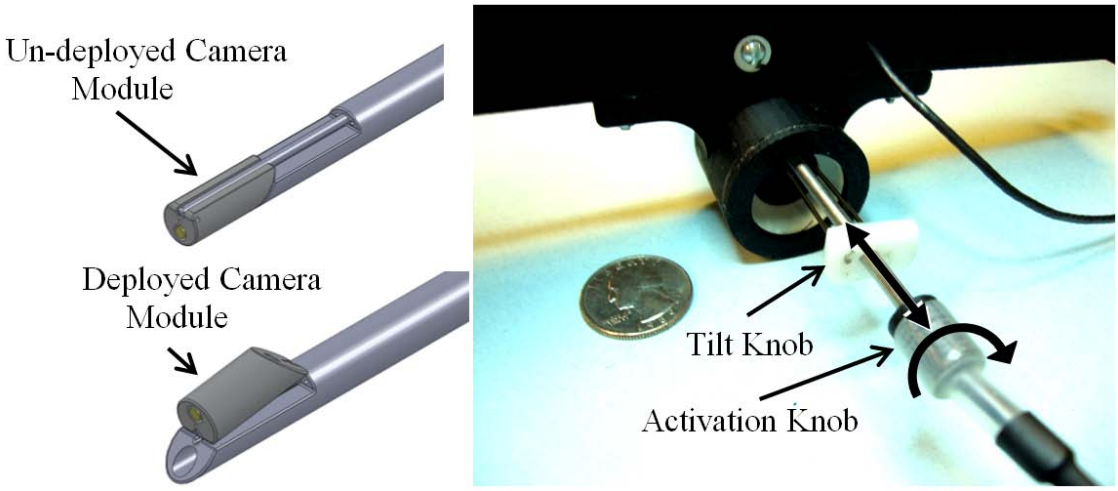

Figure 24: SILS Port Camera deployed (top-left), un-deployed (bottom-left), and activation mechanism (right).

A RS4018A-55 analog video camera uses an NTSC analog composite video output and a 1/18” (1.41 mm) CMOS sensor. The analog camera can operate between -2 degrees C and 40 degrees C offering a depth of field between 10-100 mm and a viewing angle of 55 degrees. The standard distance from the cannula end to surgical site is 100-150 mm. The data sheet for the RS4018A-55 camera used for each of the prototypes can be found in Appendix A.1. The video camera comes in a very small package (W 3.25 x H 3 x L 17.5 mm) ideal for reducing overall camera module size, see Figure 25.

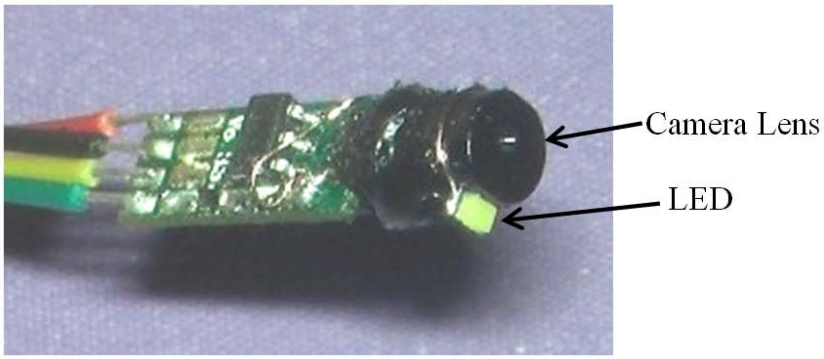

Figure 25: RS4018-55 Analog Video Camera [51].

The reduced camera module size ensures that the diameter of the cannula remains small and can be easily inserted into a SILS port. The pocket that houses the camera and LED is sealed using Loctite 3301 medical device adhesive (bio-compatible), and is used to mount a machined acrylic lens to camera modules outer face. A tilt knob translates two AS-400 polymer wedges, located at the end of a 1.25 mm outer diameter nitinol rod, under the camera module during its fully activated state to tilt the camera module up to 45 degrees from the cannula shaft. A 1.25 mm outer diameter nitinol spring was manufactured and embedded into the camera module and attached to the activation rod to store mechanical energy as the wedges rotate the module away from the cannula. A 1.25 mm stainless steel pin attaches and allows the camera module to pivot around the activation rod, See Figure 26.

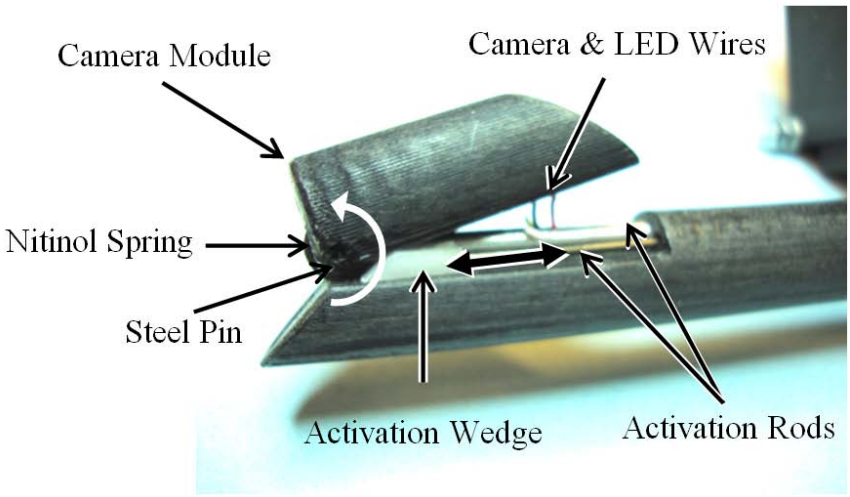

Figure 26: SILS Port Camera tilt activation.

The camera output was connected to a 17.8 cm (7") polarized LCD which is mounted onto the proximal end of the cannula and used to display the camera module image during use. The 2.5 volts and 9 volts required for Camera/LED and LCD operation respectively was supplied by 1762 Triple Output DC Power produced by BK Precision Electronic Test Instruments, See Appendix A.2.

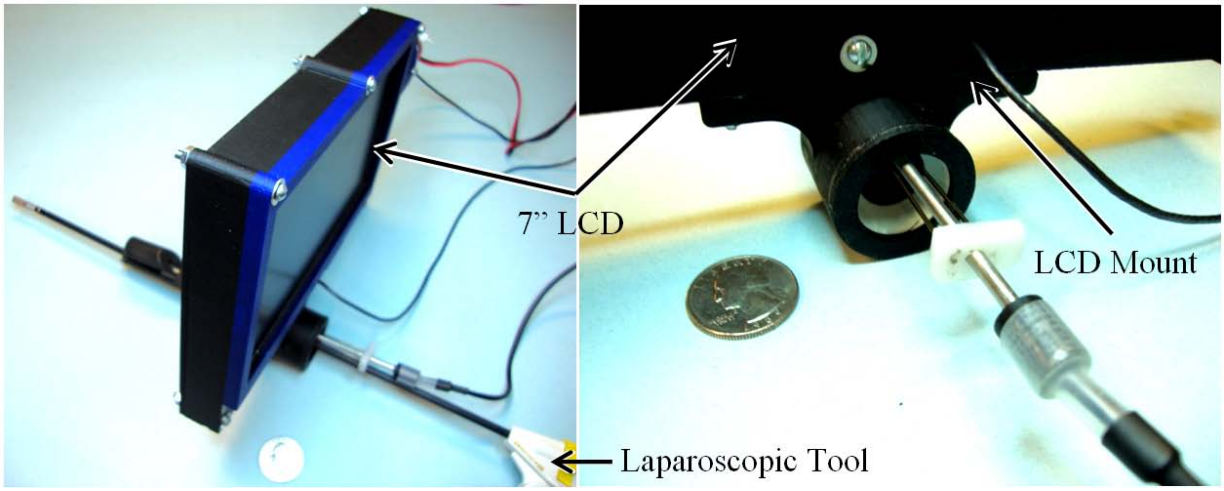

Figure 27: SILS Port Camera with 7" (17.8 cm) LCD screen.

2.3.3 Port Camera: Prototype 2

Prototype 2 was a slightly modified version of prototype 1, increasing cannula length from 100 mm to 150 mm and reducing LCD screen size from 17.8 cm (7") to 8.9 cm (3.5"), see Figure 28. Due

to the limitations of the cameras field of view as well as its lack of zoom the cannula length was extended to provide viewing distance of 150 mm from the camera module to the surgical site. The weight of the LCD screen in version one caused the device to be top heavy, thus leading to un-intentional rotation of the entire SILS Port Camera during use. In order to solve this problem an Accelevision LCD was purchased reducing the screen size from 17.8 cm (7") to 8.9 cm (3.5"), and helping distribute the center of gravity closer to the cannula shaft, see Appendix A.3.

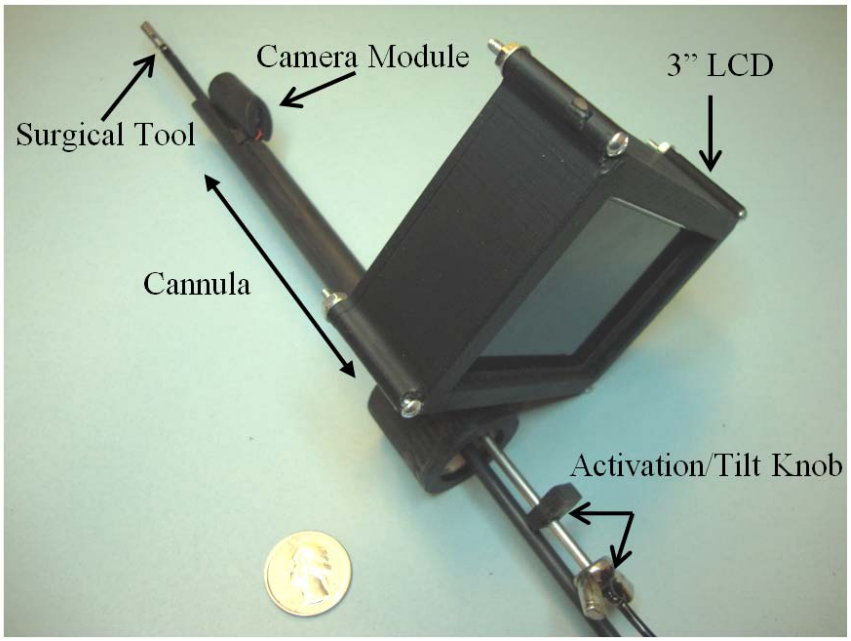

Figure 28: SILS Port Camera Prototype 2.

The camera module and cannula housing were redesigned to better accommodate the camera and LED and their wire leads. The pocket size and shape was changed to help keep the camera and LED securely fixed within the module during use. A new activation and tilt knob was developed and incorporated in order to provide smoother camera module deployment and articulation. The addition of wings to the activation knob helps the surgeon rotate to approximately 180 degrees by keeping the wings orthogonal/horizontal to the cannula's shaft in its deployed and un-deployed state, see Figure 29.

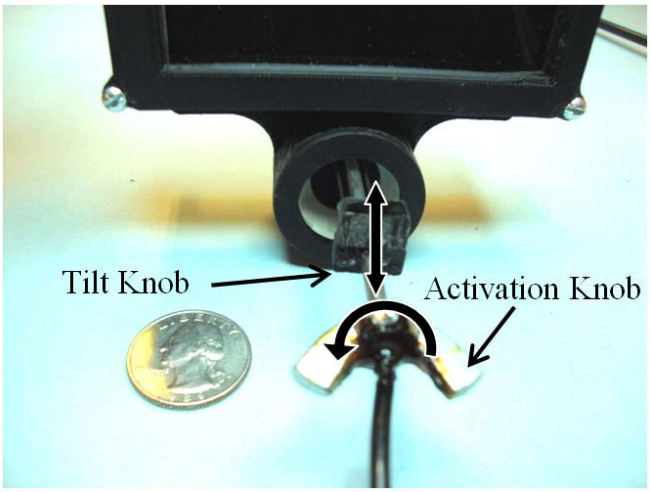

Figure 29: SILS Port Camera activation knob.

2.3.4 Prototype 2: Deployment Procedure

The SILS Port Camera can be integrated with a variety of SILS ports. Due to accessibility to Covidien's SILS port, for SILS Port Camera testing, a traditional laparoscopic entry technique is recommended for the insertion of Covidien's SILS port into the abdominal cavity. The un-deployed SILS Port camera is then inserted into one of the open channels in the port, just like a traditional cannula. Once in place the SILS Port Cameras camera module is activated, allowing for surgical tool access through its cannula. Ultimately a surgeons knowledge of SILS operations, port and entry preferences dictate what methods are used during the SILS Port Camera deployment.

2.4 Device Design: SILS Magnet Camera

The second design concept was developed after significant testing of the SILS Port Camera device, and instead focuses on completely removing the camera system away from the SILS port thus increasing range and dexterity for the surgeon's hands. The design specifications for the SILS Magnet Camera includes sealable housings which are Gamma Sterilization compatible [Somos 10120 material check]; electronics with low heat dissipation that can be coated to prevent electrical shorting [LED, Motors, and Camera]; camera controlled with one thumb, device and SILS port interaction does not inhibit tool motion; robust design that withstands heave use; ergonomically

designed to keep surgeon's posture upright, elbows in and wrists straight; cross section no more than 26 mm and length no more than 100 mm; maximum total unit cost of 500 dollars; and designed for mass production of all custom parts.

2.4.1 Device Design: SILS Magnet Camera

The development and testing effort of the SILS Magnet Camera system consisted of four phases: the testing results of the SILS Port Camera and SILS port types were reviewed, a prototype of the new SILS device concept was developed, an experimental evaluation of the device was conducted using surgical residents, and the device was tested in a live porcine model. The prototype has the following features: 1) Rapid prototyped using Somos 10120 polymer (high feature resolution), 2) A RS4018A-55 analog video camera utilizing a CMOS video imager with an NTSC output, 3) A single, low-power, high efficiency 5 mm, 15 degree white LED, and 4) The camera has 360° of pan, 90° of tilt, and 3 inches of translation. Future prototypes will be battery powered and wireless; this version uses an external power supply.

2.4.2 SILS Magnet Camera: Prototype 3

Prototype 3 focuses on solving the limited field of view and range in tool motion associated with a traditional laparoscopic set up and the SILS Port Camera. Traditionally once the SILS port has been inserted into the incision the laparoscope and two surgical tools are inserted into one of its three channels. The laparoscopes' camera and lens system are housed in a handle (*ex vivo*) and is operated by an assistant during surgery. A traditional SILS setup has the assistant's hand (laparoscope control) and each of the surgeons hands (surgical tool control) operating in roughly the same area, making operational space tight with frequent collisions between hands and tools, see Figure 30 [52].

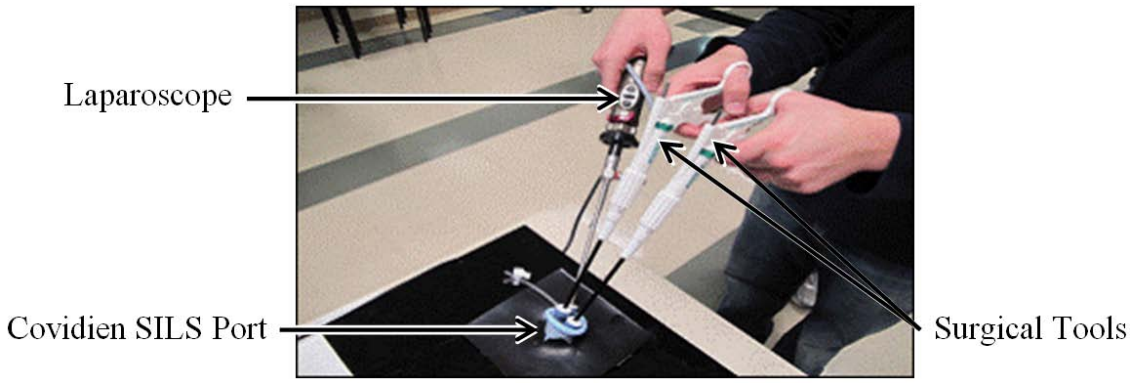

Figure 30: Typical SILS surgical tool and laparoscope operation [52].

To help alleviate the dexterity challenges of using SILS the SILS port itself can be rotated to allow for different bi-lateral tool motion, see Figure 31 [53].

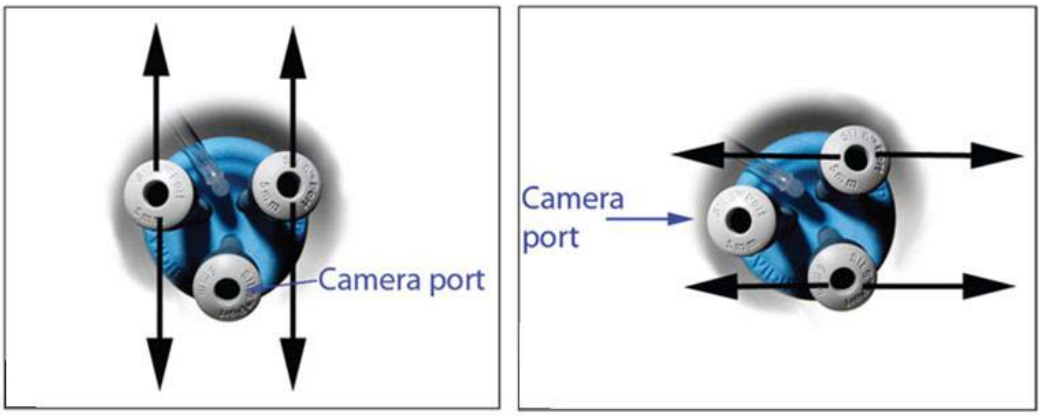

Figure 31: Coviden SILS Port. Vertical tool operation (left). Horizontal tool operation (right) [53].

By restricting the laparoscopes motion apex to the incision point the assistant is only able to provide a sweeping view of the surgical site, thus creating blind spots to the sides and behind the point of operation. A few different laparoscope designs have been developed offering tilt-able tips of 15 and 45 degrees to enable a slightly modified field of view.

By decoupling the camera system from an inline path with the incision and increasing the cameras systems range of motion the need for a dedicated laparoscope port can be removed. This reduces the number of pole like tools from 3 down to 2, allowing for a greater range in tool motion and opening up valuable operating real-estate. This SILS Magnet Camera module includes three

degrees-of-freedom: one translational motion and two rotations. During use, the device is inserted through a 26 mm incision in the umbilicus, followed by a SILS port. The SILS Magnet Camera is mounted to the abdominal ceiling using one of two methods: fixation to the SILS port through the use of a rigid ring and cantilever bar, or through the use of an external magnetic handle. The SILS Magnet Camera features can be broken down into two categories: camera mobility and SILS device mounting, see Figure 32.

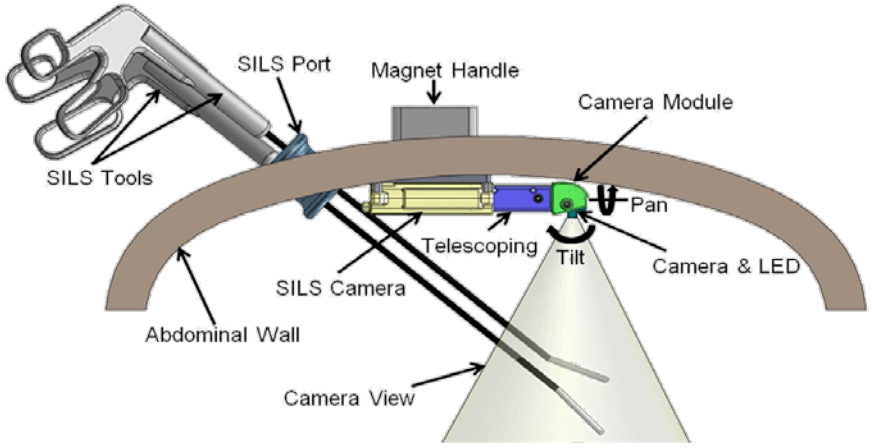

Figure 32: SILS Magnet Camera deployed in vivo.

Camera Mobility

Remote viewing of the abdominal cavity is accomplished by three motors which control the tilt, pan, and telescoping camera module features. The camera module has an overall size restrictions of (L 26 x W 12 x H 26 mm) to ensure that it can still be safely inserted through a 26 mm incision. Two (D 6 x L 24 mm) dc micro-mo motors (Faulhaber 0615 C 4.5 S) are used to provide the tilt and pan feature, see Appendix A.4. The micro-mo motors can be ordered with different gear head attachments to provide a range in output speed. The motors operate at 4.5 volts, 0.12 amps, and provide an output of 20,000 revolutions per minute (rpm), see Figure 33.

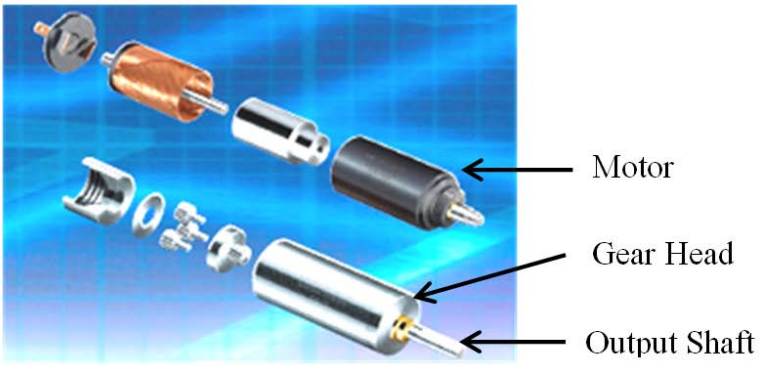

Figure 33: 6 Volt DC Micro-Mo 6 mm motor[54].

Flanged ball bearings are used to reduce friction and binding of motor shafts and moving components. Bearings were used to support all rotating shafts and mechanical components in the SILS Magnet Camera device.

Tilt and pan was created using a gimbal like design. A gimbal is a structure that allows the rotation of a parent object (camera module) around one axis. The parent object contains another pivot orthogonal to the initial rotation axis allowing for a rotation of a child object (camera/LED mount) around a perpendicular degree of freedom, see Figure 34.

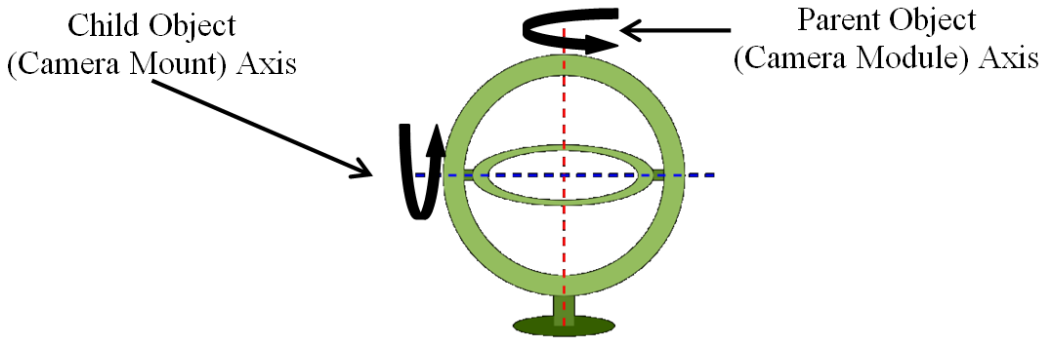

Figure 34: Gimbal degrees of freedom [55].

Normally in gimbal applications one motor controls the parent object (pan degree of freedom). The parent object contains the second motor to control the child object (tilt degree of freedom). Due to the max size restrictions for the camera module (L 26 x W 12 x H 26 mm), the tilt motor could not be added to the module without exceeding design specifications.

To keep the camera module size small and its weight below 8 grams the tilt and pan motors were offset from a co-linear position with the camera module and glued into a stationary housing (inner motor housing). To transmit the rotation force generated by the two motors positioned lengthwise down the SILS device, special coupling shafts were glued to the motor shafts and press fit into 1.4 mm (0.055”) flanged ball bearings. The bearings were then glued into the inner motor housing and used to reduce binding and frictional losses to the motors, see Figure 35.

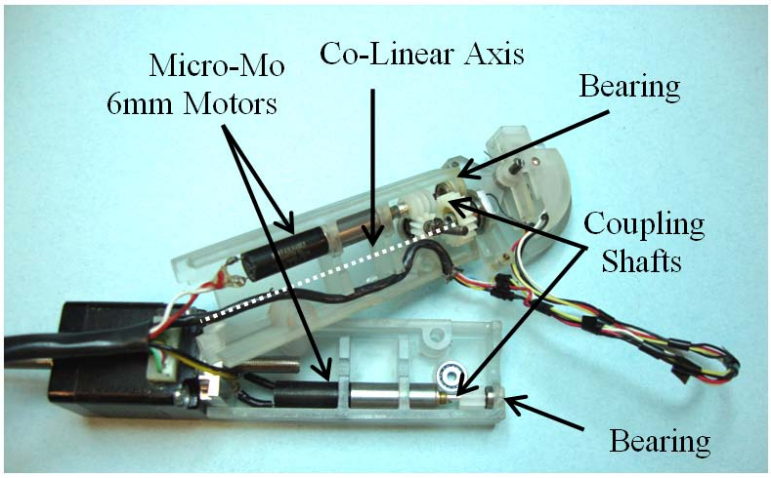

Figure 35: SILS Magnet Camera motor mounting and operation.

A 3.175 mm (0.125”) hollow aluminum shaft was attached to the camera module using a T-Plate and fixed to the inner motor housing by being press fit into a glued 3.175 mm (0.125”) flanged ball bearing. The bearing allows for the camera module to rotate around one degree of freedom, see Figure 36.

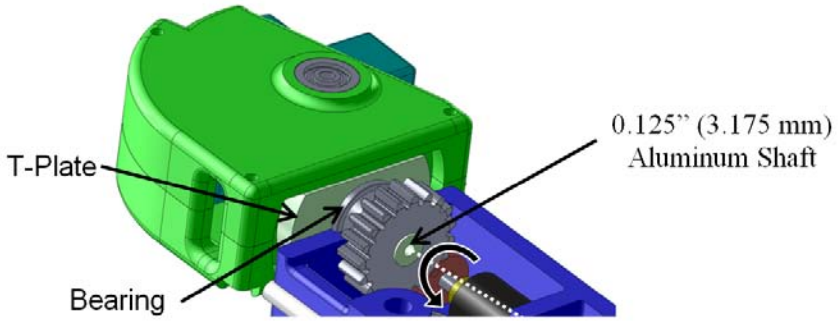

Figure 36: SILS Magnet Camera camera module mounting mechanism.

By using a pair of spur gears, a 10 mm pitch diameter acrylic spur gear press fit onto the camera module shaft and a 4 mm pitch diameter acetal motor gear press fit onto the pan motor coupler, the pan motor is able to rotate the camera module while keeping a co-linear path to the camera modules rotation axis open allowing for a tilt mechanism to be integrated, see Figure 37.

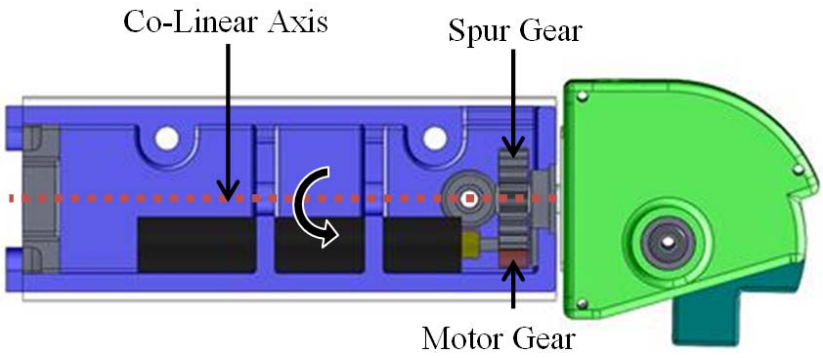

Figure 37: SILS Magnet Camera pan mechanism.

Tilt was provided by using a spool and anchor technique. A worm/worm gear pair is used to provide rotation to a spooling shaft. The spooling shaft is centered in line with the camera module rotation axis and fixed to the inner motor housing through the use of two 1.4 mm (0.055”) flanged ball bearings. The 5 mm pitch diameter acetal worm gear is press fit onto the spooling shaft and meshes with the 5.5 mm pitch diameter acetal worm connected to the tilt coupler. By running a cable from the spooling shaft up through the camera modules’ hollow aluminum shaft and mounting it to the back side of the camera mount, the fully deployed position (45 degrees) is achieved as cable slack is taken up by the spool. One end of a torsion spring is fixed to the camera mount and the other end is fixed to the camera module, allowing for mechanical energy to be stored in the spring as the spooling cable pulls the back end of the camera mount towards the spooling shaft. To provide the down tilting feature the spooling shaft is rotated in the opposite direction to provide slack in the cable, thus using the stored energy in the spring to return the camera mount to its original/neutral position (-45 degrees), see Figure 38.

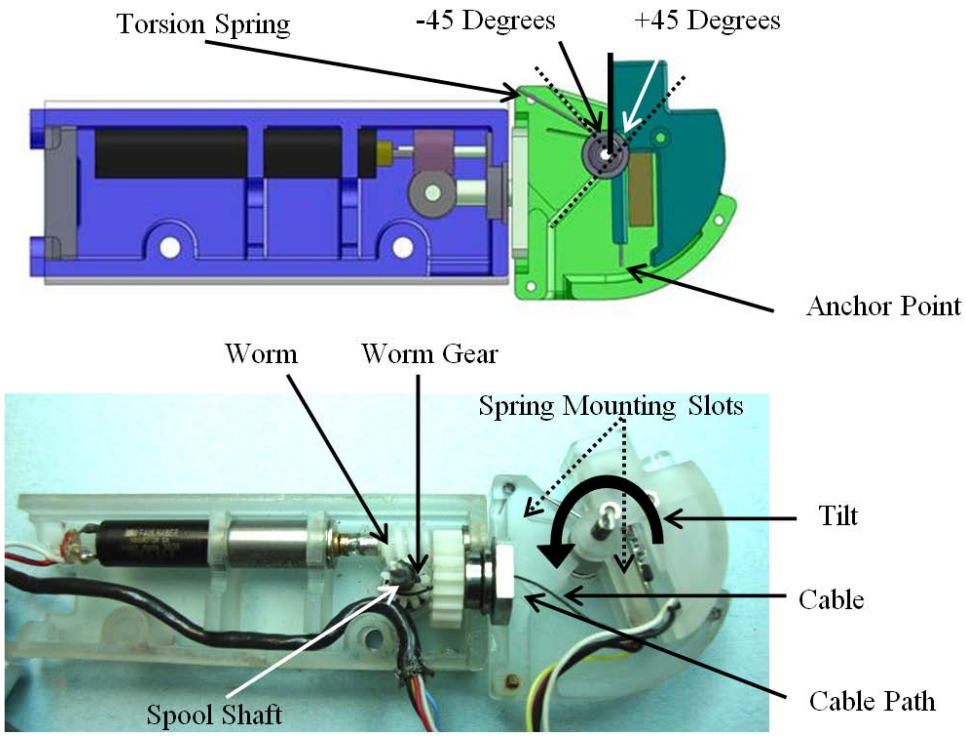

Figure 38: SILS Magnet Camera tilt mechanism

Translation of the camera module is provided by a Size 8 non-captive Haydon Kerk linear actuator, see Appendix A.5. Linear actuators are motors that use non-linear motion to create linear motion by either using mechanical, hydraulic, pneumatic, piezolectirc, or electro mechanical means [56]. The Size 8 linear actuator is a mechanical actuator that rotates an actuator nut which in turn moves a screw shaft in a line. During use the screw shaft is not allowed to rotate to provide either linear movement of the screw or in this case the movement of the motor. The screw is fixed to the outer motor housing, which is fixed to the abdominal wall, whereas the motor is attached to the inner motor housing and allowed to move in one translation degree of freedom, thus providing translation of the motor, inner housing, and camera module. The maximum translation distance is limited by the 7.62 cm (3") screw allowing for 5.6 cm (2.2") of displacement, see Figure 39.

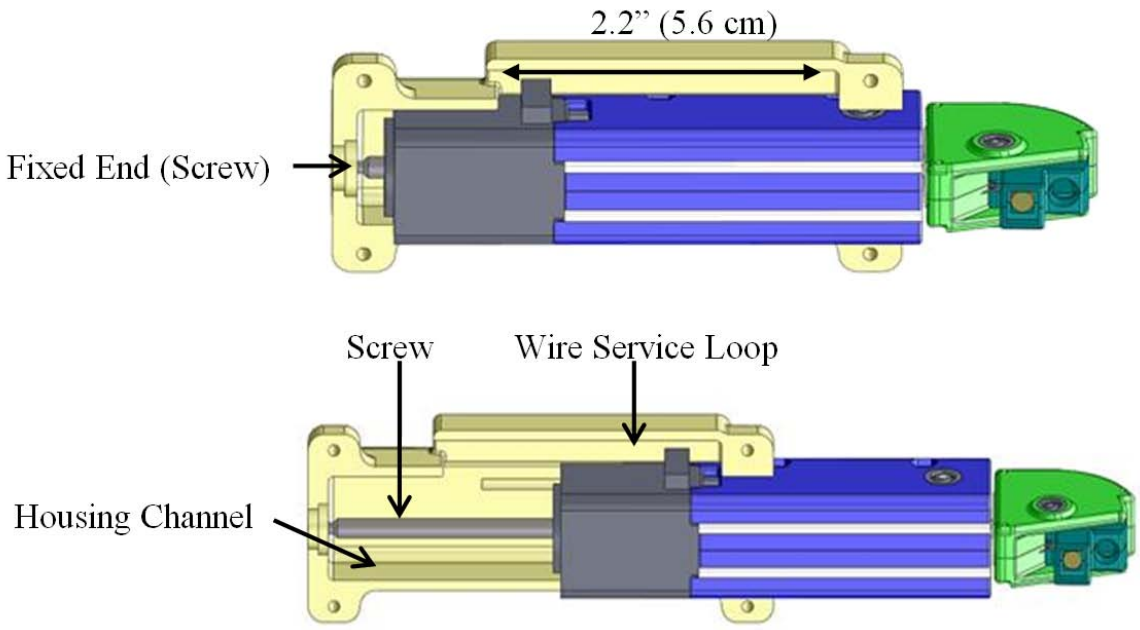

Figure 39: SILS Magnet Camera un-translated state (top) and Translated state (bottom).

The SILS device housings serve as a structural support for the internal motors, camera/LED, shafts/bearings, and provide sealing of electrical components to keep them dry during use. The housings were designed using SolidWorks and printed by the Protogenic Company. Somos 10120 was chosen as the printing material due to its high printing resolution, can be UV cured, bio compatible, and has a high structural strength. Model features were limited to feature thicknesses no less than 0.51 mm (0.02”).

Gears, gear heads, and motors were sized to obtain a camera pan and tilt speeds of 15 rpm and 24 rpm respectively. The maximum output speed of the 6 mm micro-mo motor is 20,000 rpm which can be applied to multiple gear heads offering a 4:1 to 4096:1 gear reduction, see Appendix A.6. The output torque from each gear ahead is approximately 25 mNm. In order to determine the gear head needed to provide adequate torque and rotation speed for the pan and tilt features, the design specified torque and rpm were used to back out motor torque and output speed.

Torque

The camera module was assumed to be a cuboid (L 26 x W 12 x H 26 mm) with a mass of 7.5 grams providing an inertia of 512.5 g*mm^2. To provide a quick turning response (pan) the angular acceleration for the camera module to get up to a steady state rotation of 15 rpm within 0.25 second was found to be 6.3 rad/s^2.

$$I_{Cuboid}=\frac{1}{12}*m*\left(L^2+W^2\right)=\frac{1}{12}*7.5g*\left(26mm^2+12mm^2\right)=512.5g*mm^2 \quad (1)$$

$$\alpha=15\frac{rev}{min}*2\pi*\frac{1}{60s}*\frac{4}{1s}=6.3\frac{rad}{s^2} \quad (2)$$

$$T=I_{Cuboid}*\alpha=512.5g*mm^2*6.3\frac{rad}{s^2}*\frac{1m}{1000mm}=0.33\ mN*m \quad (3)$$

From Eq. 1-3 the required torque to turn the camera module is 0.33mNm which is significantly lower than the 25 mNm offered by the micro-mo motor.

The spooling shaft is used to tilt the camera mount up to 90 degrees from its default position. A torsion spring stores the energy and releases the energy to rotate the camera mount back to its default position. The torque required to tilt the camera mount is governed by the stiffness and maximum deflection of the torsion spring. It takes approximately 1.275 N to deflect a 8.9 cm (3.5") floppy disk torsion spring to the required 90 degrees. Using the force exerted on the spring, the distance from rotation to the cable anchor (spring moment arm length in mm), and the deflection between the spring arms in degrees the spring constant can be found.

$$k=\frac{P*M}{D}=\frac{1.275\ N*12mm}{90^o}*\frac{1m}{1000mm}=0.00017\frac{Nm}{degree} \quad (4)$$

Where k is the spring constant (Nm/degree), P is the force exerted on the spring (N), M is the moment arm (mm), and D is the deflection (degrees). From Eq. 4 the spring constant was found to be 0.00017 Nm per degree.

The spring constant is used to help size the tilt motor to ensure the spooling shaft can provide sufficient torque to deflect the spring 90 degrees. A worm to worm gear drive train is used to provide

a large speed reduction between cross axis shafts, to lock the spooling shaft allowing the tilt motor to be turned off and the position of the camera mount to be maintained, and to maintain a high power transmission between the motor and the spooling shaft. Initial torque calculations for the worm gear train was developed using the 6 mm micro-mo motor due its small size and high torque output of 25 mNm. To determine the output torque of the spooling shaft the tangential force on the worm and the axial force on the worm were calculated.

$$F_{wt}=F_{ga}=2*\frac{M_1}{d_1}=2*\frac{25mNm}{5.5mm}*\frac{1000mm}{1m}*\frac{1N}{1000mN}=9.1N \quad (5)$$

Where F_{wt} is the tangential force on the worm (N), M_1 is the motor/worm torque (Nm), and d_1 is the reference/pitch diameter of the worm (mm). From Eq. 5 the tangential force on the worm, 9.1 N, is used with the worm tooth geometry and the coefficient of friction between the acetal gears to find the axial force on the worm.

$$F_{wa}=F_{gt}=F_{wt}\frac{\cos(\alpha_n)-\mu*\tan(\gamma)}{\cos(\alpha_n)*\tan(\gamma)+\mu}=9.1N\frac{\cos(20^o)-0.4*\tan(22^o)}{\cos(20^o)*\tan(22^o)+0.4}=9.33N \quad (6)$$

Where F_{wa} is the axial force on the worm (N), F_{wt} is the tangential force on the worm (N), α_n is the normal pressure angel of the worm (degrees), γ is the worm lead angle (degrees), and μ is the coefficient of friction between the acetal gears. From Eq. 6 the axial force on the worm was found to be 9.33 N. Combining Eq. 5-6 the spooling shaft torque can be determined.

$$M_2=\frac{F_{wa}*d_2}{2}=\frac{9.33N*5mm}{2}*\frac{1m}{1000mm}*\frac{1000mN}{1N}=23.3\ mNm \quad (7)$$

Where M_2 is the spooling shaft torque (mNm), F_{wa} is the axial force on the worm (N), and d_2 is the reference/pitch diameter of the worm gear (mm). From Eq. 7 the spooling shaft force was calculated to be 23.3 mNm which is less than the output torque of 25 mNm (for continuous operation) provided by the micro-mo motor. The micro-mo motor is able to produce up to 35 mNm of torque for short durations, making it an ideal choice for the tilt application.

Rotation Speed

Using the desired camera rotation speed of 15 rpm the pitch diameter for each spur gear could be determined. The input speed to the gear head is 8000 rpm, using a gear head reduction of 256:1 and a spur gear ratio of 2.08:1 the output rotation speed of 15 rpm can be achieved. Due to limitations of housing size a 10 mm spur gear and 4 mm motor gear were used to obtain a ratio of 2.375:1.

$$\text{output}_{\text{speed}}=\text{input}_{\text{speed}}*\text{gear}_{\text{head}}*\text{spur}_{\text{gear ratio}}=8000\frac{\text{rev}}{\text{min}}*\frac{1}{256}*\frac{1}{2.375}=13.15\ \frac{\text{rev}}{\text{min}} \quad (8)$$

From Eq. 4 the spur gear ratio provides a camera rotation speed of 13.15 rev/min which meets the design specifications.

The desired tilt time for the camera mount to rotate from its 45 degree down position to a 45 degree up position was set as 8 seconds allowing for the pitch diameter for the worm gear train and the motor gear head to be selected. To determine the rotation speed needed to rotate the camera mount 90 degrees in 3.5 seconds the distance from the cable mount (down state) to the triangular stop was calculated using camera module geometry, Figure 40.

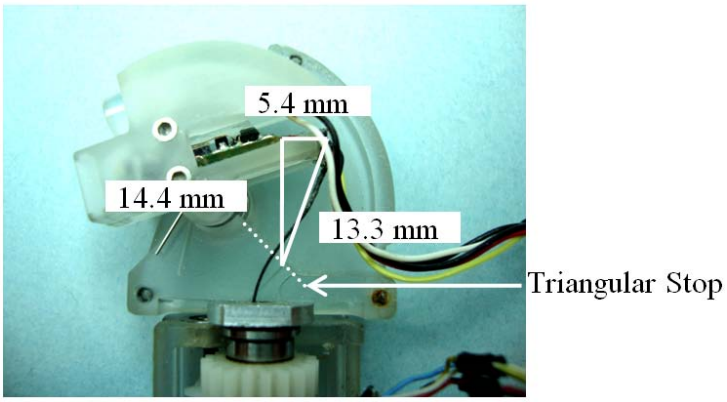

Figure 40: Cable length calculation

The required rotation speed of the spooling shaft is acquired by using its circumference and the total length of cable which is reeled in, see Eq. 9.

$$\text{Speed}_{\text{shaft}}=\frac{13.3\text{mm}}{3.5\text{s}}*\frac{1\text{rev}}{3\text{mm}*\pi}=0.4\frac{\text{rev}}{\text{s}} \quad (9)$$

Using the desired rotation speed of 0.4 rpm the pitch diameter for the worm and worm gear could be determined. The input speed to the gear head is 8000 rpm, using a gear head reduction of 64:1 and a spur gear ratio of 5.2:1 the output rotation speed of 0.4 rpm can be achieved. Due to limitations of housing size a 5.5 mm pitch diameter worm and 5 mm pitch diameter worm gear were used to obtain a gear ratio of 5:1.

$$output_{speed}=input_{speed}*gear_{head}*r_{gear\ ratio}=8000\frac{rev}{min}*\frac{1}{64}*\frac{1}{5}*\frac{1min}{60s}=0.42\ \frac{rev}{s} \qquad (10)$$

From Eq. 10 the spur gear ratio provides a camera rotation speed of 25.2 rpm which is within design specifications.

SILS Magnet Camera Housings

The SILS device consists of 4 major housing components: outer motor housing, inner motor housing, camera module, and camera mount. Each housing component was designed to minimize SILS device size, orient and fix components, offer leak protection to electronics, provide wire routing, and be easily assembled/disassembled, see Figure 42.

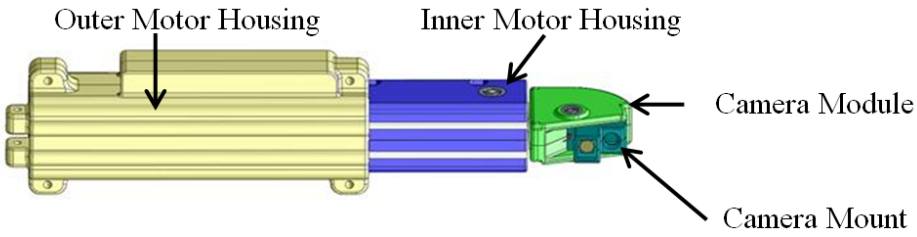

Figure 41: SILS Magnet Camera housing layout.

The camera mount was developed using the clam shell housing technique, which allows the camera and LED to be clamped tightly into form fitted depressions. The clam shell method bisects the housing along a line of symmetry, allowing for easy assembly and disassembly. A lens cover was made out of acrylic using an Epilog CNC laser Cutter, to protect the Camera from intra-abdominal fluid. The lens, camera, LED, and torsion spring are inserted into one half of the camera mount and are held in place when the other half of the mount is placed on top. The two halves of the

housing are then screwed together using 0/80 x 8.9 mm (5/16”) socket head screws. The camera and LED wires are then run out the back of the camera mount into a service loop located in the camera module, see Figure 42.

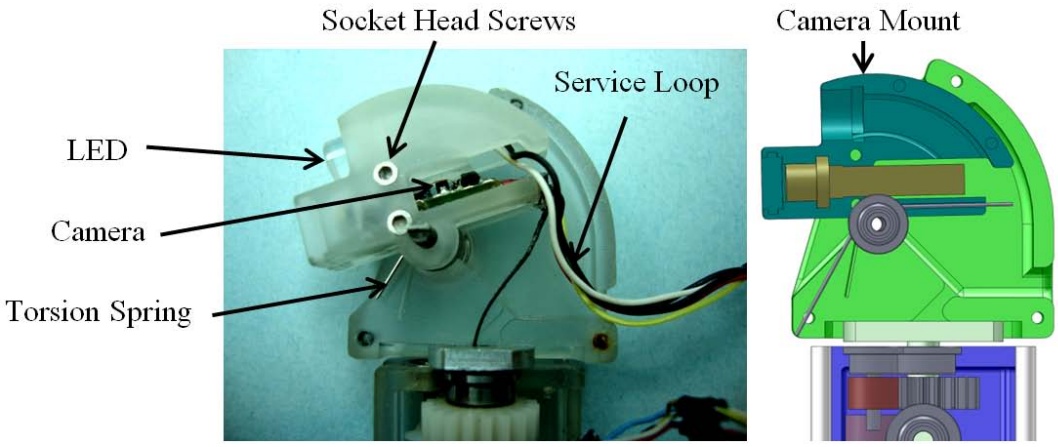

Figure 42: SILS Magnet Camera camera mount assembly.

Once the camera mount is assembled it is press fit onto the tilt rotation shaft. The camera module uses the clam shell technique to support the tilt rotation shaft and allow the camera mount 1 degree of freedom. Flanged ball bearings (1.4 mm or 0.055 inch) are glued into each half of the camera module, then the camera mount and tilt rotation shaft is press fit into one of the bearings. The camera mount is aligned in the module so the torsion spring fits into a groove. The groove serves as the other mounting point for the spring, where the camera mount contains the other end. An equilateral triangular extrusion in each half of the camera module serves as a mechanical stop for the rotation of the camera mount. Essentially the camera mount rotates at the tip of the triangle in a see-saw like motion. The top of the camera module housing is formed to the shape of the camera mount to keep intra-abdominal fluid from leaking into the gimbal. The other half of the camera module is then press fit onto the tilt shaft and each half is screwed together using three 0/80 x 8.9 mm (5/16”) socket head screws. In order to be able to dissemble the camera module the t-plate and camera module rotation shaft are glued into one half of the module, allowing for the other half to be detached once the three

screws are removed. The wires from the camera and LED are run out of an access slot located at the base of the camera module, see Figure 43.

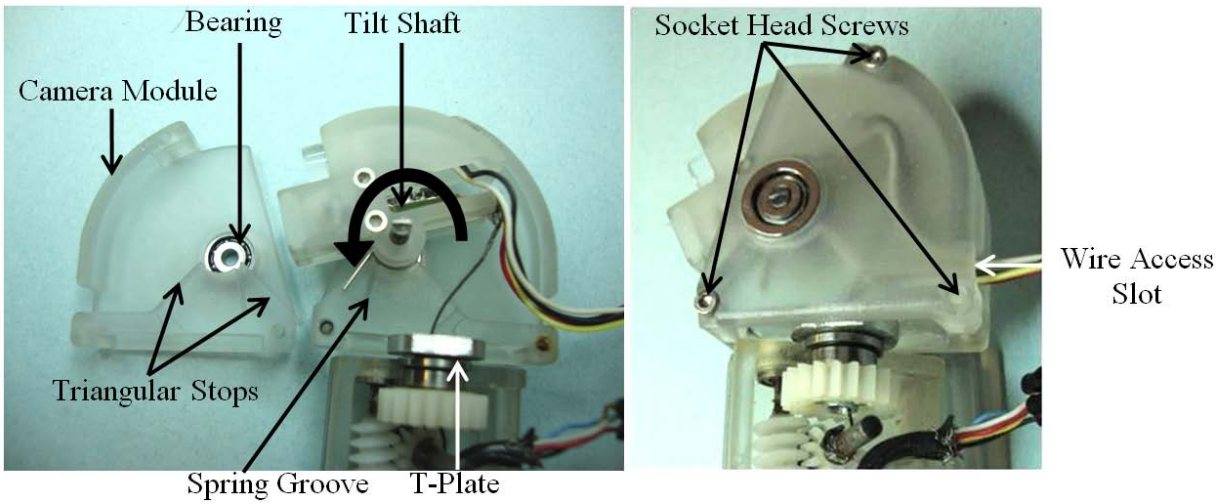

Figure 43: SILS Magnet Camera camera module assembly.

The gimbal is articulated by two motors located in the motor inner housing. Each half of the clam shell housing contains 1 micro-mo motor, one for camera module tilt, and the other for camera module pan. Each motor shaft and its coupling shaft are attached by 1.4 mm (0.055”) flanged ball bearings located at the top of the housing. Each side of the inner motor housing has one 1.9 mm (0.075”) flanged ball bearing inserted to suspend the spooling wire. The wires from the camera module are routed into an access slot located between the two halves of the inner motor housing and are combined with the motor wires at the base of the housing, see Figure 44.

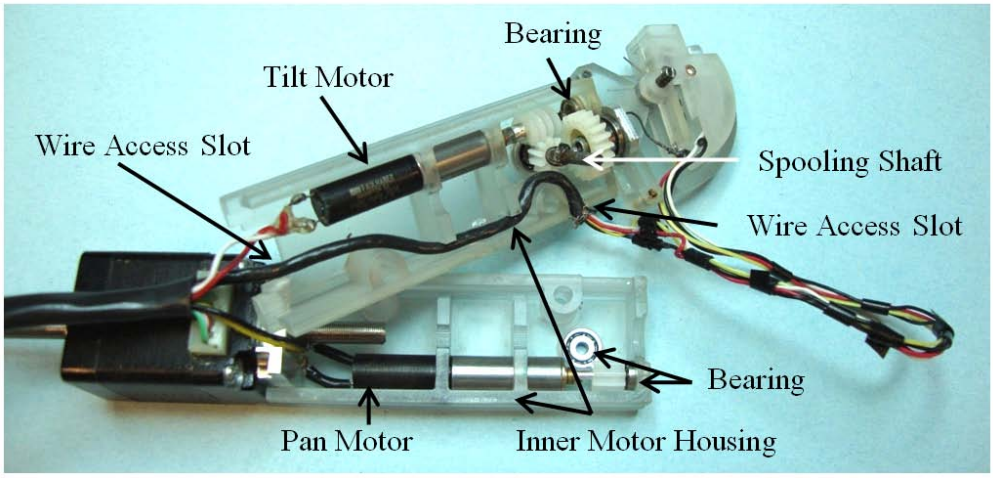

Figure 44: SILS Magnet Camera gimbal motor locations.

The camera module and inner motor housings can be translated away from the outer motor housing to provide a zoom like feature to the camera field of view. A Haydon Kerk Size 8 linear actuator with a 7.62 cm (3") screw is used to accomplish the translation. A square mounting bracket with corner notches is glued to the top face of the linear actuator. The clam shell design of the inner motor housing is used to embed housing feet in the mounting bracket notches, securely fixing the linear actuator to the inner motor housing, see Figure 45.

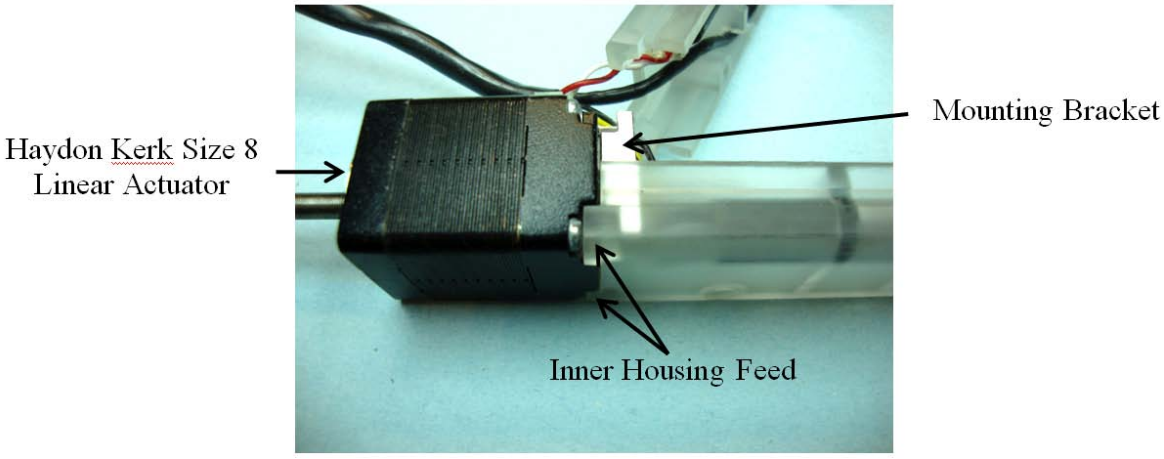

Figure 45: SILS Magnet Camera linear actuator mounting bracket.

The two housings are screwed together using two 4/40 socket head screws which are placed into a counter bore in one half of the inner motor housing and screw into two 4/40 nuts embedded in the

other half. A cylindrical channel runs down the length of the inner motor housing to allow the translation of the linear actuators screw during use. The camera, LED, and micro-mo motor leads are routed through the base of the inner motors housing and are combined with the linear actuator wires, see Figure 46.

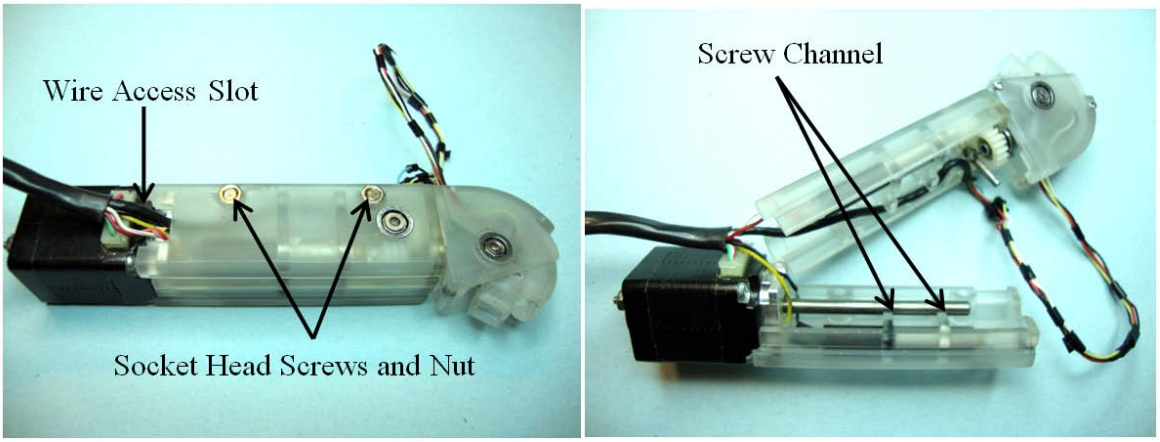

Figure 46: SILS Magnet Camera inner motor housing assembly.

The outer motor housing was developed using the clam shell housing technique, which fixes the linear actuator's screw in place, provides a channel for the inner motor housing to translate along, supports two different mounting modules to be attached, and allows for easy assembly and disassembly. The housing contains a 5.6 cm (2.2") long wire service loop, allowing the wires to move with the inner motor housing during telescoping. The top half of the housing uses a press fit 4/40 nut to mount and fix the linear actuators screw. First the linear actuator and inner motor housing are placed into top half of the outer motor housing , once the screw has been fixed to the embedded nut and the wires are run out the service loop the bottom half of the housing is placed and screwed to the top using 4/40 socket head screws, see Figure 47.

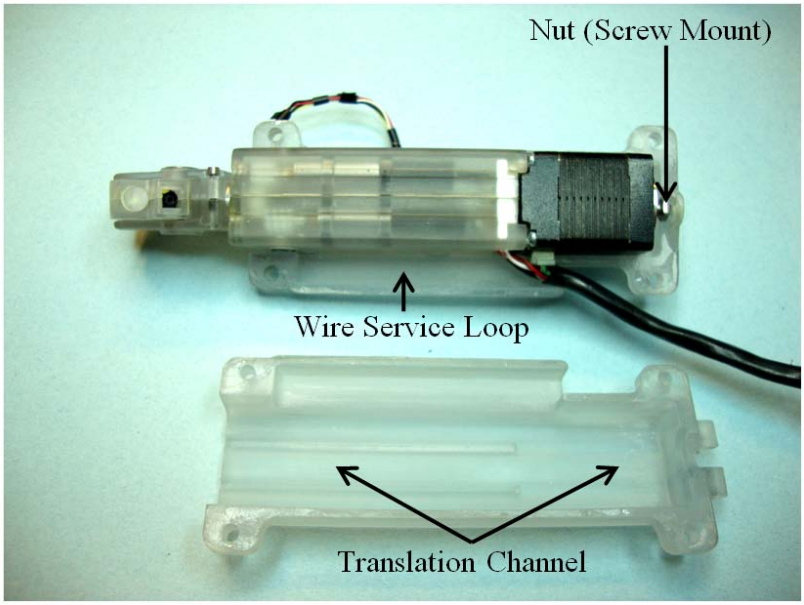

Figure 47: SILS Magnet Camera outer motor housing.

Mounting

The top half of the outer motor housing contains a mounting tab allowing for a hook and ring to be attached. The ring slips around the base of the Covidien SILS Port, allowing for the SILS Magnet Camera device to be firmly connected to the port, and suspending it inside the abdominal cavity. The hook, cantilever bar, extends the base (proximal end of the SILS Magnet Camera) 31.75 mm (1.25”) away from the port allowing for surgical tools to be used near the abdominal wall without colliding with the outer motor housing, see Figure 48.

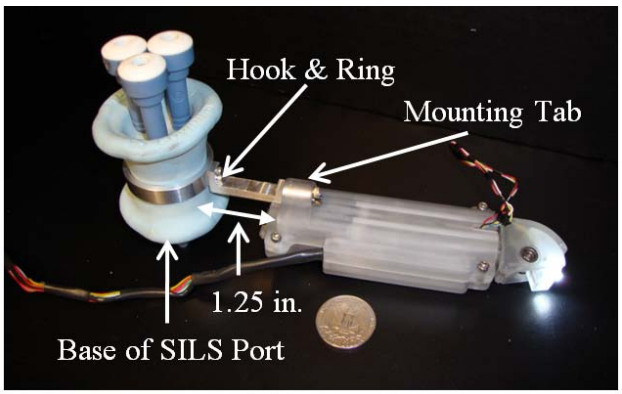

Figure 48: SILS Magnet Camera hook & ring mounting system.

Before the two outer motor housings are screwed together a magnet backing can be added to the top housing, allowing it to be used with the hook and ring or separately. The magnet backing consist of four embedded W 12.7 x L 19.1 x H 3.175 mm grade N42 Neodymium (NdFeB) rectangular magnets. The rectangular magnets are oriented to be attracted to two D 25.4 x L 25.4 mm N52 Neodymium (NdFeB) cylindrical magnets located *ex vivo* in a magnet handle. The magnet system can be used in conjunction with the hook and ring mount to rotate the entire SILS Magnet Camera around the incision point, and used alone to suspend and move the SILS Magnet Camera around the abdominal cavity, see Figure 49.

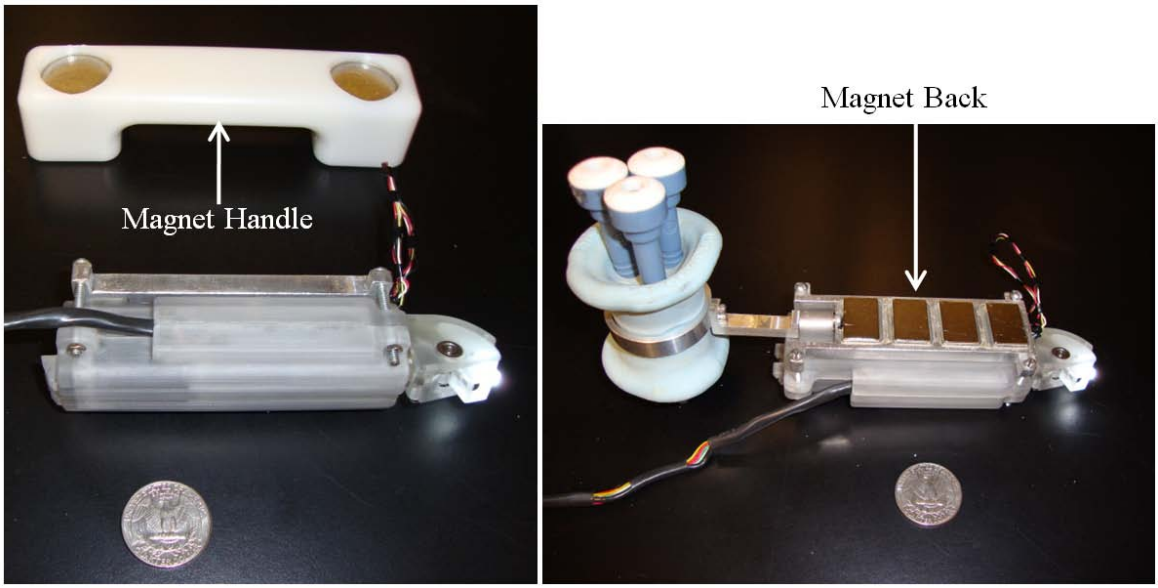

Figure 49: SILS Magnet Camera magnet mounting system.

The magnets were purchased through K&J Magnetics. The K&J magnet calculator was used to determine the size and quantity of magnets needed in *ex vivo* to suspend the 175.8 g (0.388 lb) SILS Magnet Camera with the magnet backing *in vivo* through a 25.4 mm (1”) thick abdominal wall (19.1-25.4 mm is typical wall thickness for petite patients). A D 25.4 x L 25.4 mm N52 Neodymium (NdFeB) cylindrical magnet provides a 32.9 kg (5.03 lb) pull force when attached directly to a steel plate. As the magnets distance away from the steel plate increases its pull force exponentially

decreases. Therefore the N52 magnet only offers a 235.9 g (0.52 lb) pull force when one inch away from a steel plate, which can still easily suspend the 175.8 g (0.388 lb) SILS Magnet Camera, see Figure 50.

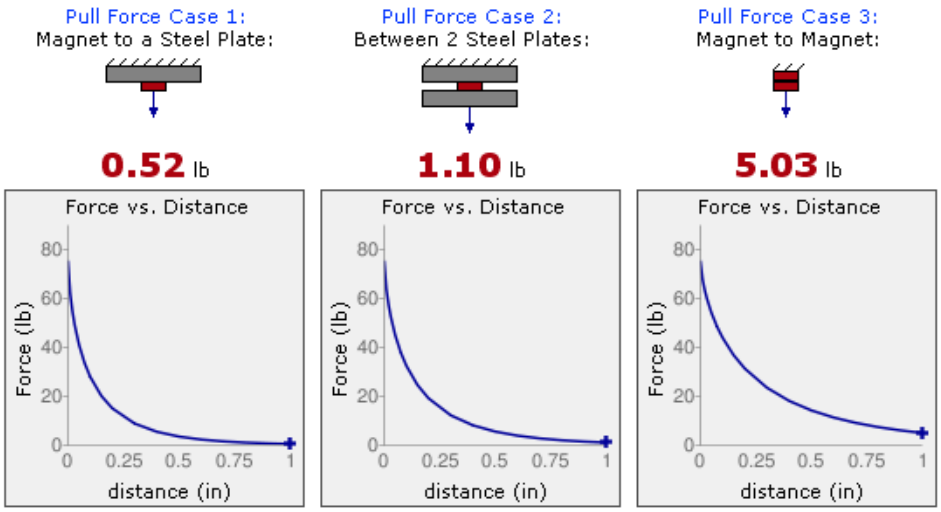

Figure 50: One inch N52 cylindrical magnet pull force [57].

To orient the SILS Magnet Camera, once it is *in vivo*, the magnet handles uses two cylindrical magnets to attract the device and keep it parallel to the handle. A reduction in the overall weight of the SILS Magnet Camera is achieved by designing a magnet backing with an aluminum frame, containing four embedded rectangular magnets, versus using a heavier steel plate. The magnet backing increases the pull force to the *ex vivo* magnet allowing for the SILS Magnet Camera to be securely suspended over a range of abdominal wall thicknesses.

Motor Control

The Series8 linear actuator used to provide translation to the camera module uses a bi-polar stepper motor to rotate the actuator nut. Stepper motors are brushless, constant power devices that have a reduction in torque as motor speed is increased. Stepper motors provide rotation of a rotor (the actuator nut) by breaking down rotation into a series of steps controlled by a clock pulse.

Each time a clock pulse is passed through a special translocation circuit, the motor rotates one step. Each step consists of turning on one of the electromagnets located around the rotor, causing it to

rotate and align with the electromagnet. For each clock pulse this process is repeated, turning on the next electromagnet and turning off the previous one, causing the rotor to continually rotate to remain aligned with the electromagnet (turned on). Stepper motors offer the benefit of being precisely controlled without a feedback loop, due to a full rotation of the actuator nut being broken down into a precise number of steps. Often times stepper motors vibrate more than other motor types due to the stepping motion of the rotor. By increasing the number of phases a motor has the rotation per step of the motor decreases offering smoother operation and a reduction in vibration [58].

Bi-Polar steppers turn on and off the electromagnets by using a single winding for each phase. In order to alternate between attraction and repulsion in the electromagnets, the current in the windings are reversed using an H-bridge. The reversal in the windings is controlled by a stepper driver chip allowing the polarities in the electromagnet to reverse for each step. A clock is used to control how quickly the driver controls the H-bridge, effectively dictating the step speed of the rotor [59].

There are three main types of stepper motors: permanent magnet, hybrid synchronous and variable reluctance. Permanent magnet steppers utilize the attraction/repulsion of the rotor (actuator nut) and the stator electromagnets, whereas variable reluctances steppers use the attraction between the rotor and the stator magnet poles. Hybrid synchronous steppers use a combination between the permanent magnet and variable reluctance steppers to increase the power of the stepper motor while keeping its package size small [60].

Choosing the stepper motor type was determined off the following requirements: the linear actuator needs to move the combined weight of the inner motor housing and camera module, 79.4 g, 76 mm (3”) in under twenty seconds and have a cross-section less than 26 mm. Haydon Kerks Series 8 Bi-Polar hybrid stepper motor was selected for its high pull/push force up to 45 N, its small package size 21 x 21 mm, and high step resolution of 1.8 degrees per step. The high step resolution provides smoother operation and less vibration in the motor. An EDE1204 bi-polar stepper driver operated by two 4 MHz clocks provides a maximum rotation speed from an L293NE H-bridge of

1.18 rpm at 1.8 degrees per step, see Appenndix A.7. Using the output speed from the H-bridge, a screw size can be determined by the linear distance it travels per step, see Eq. 11.

$$v_{linear}=s_{driver}*D_{step}*d_{step} \tag{11}$$

$$v_{linear}=1.18\frac{rev}{s}*\frac{200\ step}{1\ rev}*\frac{0.02mm}{1\ step}=4.67\ \frac{mm}{s} \tag{12}$$

Where v_{linear} is the linear speed the screw travels (mm/s), s_{driver} is the output revolutions per minute from the stepper driver & H-bridge combo (rev/s), D_{step} represents the degrees the rotor/actuator nut rotates per step (1.8^{o}), and d_{step} is the linear travel per step the screw offers (mm/step). From Eq. 12 it was determined that the EDE1204 stepper driver combined with a screw size of 0.02 mm per step (AD in Haydon Kerk catalog) will move the screw 4.67 mm/ s. Eq. 11-12 combine the speed at which the screw travels per step and the required travel length, of 76 mm (3”), to determine total travel time.

$$t_{travel}=d_{required}*\frac{1}{v_{linear}} \tag{13}$$

$$t_{travel}=76mm*\frac{1s}{4.7\ mm}=16.3\ s \tag{14}$$

Where t_{travel} is the time it takes for the screw to travel 76 mm (s), $d_{required}$ is the required screw travel length (mm), and v_{linear} is the linear speed the screw travels (mm/s). From Eq. 14 it was determined that a screw size offering 0.02 mm per step will allow the linear actuator to travel 76 mm (3”) in 16.3 seconds meeting the required deployment time of under 20 seconds. The force versus speed curves were checked to ensure the linear actuator could push or pull 79.4 g at a speed of 0.47 mm/s.

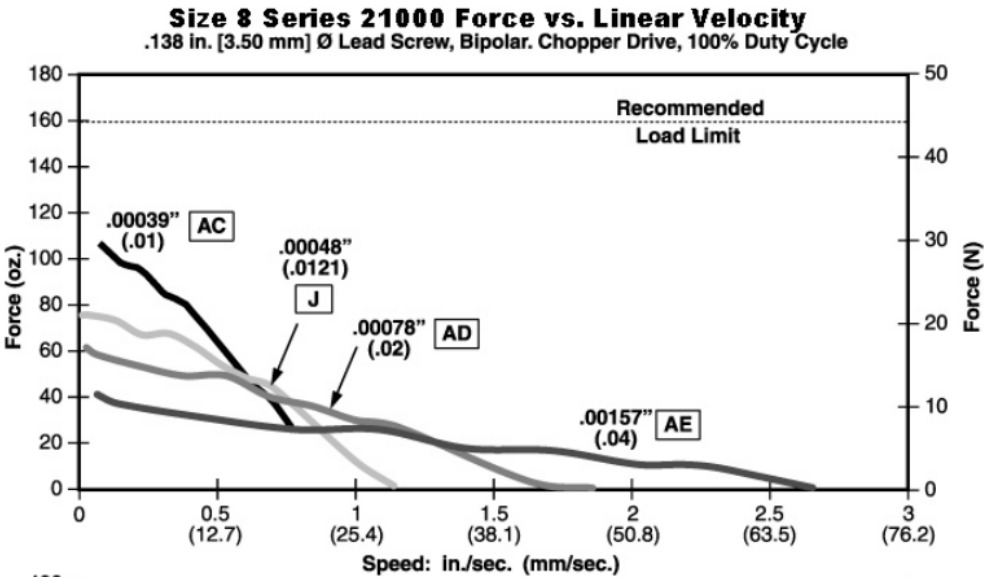

Figure 51: Size 8 Linear actuator force vs. speed curves [61].

From Figure 51 the AD screw size (0.02 mm/step) provides a push or pull force of 14 N which is much greater than required 0.78 N.

A hand held controller was built to actuate the two DC micro-mo motors, and the linear actuator. The controller housing consists of a W 76 x L 127 x H 38.1 mm grey plastic box, three 5A-28V DC double pole double throw (DPDT) momentary switches, a 15 pin connector, a bi-polar stepper driver, and two 4MHz oscillators, see Figure 52.

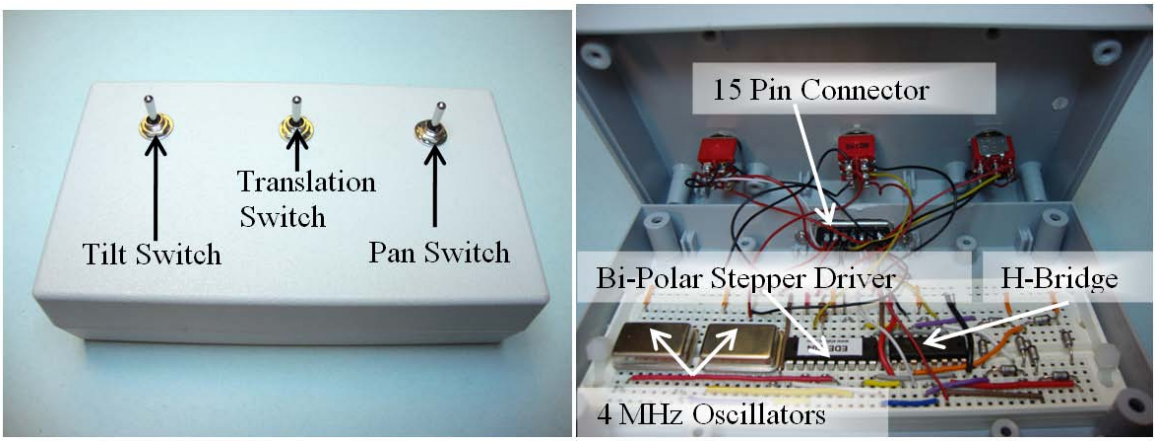

Figure 52: SILS Magnet Camera control box (left) and linear actuator circuit (right).

One side of a BK Precision power supply is used to supply the motor power inputs and outputs. The wires coming from the power supply and the SILS Magnet Camera's motors are soldered onto a male 15 pin connector which interfaces with a female connector in the controller. The power supply provides 5 volts to the bi-polar stepper driver circuit and motor, and 4.5 volts to each micro-mo motor. Inside the controller the power supply pins are hooked up to three DPDT momentary toggle switches which connect or break the motor circuits. Two 4MHz oscillators control the clock speed of an EDE1204 bi-polar stepper driver which outputs a voltage signal to a L293NE H-Bridge ultimately polarizing and depolarizing the windings on the linear actuator causing the actuator nut to rotate, see Appendix A.7 for complete electrical schematic.

The camera and LED are run off 3.5 volts and 20 mA powered by the other half of the BK Precision power supply. These components are kept separate from the controller, due to the low current consumption of the camera module versus the motors, see Figure 53.

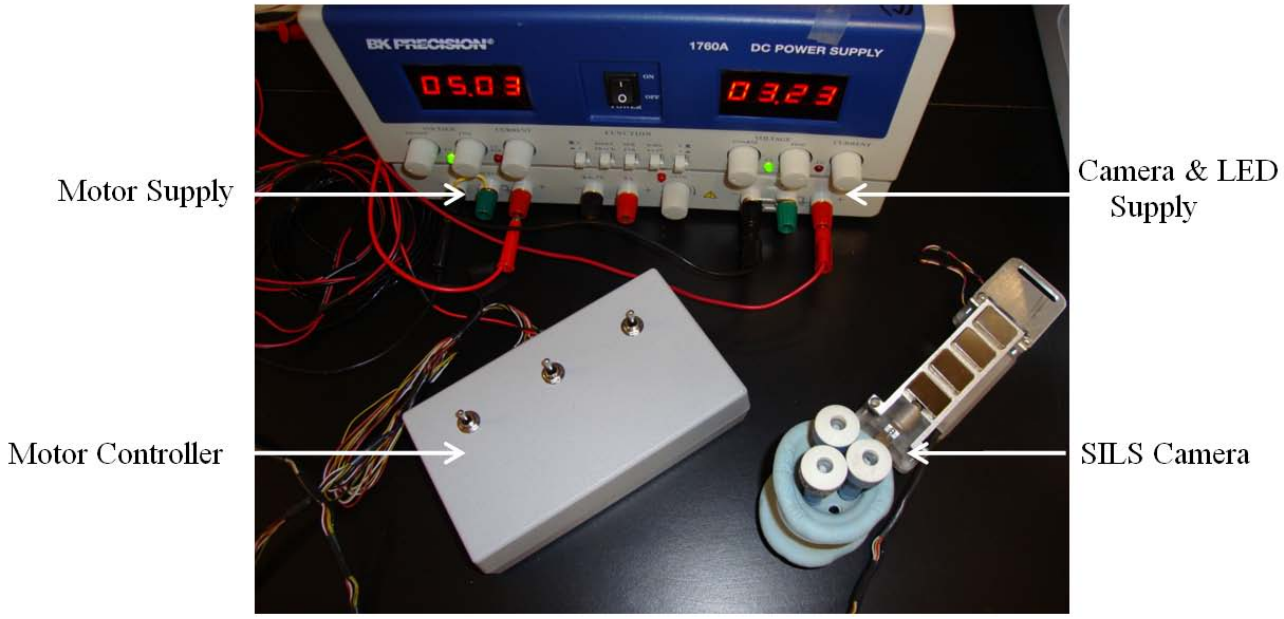

Figure 53: SILS Magnet Camera power supply hook up.

2.5 Video System Evaluation

The vision system must provide a clear and accurate visual representation of the surgical site to allow for easy tissue identification and manipulation. The two design factors for the camera system are size and overall image quality, while reducing the overall size of the camera system typically reduces the image quality. The RS-5018 analog video system used in the three prototypes was evaluated by comparing it to a leading industry laparoscope, the Stryker high definition camera and scope (model number 1188HD). Sharpness, colorfulness, brightness, lightness, hue, and chroma between the RS-5018 and Stryker camera systems have been compared in another paper [50].

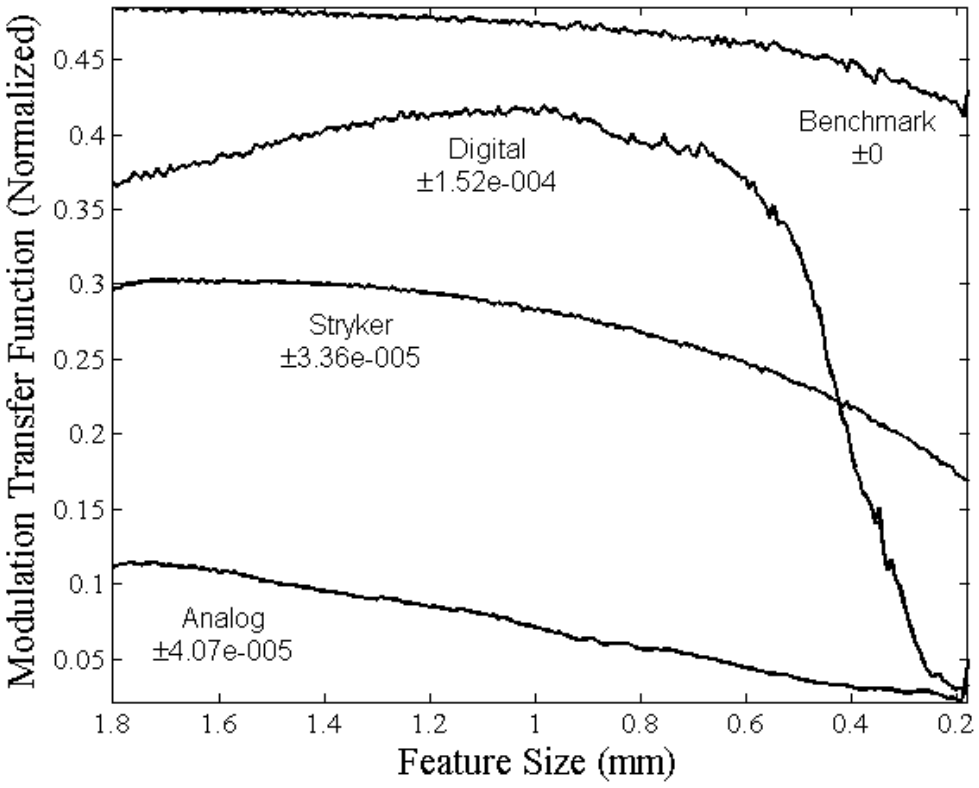

Figure 54: Contrast vs. feature size comparison of the Stryker 1188HD, Analog RS-5018, and Digital OV7690 video systems [50] .

The analog video system performs poorly in comparison to the HD Stryker laparoscope system offering one third of the contrast vs. feature size and half of the color quality, see Figure 54 [50]. Due to the reduced performance of the analog system the paper introduces a digital video system (Omni Vision OV7690) as a replacement and compares it to the HD Stryker laparoscope.

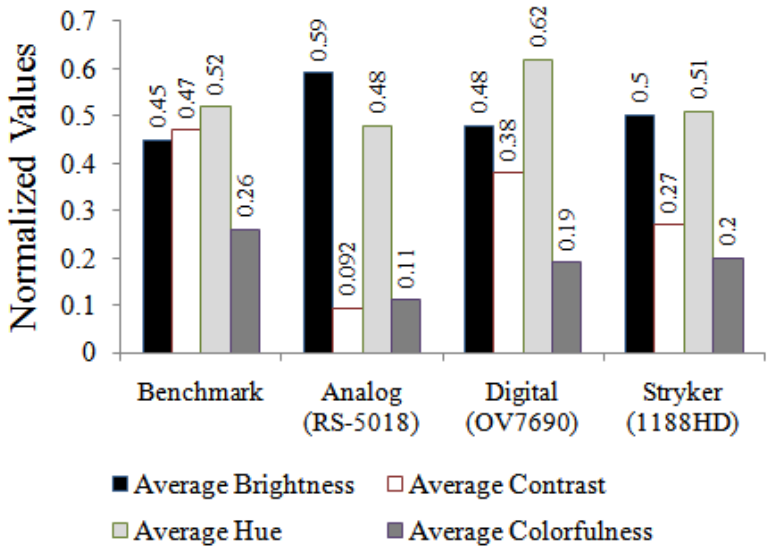

Figure 55: Color quality comparison of the Stryker 1188HD, Analog RS-5018, and Digital OV7690 video systems [50].

The Omni Vision system outperforms the HD Stryker laparoscope in average brightness and contrast down to feature sizes of 0.4 mm where the increased pixel density of the Stryker system allows for smaller feature resolution, see Figure 55 [50]. The digital system offers comparable performance to that of the Stryker system; however due the relatively large size of the Omni Vision system (L 12 x W 12 mm) it becomes impossible to integrate into the prototype design. Even though the analog system performs visually worse than the digital system it still offers relatively clear video images with decent contrast and color hue for a range of feature sizes in a small package size (W 3.25 x H 3 x L 17.5 mm), making the analog system a more viable choice for prototype development.

Chapter 3 - Participant Study

To prove functionality of each of the prototypes an evaluation study was created to compare the performance of the SILS devices with a typical SILS setup. A minimally invasive environment (MIS) environment was set up for participants to perform two tasks that closely mimic various functions that a surgeon would perform during common MIS procedures: tissue identification, and stretch/dissect respectively. The surgical tasks represent two of the most common procedures that surgeons perform. The tasks test the participant's spatial accuracy, depth recognition, ability to discern between similar tissues, and ability to make an accurate cut with both the SILS devices and a traditional laparoscope. Each task is evaluated using completion time and accuracy.

3.1 IRB Test Protocol

A human testing application was submitted to the institutional review board (IRB) at the University of Colorado Boulder by the Advanced Medical Technologies Laboratory group (AMTL) for permission to test with human volunteers. The application was reviewed and the IRB decided the tasks and testing presented no harm to the participants and ruled Exempt, allowing for testing to be performed.

3.2 Participant Criteria

Participants were required to be associated with UCB academia and not be a part of the AMTL. Participants were selected regardless of age, gender, surgical experience, and hand dominancy. A minimum goal of 30 participants was initially set to ensure that the sample size would be large enough for the calculation of probability distributions and a 95 percent confidence interval.

3.3 Surgical Simulation Cavity: MIS Environment

The evaluation of the SILS device and traditional SILS setup were performed in a MIS environment to most accurately mimic their use in a real surgery. The participant study was performed using a surgical simulation box, which represents the abdominal cavity with pre-

positioned incision/access points. Traditionally surgical simulation is used to train and help familiarize residents and surgeons with laparoscopic and SILS techniques, allowing for a safe learning environment for surgical tool operation. A Laparoscopic – Minimally Invasive Training System (MITS TRLCD03) manufactured by 3-d med was loaned to the AMTL by the Anschutz medical campus to serve as the MIS simulator for the participant study, see Appendix A.8. The Trainer features seven cannula access ports, an integrated camera, light and LCD system, see Figure 56.

Figure 56: 3-Dmed's minimally invasive training system [62].

3.4 Configurations

Port Camera

Three different device configurations were developed to test the SILS Port Camera versus a traditional SILS setup. The configurations are designed to evaluate the SILS Port Camera performance versus a traditional SILS set up, and to evaluate the on-patient LCD screen versus the industry standard off-patient monitor. Configuration A represents a typical SILS set up, with two of the channels in the SILS port being used for surgical tools, and the third channel being dedicated for

the laparoscope. Configuration B dedicates one of the SILS channels for an articulating tool, and another SILS channel for the SILS Port Camera. A straight tool is then passed through the channel in the SILS Port Camera, where the Participant relies on the SILS Port Camera LCD for visual feedback from the camera module. Configuration C is set up in the same fashion as B, however an off-patient monitor located above the simulation box is used to display the visual feedback from the camera module to represent a traditional SILS set up, see Figure 57. The surgical trainers built in defuse internal light source was used to illuminate the inside of the trainer for each configuration. The laparoscope implemented the analog RS-5018 video camera to keep the image quality the same between configurations, thus the participant study does not include the evaluation of light source origin and intensity or video quality.

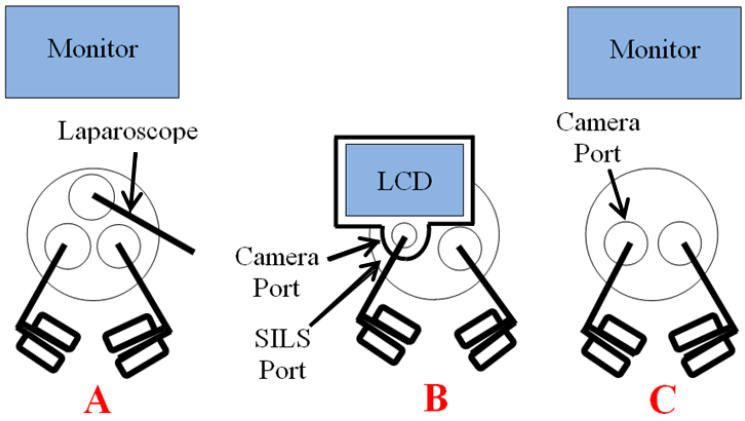

Figure 57: SILS Port Camera ball drop and cut task test configurations.

SILS Magnet Camera

The number of configurations for the SILS Magnet Camera testing was reduced from 3 to 2 with the decoupling of the SILS device from the SILS port and the removal of the on-patient LCD. The two configurations are designed to only evaluate the SILS Port Camera performance versus a traditional SILS set up. Configuration A represents a typical SILS set up, with two of the channels in the SILS port being used for surgical tools, and the third channel being dedicated for the laparoscope. Configuration B dedicates two channels in the SILS port for surgical tool insertion and leaves the

third channel unoccupied, see Figure 58. Both configurations use an analog RS-5018 video camera and a L23 LED to illuminate and view the inside of the trainer. The trainers built in light source directly interfered with the mounting of the SILS device in configuration B, thus it was removed and both configurations rely solely on the L23 LED for lighting. The participant study does not include the evaluation of light source origin and intensity or video quality.

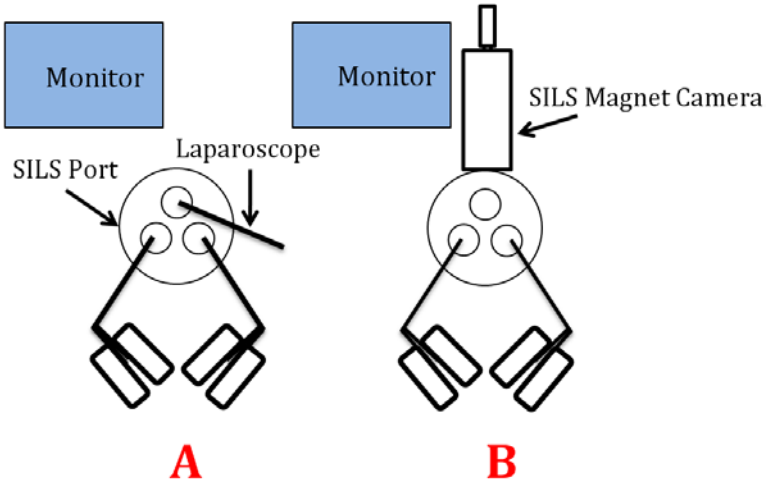

Figure 58: SILS Magnet Camera ball drop and cut task test configurations.

3.5 Trainer and LCD Placement

The trainer was located on a table top set 76.2 cm (30”) above the ground. For the Port Camera testing the LCD screen was located 15.2 cm (6”) from the top of the table, 40.6 cm (16”) to the left of the trainer, and 20.3 cm (8”) behind the front face of the trainer. During the SILS Magnet Camera testing the LCD was moved to 66 cm (26”) from the table top and 40.6 cm (16”) behind the front face of the trainer to keep the participants in line with the trainer and LCD, See Figure 59.

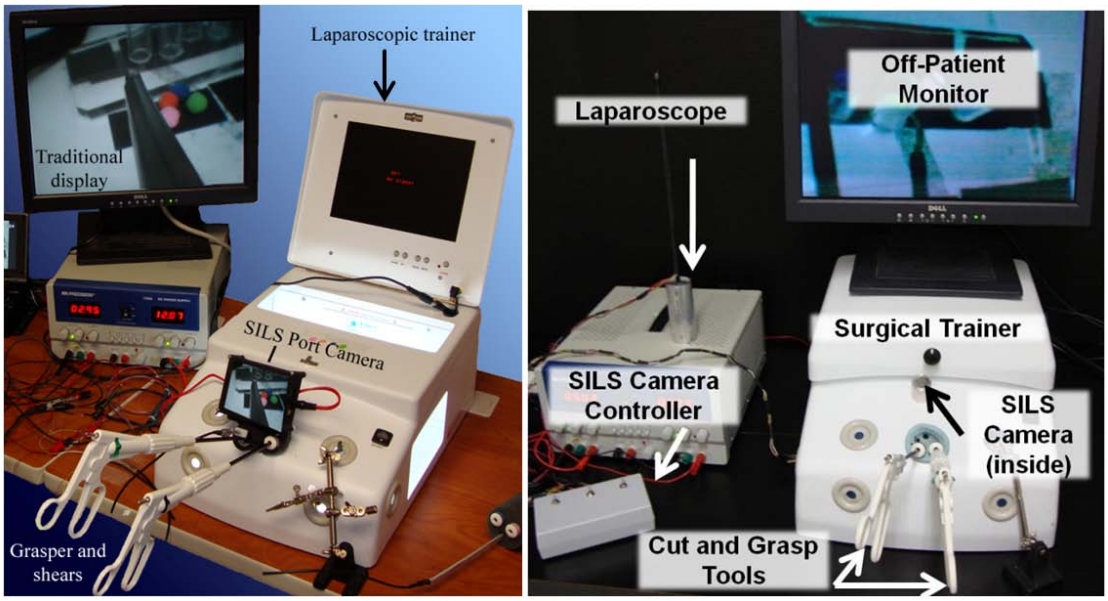

Figure 59: Monitor and LCD locations SILS Port Camera (left) and SILS Magnet Camera (right).

3.6 Task and Configuration Order

The participants perform both tasks for each configuration. The tissue identification task (ball drop task) requires the use of one grasping tool to individually pick up a series of different colored balls and drop them in their corresponding colored bin. The tissue stretch and dissect task (cut task) requires the use of both a grasping and cutting tool to grab, stretch, and cut along a marked line located on three separate rubber band strips, see Figure 60.

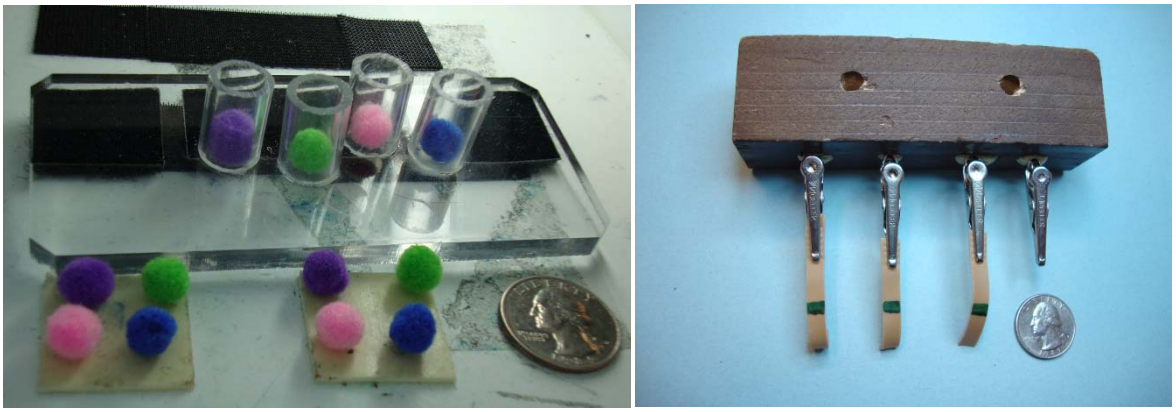

Figure 60: Ball drop task (left) and cut task (right).

Operating in a MIS environment reduces tactile perception, restricts camera field of view, requires use of specialized surgical tools, operation in a confined space, and performing unfamiliar tasks. As participants become acclimated to tool control and task interaction in the MIS environment they will perform the tasks with greater and greater ease. To account for this learning curve task and configuration order were taken into consideration.

For instance, if participant one is asked to perform the ball drop task and participant two is asked to perform the cut task, then both participants are asked to perform the ball drop task which participant will perform the best on the last ball drop task? Participant two will perform the final ball drop task more efficiently than participant one due to their initial experience with the harder cut task.

The same concept can be applied to configuration order. Since each task is performed on every configuration the participant's learning curve plays an important role. Each time a task is done the participant will improve as they become more acclimated to the MIS environment. If configuration order remains consistent between participants, the last configuration will be performed when the participant has the most experience with the task. To avoid falsely weighing the task results for each configuration, the configuration order is randomized for each participant.

Due to the increased difficulty of the cut task versus the ball drop task it was determined that participants should start with the easier of the two to give them the chance to become acclimated to the MIS environment. Each participant performs the ball task first for each configuration (randomized) followed by the cut task for each configuration (randomized).

3.7 Participant Time Allocation

After running through the study with volunteers in the AMTL it was decided that each task should take no more than 200 seconds to complete with 120 seconds of set up time between tasks. Participants were asked to commit 40 minutes of their time in order to complete each task on every configuration and answer a set of survey questions.

3.8 Ball Drop Task: Tissue Identification

The success of a MIS operation relies heavily on the surgeon's ability to accurately control tool location, and read depth perception in the field of view provided by the camera system. The ball drop task helps to familiarize the participant with laparoscopic tool control in a remote viewing environment with limited depth perception. The goal of the ball drop task is to test the participant's spatial accuracy, depth recognition, and ability to discern between similar tissues with the camera system provided.

The participants are asked to use a grasping laparoscopic tool to move 4 different colored 8.9 mm puff balls from a pick up pad and place them in their corresponding colored bins. The bins are represented by a L 76.2 x W 51 mm acrylic platform that is velcroed to the base of the trainer. There are four L 17.8 x D 12.7 mm hollow cylinders located atop the acrylic platform; each contains one of the four colored balls, see Figure 61.

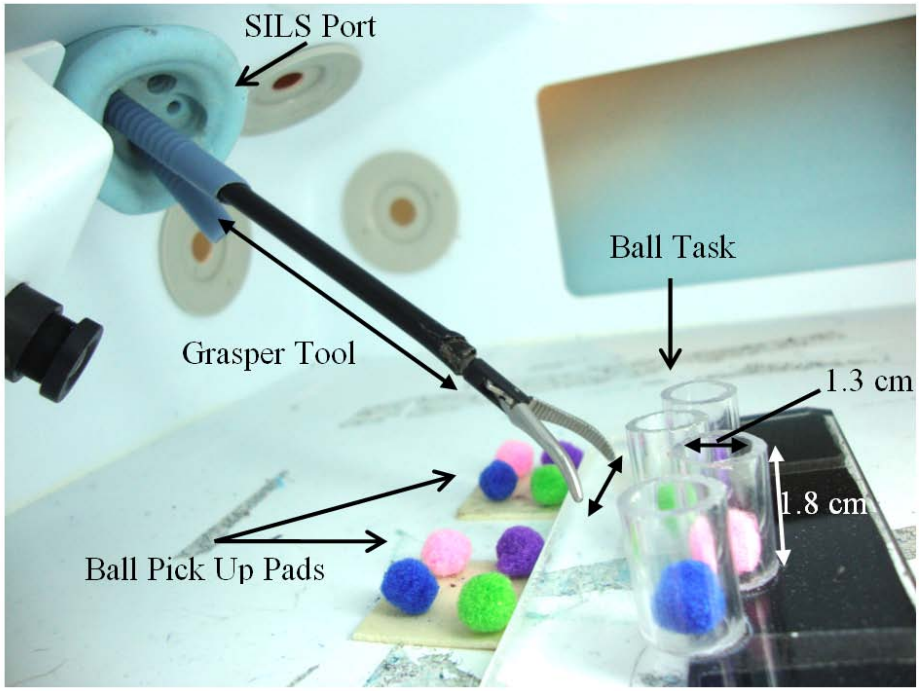

Figure 61: Ball drop task setup.

Participants needed to locate the articulating end of the tool (grasping mechanism) in the camera field of view, open and close the jaws, rotate the jaws, position the jaws at different heights and move them in longitudinal and latitudinal directions in order to complete the task.

3.9 Ball Drop Task: Evaluation and Scoring

The ball drop task is a time based test, where time starts when the participants grab the first ball and ends when they place the last ball in the corresponding bin. The participants can move each of the four balls to their corresponding bin in any order they choose but must make sure each ball is placed completely inside the bin before the time is recorded. Errors are kept track through the use of tick marks and are assessed each time a participants drops a ball that had been picked up or mismatches a ball to a different colored bin. Errors have no direct effect on task completion time but instead are a penalty associated with the configuration instead of with the timed task.

3.10 Participant Instructions

3.10.1 Background Info

The following was said to each participant during the beginning of the study:

> "Minimally invasive surgery is an alternative for some surgical procedures versus open surgery. Open surgery requires the use of one large incision in the patient's skin or body cavity to allow access to the point of interest. MIS uses trocars and cannula ports (*show them trocar and port, and insert it into the trainers access point*) to reduce incision size and makes use of a camera system (*show them the laparoscope and prototypes*) to provide a field of view of the point of interest. Once the ports are inserted carbon dioxide is pumped into the abdominal cavity to inflate it and provide a working area for the surgeon (*explain the inside of the trainer*). This laparoscopic trainer simulates an abdominal cavity and typical insertion point; it is used to train surgical residents on proper MIS techniques (*show them trainer*). Single incision laparoscopic surgery is a variation of MIS that uses one incision typically located at

the patients belly button followed by the insertion of a specialized port to allow tool and vision access to the point of interest (*show them SILS port and SILS tools*). This is one design a SILS tool can take; it is different from a straight tool in the sense it can be articulated and crossed with a similar tool to provide better triangulation and leverage at the surgical site (*articulate tool show how they are used in a SILS port*). MIS offers many benefits versus open surgery by reducing trauma to the patient with smaller incisions, provides quicker recovery times, and reduces the chance of infection. SILS is very popular, because the belly button incision is not noticeable leaving no visible scarring after the operation. However, by restricting tool and camera motion to one incision several mechanical problems arise such as tool to tool interference. To address this problem two separate camera devices have been developed to be used with two different tasks."

3.10.2 Ball Drop Task: Participant Instructions

The following was said to each participant during the beginning of the study:

"The ball drop task will require you to use a laparoscopic grasper tool to grab and move four colored balls to their corresponding colored bin (*show the participants the ball drop set up on the off-patient LCD screen*). You will act as the surgeon controlling the tool, and I will be your assistant and orient the camera systems.

This is a typical surgical grasper tool, the grasping end (*point it out*) can be articulated by placing your hand into the finger grips (*point them out*) and pulling back while pushing forward with your thumb (*demonstrate*). By leaving your index finger free you can articulate this rotation wheel to change the orientation of the grasping end in order to get a different angle on any object you want to grab (*show them*). If you look closely at the grasping end you will notice that it is curved (*point it out*) you can use this feature when you decide how to pick up the colored balls. This

is a SILS specific tool in the sense that you can move the grasping end out angling it away from the tool shaft by using your free hand to rotate the activation knob (*show them*). This can be useful if you drop or knock a ball behind the bins and you need to reach down from the top to grab it (*show them*). Go ahead and take the tool in your dominate hand (*give them the tool*) and experiment with each feature (*make sure they open and close the jaws, rotate the jaws, and extend the jaws out an angle from the shaft*). Do you have any questions about how to interact with the grasper tool?

This is where you will insert the tool, and this is the location of the camera system (*show them*). Please go ahead and insert the grasper tool into this port in the laparoscopic trainer (*point out the port*). Please do not touch any of the balls on the pad. Please locate the end of the tool within the field of view of the camera (*wait until they have found the tool*). Now articulate each feature of the tool once again (*wait until they have done so*). Now please touch the base of the trainer and each one of the bins in order to get a feel for the depth perception.

This is a time based experiment meaning you should compete the task as quickly and accurately as possible. Time starts when you grab the first ball and ends when the last ball is placed into its bin (*point out the pickup pad and the bins*). You can move the balls to their bins in any order you would like. The time will be stopped when the last ball is placed into its bin; however you must ensure that each ball is located completely inside of its bin before the time will be stopped. There are two different pickup pads please just stick to one. The second pad is there if you drop a ball and are unable to collect it with the grasper tool. In this situation please grab a ball of the same color that has been lost and then proceed using the original pad. You may pick either pad just stick to using one for the duration of the test. You will be penalized if you drop a ball once you have picked it up or place the ball in the wrong colored bin.

The balls are about the same size as their corresponding bins, it can help to grab the ball on the upper hemisphere to allow for part of the ball to be positioned into the bin before it is released. If the ball is grabbed on the bottom typically part of the tool will end up the bin and during release the ball will be popped out of the bin. Do you have any questions about the procedure? Please begin as soon as you're ready."

3.10.3 Cut Task

Most MIS require surgeons to make accurate cuts for tissue resection and dissection by coordinating the motion and articulation of two surgical tools. The goal of the cut task is to test the participant's spatial accuracy, depth recognition, ability to discern between similar tissues, and make accurate cuts with the camera system provided.

The participants are asked to use a grasping laparoscopic tool to stretch out 3 rubber bands and cut along a marked line. Each rubber band is 25.5 mm long and 6.5 mm wide with a 4 mm wide mark located 15 mm from the free end. The other end of the rubber band is clipped to a L 127 x W 25.4 x H 25.4 mm wooden block which is velcroed to the bottom of the laparoscopic trainer, see Figure 62.

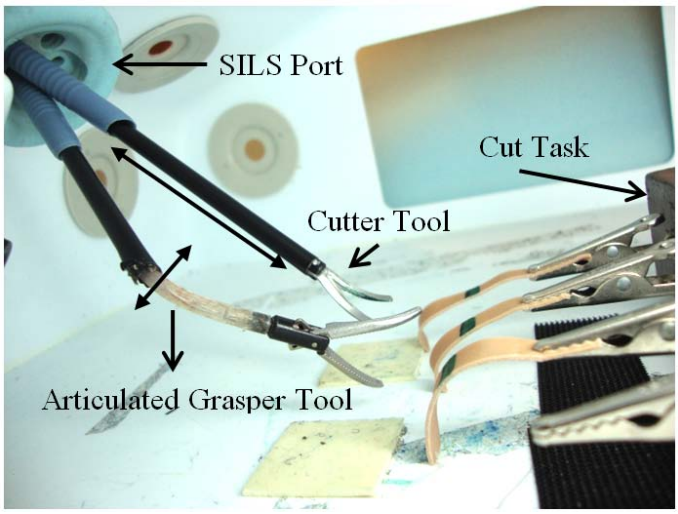

Figure 62: Cut task setup.

Participants need to locate the articulating end of the grasping tool (grasping mechanism) in the camera field of view, open and close the jaws, rotate the jaws, position the jaws at different heights

and move them in longitudinal/latitudinal directions in order to grab and stretch the free end of the clipped rubber band. Once the rubber band has been stretched the participants need to locate the articulating end of the cutter tool in the camera field of view, open and close the jaws, rotate the jaws, position the jaws at different heights and move them to the marked line in order to dissect the free end.

3.11 Cut Task: Evaluation and Scoring

The cut task is a time based test, where time starts when the participants grab the first rubber band and ends when the last rubber band is cut. The participants can cut the rubber bands in any order they choose and can discard the dissected ends anywhere on the base of the trainer. Errors are kept track through the use of tick marks and are assed each time a participants cuts 1 mm outside of the marked line. Errors have no direct effect on task completion time but instead are a penalty associated with the configuration instead of with the timed task.

3.11.1 Cut Task: Participant Instructions

The following was said to each participant during the beginning of the study:

> "The cut task will require you to use a laparoscopic grasper tool to grab and stretch a rubber band followed by the use of a laparoscopic cutting tool to cut along the marked line (*show the participants the wooden block and the rubber bands*). This is a typical surgical cutter tool, the cutting end (*point it out*) can be articulated by placing your hand into the finger grips (*point them out*) and pulling back while pushing forward with your thumb (*demonstrate*). By leaving your index finger free you can articulate this rotation wheel to change the orientation of the grasping end in order to get a different angle on any object you want to cut(*show them*). Go ahead and take the tool in your dominate hand (*give them the tool*) and experiment with each feature (*make sure they open and close the jaws, rotate the jaws, and extend the jaws*

out an angle from the shaft). Do you have any questions about how to interact with the grasper tool?

This is a traditional straight laparoscopic tool in the sense that you cannot articulate the end as was done with the grasper (*point out the difference*). I recommend using the cutter in your dominate hand and the grasper in your off hand; however you may choose which hand feels best for each tool. Please insert a tool into these two sub channels in the SILS port *(remove the SILS port from the trainer box and hold it while they insert the tools*). Once the tools have been inserted you can deploy the grasper tool and cross its tool path with the cutter tool in a scissor like motion (*show them*); what this does is add distance between your hands allowing you greater tool motion and dexterity. By using the articulation knob on the grasper tool (*point it out*), you can orient the grasping end to grab the rubber band from the side ensuring a good attack angle and that the end of the tool does not obstruct the camera view. Crossing the tools changes their control and how you perceive them on the LCD. Your grasper hand will control the tool on the opposite of the monitor (*show them*), so when you move your tool left it will move right on the screen and vice versa. Go ahead and grab the end of one of the rubber bands (*place the wooden block on the table*) and stretch it orthogonal to its resting state to expose the line in a parallel path to you cutting tool motion (*wait for them to grab the end and expose the line for cutting*). Please do not cut the rubber band but move the blades in line to get a feel for the motion. I recommend keeping the cutting tool on top of the grasper tool to minimize tool interference. For instance if you stretch the rubber band downwards and your cutting tool is below the grasper tool you will be unable to reach the line with the cutting end (*show them*). It is important that you orient the cutting end with the rotation knob so it is cutting perpendicular to the rubber band to avoid any mis-

cuts. If you don't like the grasper tool fully deployed, you can change deployment as you see fit, if you would like to switch tool hands do so now. Do you feel comfortable with the operation and deployment of the tools? Please remove the tools (*re-insert the SILS port into the laparoscopic trainer*). Please insert your tools into the SILS port and locate them on the display. Please do not touch the rubber bands yet, but touch the bottom of the trainer, deploy your tools, and get them oriented to the position you feel most comfortable with. Go ahead and mimic the grasping, stretching, and cutting process in the air. When you feel comfortable with the tools and we will begin the task.

This is a time based experiment meaning you should compete the task as quickly and accurately as possible. Time starts when you grab the first rubber band and ends when the last rubber band is cut. You can cut the rubber bands in any order you would like. Please just discard the dissected rubber band pieces anywhere on the bottom of the laparoscopic trainer. You will be penalized if you cut 1 mm outside of the marked line. Do you have any questions about the procedure? Please begin as soon as you're ready."

3.12 Task Set Up: Test Dimensions

The laparoscopic trainer box offers a 44.5 x 31.8 x 21.6 cm internal operation space. The ball drop and cut tasks are located near the middle of the trainer, 10.2-20.3 cm away from the umbilicus insertion point. Most port incisions are located within 15 cm of the surgical site to ensure the surgical tools have extra range of motion to accurately perform the surgical tasks. The built in laparoscopic trainer camera was suspended from the middle right incision point and connected to a Sony digital high definition videocassette recorder (Gv-HD700) recorder to save the task results for each participant, see Appendix A.9. A top down diagram of the trainer and the task locations can be seen in Figure 63.

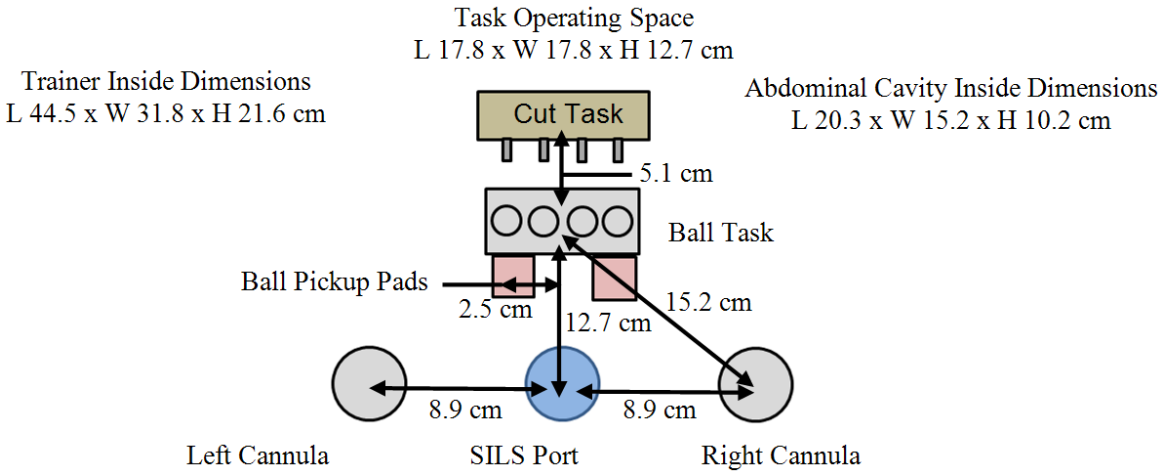

Figure 63: Test setup inner dimensions.

3.13 Penalty and Task Difficulty Reasoning

The goal of the tasks is to help distinguish each camera system's ability to provide the best view possible for the participant during the test. A previous study was done by another AMTL student to determine bin, mark line, and cut tolerance size. The goal of the study was to determine how difficult each task should be to provide the best data on the device viewing systems. He found that if the bin size was much larger than the ball size it was relatively easy to drop the balls in, thus reducing the visual benefits that each camera systems could provide while completing the task. To make the camera system's differences more pronounced the bin size was reduced to the ball size, requiring the participants to accurately deposit the balls in the bin. A cut tolerance of 1 mm was added to the 4 mm wide marks on the rubber band to make the cut task easier. The reduction of cut task difficulty reduces the task time bringing the focus more to the field of view each camera system provides of the cut mark rather than the participant's ability to line up for a perfectly straight cut.

Penalties for each task are applied directly to the current configuration instead of the task completion time. It was hypothesized that participants who rush through each task reduce their task completion time at the expense of making more errors, and participants who take their time completing each task increase their overall task completion time but make fewer errors. To account

for the reduced completion time a task penalty time is added to total task completion time for each error. This time penalty is based on the difference between the task completion times of a participant who made errors versus one who made no errors. However using a fixed time penalty does not affect the results linearly, being more severe for low completion times versus high completion times. For example, if a participant completes the ball drop task in 30 seconds with no mistakes for configuration A, and completes the ball drop task in 35 seconds with one mistake for configuration B there is a 14 percent difference in completion time. If a time penalty of 15 seconds is applied to configuration A then there is a 40 percent difference in completion time. If the participant took 150 seconds for A and 160 seconds for B and the same 15 second penalty is applied the percent difference changes from 14 to 6%. Developing a time penalty that is appropriately weighted for each participant in comparison to their own task completion times and the completion times of other participants is to difficult and would skew task completion data. To avoid distorting the task time data the penalties are instead applied to the configuration itself, allowing for task times to be compared and configuration errors to be compared.

3.14 Questionnaire

Further evaluation of each camera system was provided by the participants at the end of the study. Each participant was asked a series of questions about the functionality of each camera system, the test set up, and for their personal input. Each question was verbally read by the study proctor and the participants were asked to reply on a scale of one to five: 1 is strongly disagree, 2 is disagree, 3 is neutral, 4 is agree, and 5 is strongly agree.

A questionnaire was developed specifically for each prototype, focusing heavily on the prototype features, see Figures 64-65.

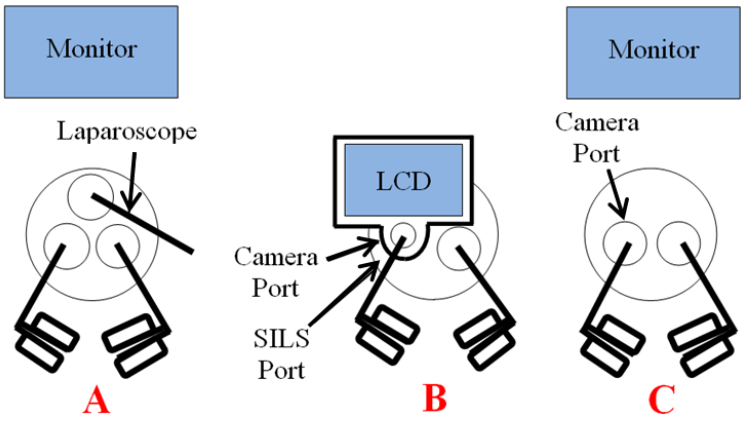

1	I was well briefed about the Ball Task.
2	I was well briefed about the Cut Task.
3	The Cut Task was difficult with configuration A
4	The Cut Task was efficient with configuration A
5	The Ball Task was difficult with configuration A
6	The Ball Task was efficient with configuration A
7	The Cut Task was difficult with configuration B
8	The Cut Task was efficient with configuration B
9	The Ball task was efficent with configuration B
10	The Ball Task was difficult with configuration B
11	The Cut Task was difficult with configuration C
12	The Cut Task was efficient with configuration C
13	The Ball task was efficent with configuration C
14	The Ball Task was difficult with configuration C
15	I was satisfied with the image on the monitor in configuration A
16	I was satisfied with the image on the LCD in configuration B.
17	I was satisfied with the image on the monitor in configuration C
18	I was satisfied with the depth perception of configuration A
19	I was satisfied with the depth perception of configuration B
20	I was satisfied with the depth perception of configuration C
21	I was satisfied with monitor's placement in configuration A.
22	I was satisfied with monitor's placement in configuration C.
23	The monitor screen was of adequate size to perform the Tasks.
24	I was satisfied with the LCD placement on the simulator in configuration B.
25	The LCD screen was of adequate size to perform the tasks in configuration B.
26	Configuration A had sufficient functionality.
27	Configuration B had sufficient functionality.
28	Configuration C had sufficient functionality.
29	I can perform the Cut Task better with…
30	I can perform the Ball Task better with…

Figure 64: SILS Port Camera participant questionnaire.

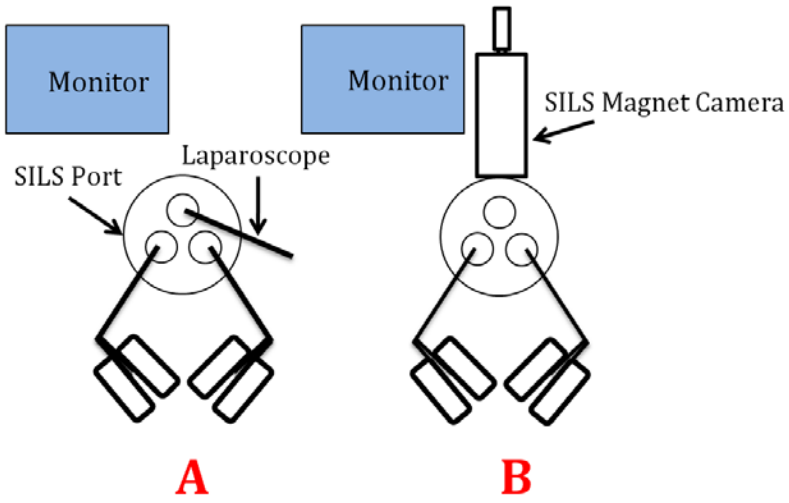

1	Were you well briefed about the Ball Task.
2	Were you well briefed about the Cut Task.
3	Was the Cut Task was difficult with configuration A
4	Was the Cut Task was efficient with configuration A
5	Was the Ball Task was difficult with configuration A
6	Was the Ball Task was efficient with configuration A
7	Was the Cut Task was difficult with configuration B
8	Was the Cut Task was efficient with configuration B
9	Was the Ball task was efficent with configuration B
10	Was the Ball Task was difficult with configuration B
11	Were you satisfied with the image on the monitor in configuration A
12	Were you satisfied with the image on the monitor in configuration B
13	Were you satisfied with the depth perception of configuration A
13	Were you satisfied with the depth perception of configuration B
14	Were you satisfied with monitor's placement
15	Were you satisfied with the movment speed of the camera in configuration B
16	Were you satisfied with the SILS device placment in configuration B
17	Was the monitor screen was of adequate size to perform the Tasks.
18	Did configuration A had sufficient functionality.
19	Did configuration B had sufficient functionality.
20	You can perform the Cut Task better with…
21	You can perform the Ball Task better with…

Figure 65: SILS Magnet Camera participant questionnaire.

3.15 Participant Results

Participant results for both the Port Camera and SILS Magnet Camera testing were analyzed under the null-hypothesis that the task completion time is not biased to a specific configuration. Under this hypothesis a t-test was performed between configuration task times to determine if the null hypothesis is preserved. Each participant performs the surgical tasks for each configuration which is known as repeated measures, allowing for a paired t-test to be performed. It was assumed that variance of each configurations completion times are un-equal to avoid false positive (Type 1 error), and false negative (Type 2 error) errors.

The null hypothesis was not weighted in favor of one configuration over another to avoid the rejection of a true null hypothesis. This method is known as a two-tailed test which is used to reject the null hypothesis when the value of the statistical test is sufficiently small or large, versus weighting the null hypothesis in favor of one configuration out performing another which is known as a single-tailed test. Evaluating the results for a one-tailed test for a small sample size is likely to falsely support the null hypothesis due to noise in the data [63]. To avoid rejecting the true null hypothesis a two-tailed, unequal variance, two sample t-test was used to check for significance between configuration results, see Eq. 15.

$$t = \frac{\bar{\bar{X}}_T - \bar{\bar{X}}_C}{\sqrt{\frac{var_T}{n_T} + \frac{var_C}{n_C}}} \tag{15}$$

Where t is the p-value between the two groups, $\bar{\bar{X}}_T$ and $\bar{\bar{X}}_C$ are the mean values for each group (T and C), var_T and var_C represent the variance for each group, and n_T and n_C are the number of people in each group. The two-tailed, unequal variance, two sample t-test for each group comparison in the following data analysis was calculated using Microsoft Excel. The p-value is the probability that the null hypothesis will be rejected if it is true. In this case if the p-value is less than 0.05 or 5% then the null hypothesis will be rejected.

Each t-test was checked using a power analysis performed using the post-hoc method to determine if the sample size used in each device testing was large enough to reject the null hypothesis when the null hypothesis is false. The effect size is the strength of the relationship between each group and was calculated for each t-test value. Using the effect size and the mean values for each group the number of samples for a power of 0.95 or 95 % was calculated for each group comparison. In other words there is a 95% chance that the comparison will reject the null hypothesis when the null hypothesis is false (producing a Type 2 error) at the calculated number of samples.

3.15.1 Port Camera

Nineteen participants with no prior surgical experience completed the ball drop task, cut task, and questionnaire for the Port Camera performance versus a traditional Laparoscopic setup. Each participant performed each surgical task (ball drop and cut task) using configurations A, B, and C. Each participant's task completion times per configuration were normalized and then averaged to find the mean completion time for each configuration at a 90% confidence level, see Figure 66.

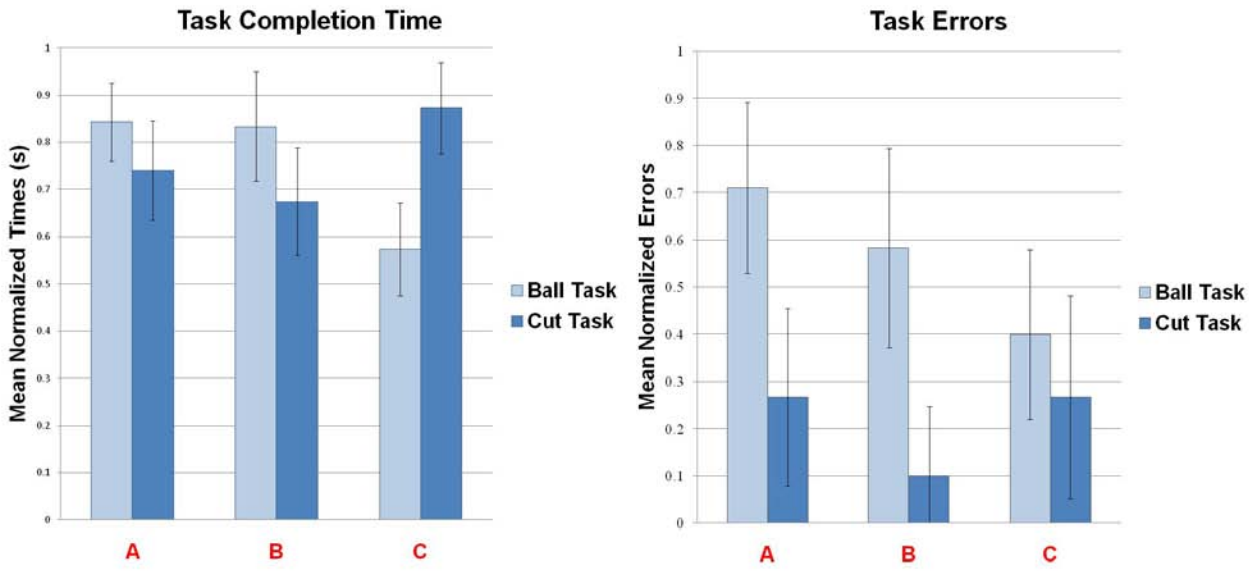

Figure 66: Mean normalized ball and cut task times (left) and errors (right).

A two-tailed, unequal variance, two sample t-test was performed between each configuration to test for significance between each configuration's task completion times. *Table 1* lists each t-test's P-values with a 90% confidence interval applied. P-values less than 0.1 reject the null hypothesis, making the results statistically significant (values in grey).

	Ball Task Times	Cut Task Times	Ball Task Errors	Cut Task Errors
A to B	0.911	0.415	0.376	0.521
B to C	0.002	0.014	0.202	0.175
A to C	0.001	0.077	0.022	0.475

Table 1: P-values indicating significant interactions between test parameters and configurations.

From Figure 66 it can be seen that SILS Port Camera with a standard external monitor (configuration C) yields faster ball task completion times than the traditional SILS setup (configurations A) and the SILS Port camera setup (configuration B) with fewer ball task errors being made. However, configuration C yields longer cut task completion times and more task errors than either configuration A and B. It was deemed from the t-test that all other interactions between configurations are statistically insignificant. Configurations A and B yield similar surgical task completion times, with both configurations performing equally for tissue identification, stretch, and dissect. Configuration C yields increased performance for tissue identification while reducing the performance of the stretch and dissect task.

A post hoc power analysis was performed to determine the power for each statistical configuration comparison. A 95% power requirement was then used to determine the number of samples needed for each configuration comparison to yield significant results.

		Ball Task Times	Cut Task Times	Ball Task Errors	Cut Task Errors
A to B	**Power**	0.031	0.105	0.116	0.08
	Sample Size	19025	359	307	580
B to C	**Power**	0.819	0.605	0.119	0.219
	Sample Size	22	37	145	125
A to C	**Power**	0.888	0.345	0.534	0.09
	Sample Size	18	75	44	475

Table 2 Power and sample size interactions between test parameters and configurations.

As the power of the comparison approaches one, the number of samples needed decreases. Table 2 shows the required number of samples for each configuration comparison to be 95% confident that significant results were obtained. The sample sizes in grey are equal to or less than the sample size of 19 used for the testing. From Table 2 it can be seen that only the comparison between the SILS Port Camera with a standard external monitor (configuration C) versus the traditional SILS setup (configurations A) produces significant results within the number of samples used for the testing. The sample size values in green exceed the sample size of 19 used; however it is feasible that up to 75 participants could complete the study. The other sample sizes listed in Table 2 are well above 75 and reach limits of 20,000 which are well outside of the realistic sample sizes that could be obtained for this study.

3.15.2 SILS Magnet Camera

Due to the lack of significant data obtained during the Port Camera testing, the minimum participant sample size was increased from 19 to 30 for the SILS Magnet Camera testing in order to improve the statistical power of the study. The 30 participants, consisting of 12 females and 18 males, completed the ball drop and cut task for configuration A and B. Each participant's task completion times per configuration were normalized and then averaged to find the mean completion time for each configuration at a 95% confidence level, see Figure 67.

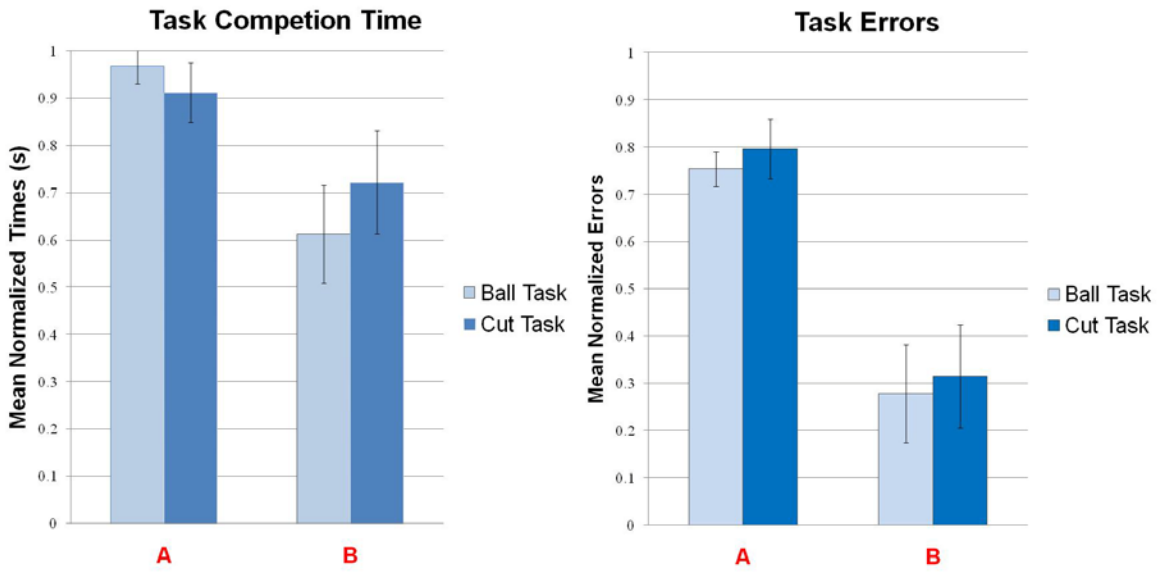

Figure 67: Mean normalized ball and cut task times (left) and errors (right).

A two-tailed, unequal variance, two sample t-test was performed between each configuration to test for significance between each configuration's task completion times. Table 3 lists each t-test's P-values with a 95% confidence interval applied. P-values less than 0.05 reject the null hypothesis, making the results statistically significant (values in grey).

	Ball Task Times	Cut Task Times	Ball Task Errors	Cut Task Errors
A to B	3.78 E -7	0.00496	9.81 E -5	4.73 E -5

Table 3: P-values indicating significant interactions between test parameters and configurations.

From *Figure 67: Mean normalized ball and cut task times (left) and errors (right)* it can be seen that SILS Magnet Camera (configuration B) yields faster ball drop and cut task completion times than the traditional SILS setup (configurations A) with fewer ball drop and cut task errors being made. It was deemed from the t-test that configuration B's reduced task completion times are significant when compared to the traditional laparoscopic setup's increased task completion times. Configuration B offers enhanced performance over Configuration A for the tissue identification, stretch, and dissect surgical tasks.

A post hoc power analysis was performed to determine the power for each statistical configuration comparison. A 95% power requirement was then used to determine the number of samples needed for each configuration comparison to yield significant results.

		Ball Task Times	Cut Task Times	Ball Task Errors	Cut Task Errors
A to B	**Power**	0.995	0.565	0.857	0.888
	Sample Size	8	38	20	18

Table 4: Power and sample size interactions between test parameters and configurations.

As the power of the comparison approaches one, the number of samples needed decreases. Table 4 shows the required number of samples for each configuration comparison to be 95% confident that significant results were obtained. The sample sizes in grey are equal to or less than the sample size of 30 used for the testing. From Table 4 it can be seen that all comparisons between the SILS Magnet Camera (configuration B) versus the traditional SILS setup (configurations A) produce significant results within the number of samples used for the testing. The sample size value in green exceeded the sample size of 13 used; however it is feasible that 8 more participants could complete the study to ensure that significant results were obtained for the cut task times.

3.16 Questionnaire Results

3.16.1 Port Camera

Each of the participants completed a survey to assess the degree of satisfaction with the SILS port camera and traditional SILS laparoscopic systems. Survey results are listed below with 95% confidence intervals.

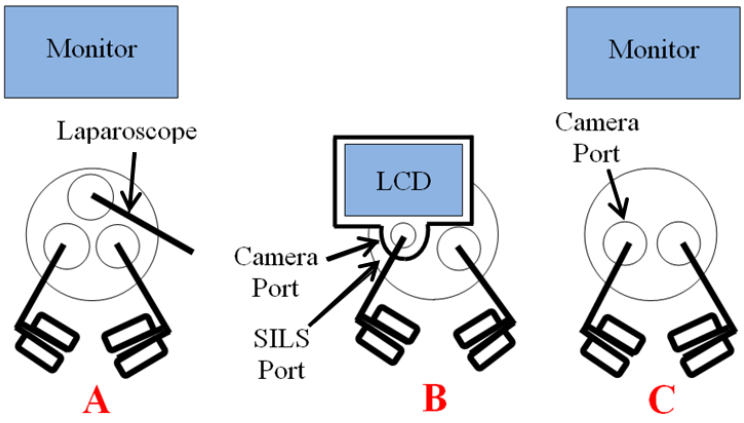

1	I was well briefed about the Ball Task.	5 - Strongly Agree
2	I was well briefed about the Cut Task.	5 - Strongly Agree
3	The Cut Task was difficult with configuration A	3 - Neutral
4	The Cut Task was efficient with configuration A	3 - Neutral
5	The Ball Task was difficult with configuration A	3 - Neutral
6	The Ball Task was efficient with configuration A	3 - Neutral
7	The Cut Task was difficult with configuration B	2 - Disagree
8	The Cut Task was efficient with configuration B	4 - Agree
9	The Ball task was efficent with configuration B	3 -Neutral
10	The Ball Task was difficult with configuration B	2 - Disagree
11	The Cut Task was difficult with configuration C	2 - Disagree
12	The Cut Task was efficient with configuration C	4 - Agree
13	The Ball task was efficent with configuration C	4 - Agree
14	The Ball Task was difficult with configuration C	2 - Disagree
15	I was satisfied with the image on the monitor in configuration A	3 -Neutral
16	I was satisfied with the image on the LCD in configuration B.	3 -Neutral
17	I was satisfied with the image on the monitor in configuration C	4 - Agree
18	I was satisfied with the depth perception of configuration A	3 -Neutral
19	I was satisfied with the depth perception of configuration B	3 -Neutral
20	I was satisfied with the depth perception of configuration C	4 - Agree
21	I was satisfied with monitor's placement in configuration A.	4 - Agree
22	I was satisfied with monitor's placement in configuration C.	4 - Agree
23	The monitor screen was of adequate size to perform the	5 - Strongly Agree
24	I was satisfied with the LCD placement on the simulator in configuration B.	3 -Neutral
25	The LCD screen was of adequate size to perform the	3 -Neutral
26	Configuration A had sufficient functionality.	4 - Agree
27	Configuration B had sufficient functionality.	3 -Neutral
28	Configuration C had sufficient functionality.	5 - Strongly Agree
29	I can perform the Cut Task better with…	2 - Configuration C
30	I can perform the Ball Task better with…	2 - Configuration C

Figure 68: SILS Port Camera participant questionnaire average answer.

From Figure 68 it can be seen that the participants believed the task difficulty was easier with the SILS Port Camera with a standard external monitor (configuration C) and the SILS Port camera setup (configuration B) versus the traditional SILS setup (configurations A). The participants indicated an overall neutral response when asked about the image quality, and ease of use of the SILS Port Camera on-patient LCD (configuration B); however they found the SIS Port Camera used with a standard external monitor (configuration A) provided sufficient image quality and monitor size. Overall the participants agreed the traditional SILS setup provided sufficient functionality where as they felt neutral about the functionality of the SILS Port Camera. Ultimately the SILS Port Camera with a standard external monitor was picked as the configuration that provided the most functionality and would be selected by the participants if the tasks were performed again.

3.16.2 SILS Magnet Camera

Each of the participants completed a survey to assess the degree of satisfaction with the SILS Magnet Camera and traditional SILS laparoscopic systems. Survey results are listed below with 95% confidence intervals.

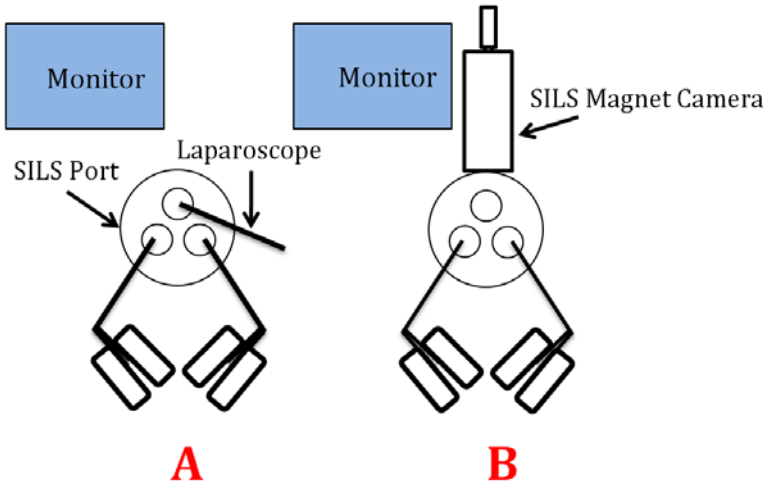

1	Were you well briefed about the Ball Task.	5 - Strongly Agree
2	Were you well briefed about the Cut Task.	5 - Strongly Agree
3	Was the Cut Task was difficult with configuration A	4 - Agree
4	Was the Cut Task was efficient with configuration A	3 - Neutral
5	Was the Ball Task was difficult with configuration A	3 - Neutral
6	Was the Ball Task was efficient with configuration A	3 - Neutral
7	Was the Cut Task was difficult with configuration B	2 - Disagree
8	Was the Cut Task was efficient with configuration B	4 - Agree
9	Was the Ball task was efficent with configuration B	4 - Agree
10	Was the Ball Task was difficult with configuration B	2 - Disagree
11	Were you satisfied with the image on the monitor in configuration A	4 - Agree
12	Were you satisfied with the image on the monitor in configuration B	4 - Agree
13	Were you satisfied with the depth perception of configuration A	3 - Neutral
14	Were you satisfied with the depth perception of configuration B	4 - Agree
15	Were you satisfied with monitor's placement	4 - Agree
16	Were you satisfied with the movment speed of the	4 - Agree
17	Were you satisfied with the SILS device placment in configuration B	4 - Agree
18	Was the monitor screen was of adequate size to	4 - Agree
19	Did configuration A had sufficient functionality.	3 - Neutral
20	Did configuration B had sufficient functionality.	4 - Agree
21	You can perform the Cut Task better with…	2 - Configuration B
22	You can perform the Ball Task better with…	2 - Configuration B

Figure 69: SILS Port Camera participant questionnaire average answer.

From Figure 69 it can be seen that the participants believed the task difficulty was easier with the SILS Magnet Camera (configuration B) versus the traditional SILS setup (configurations A). The participants indicated the image quality, and ease of use of the SILS Magnet Camera was better than the traditional SILS Setup. Overall the participants agreed the traditional SILS setup provided sufficient functionality where as they felt neutral about the functionality of the traditional SILS setup. Ultimately the SILS Magnet Camera was picked as the configuration that provided the most functionality and would be selected by the participants if the tasks were performed again.

Chapter 4 - Porcine Study

To prove SILS and Port Camera surgical feasibility both prototypes were tested in their own live porcine models at the University of Colorado's Anschutz medical Campus at different points in time. The goal of each study was to perform an exploratory surgery of the peritoneal cavity, and a basic SILS procedure. A protocol for the porcine study was approved (IACUC protocol number 87909-05-1D) by the IRB prior to the study, and in both porcine studies an experienced laparoscopic surgeon performed the MIS procedures.

4.1 Port Camera

A gallbladder removal, cholecystectomy, was chosen for the MIS procedure is a common MIS procedure that has been used to evaluate several new MIS techniques. The animal was placed dorsal recumbently, and under general anesthesia. The surgeon made a 2.5 cm incision in the umbilicus and the SILS Port from Covidien was inserted in accordance to Covidien's SILS insertion procedure [64]. Pneumoperitoneum was induced through the SILS port allowing for insufflation of the peritoneal cavity. A 5mm incision was introduced to the costal arch on the right side of the animal and the abdominal cavity was explored with a STORZ Laparoscope.

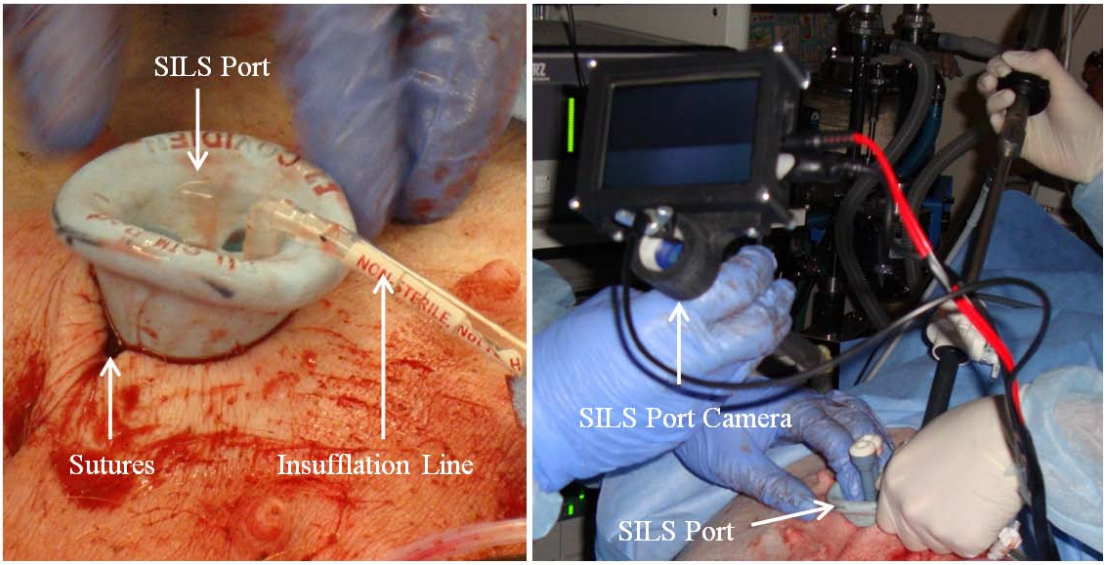

Figure 70: SILS Port insertion (left) and SILS Port Camera insertion (right).

The SILS Port Camera was then inserted into the mid channel in the SILS Port, see Figure 70. The surgeon rotated the activation knob 180 degrees followed by pulling the knob 35 mm away from the device to deploy and lock the camera module into place. Once the camera module was deployed the surgeon inserted a laparoscopic surgical grasper through the SILS Port Camera's cannula, see Figure 71.

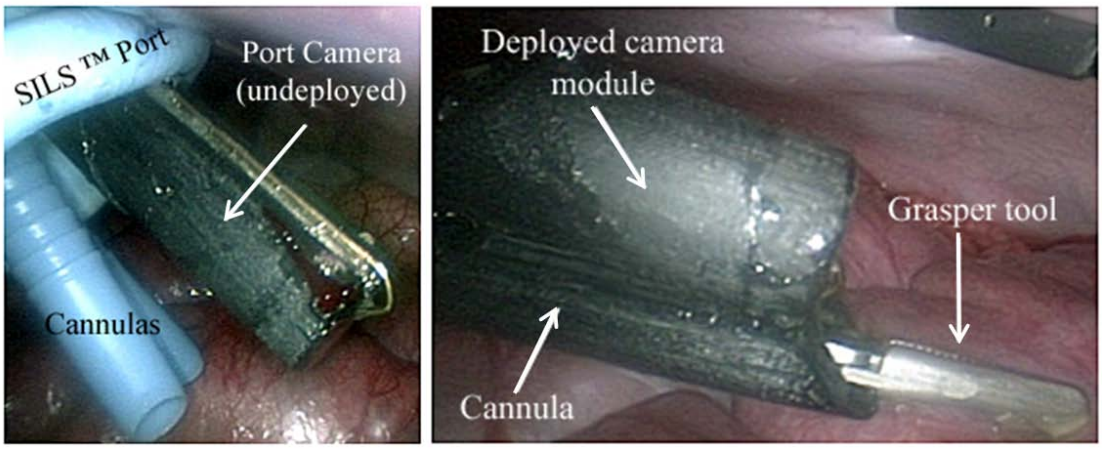

Figure 71: SILS Port Camera undeployed (left) and deployed (right).

A second articulating grasper was inserted through an open channel on the SILS port and positioned to allow the surgeon to triangulate and probe the surgical site, see Figure 72.

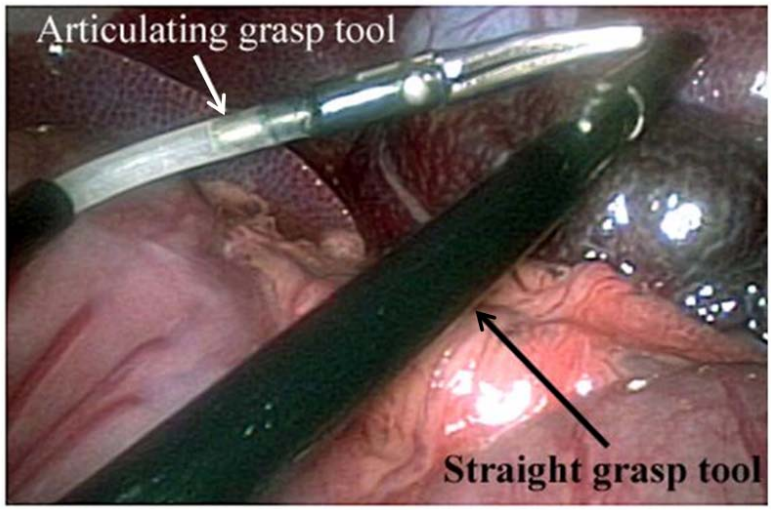

Figure 72: Tool triangulation of a straight and articulated grasping tool.

During the procedure the third channel in the SILS port was left unoccupied. During use, the SILS Port Camera's cannula inhibited the second surgical grasper's range of motion, making it impossible to suspend the gallbladder. The SILS Port was rotated 90 degrees to improve the bi-lateral range of the grasper tools motion, when this did not alleviate the interference an additional 5 mm trocar and straight grasper tool was inserted to perform the suspension of the gallbladder. The SILS Port Camera's articulating grasper was used to expose the cystic duct. A 5 mm clip applier was inserted through the Port Cameras channel to seal around the excision point on the cystic duct and artery. After the clips were applied an articulating cutting tool was inserted through the SILS port to excise the cystic duct and artery, see Figure 73.

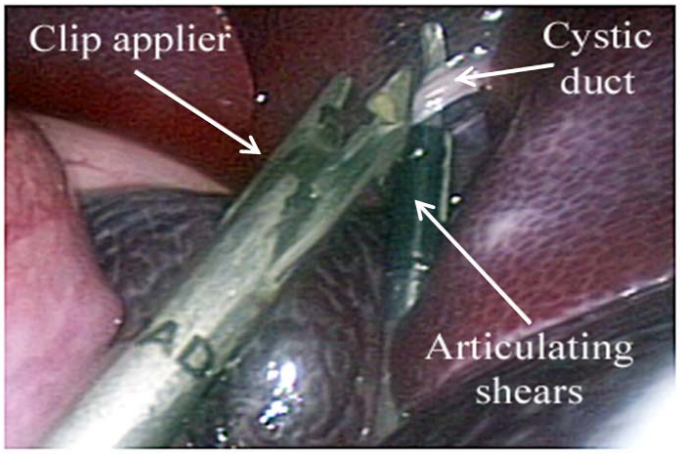

Figure 73: Clipping the cystic duct of the gallbladder.

The surgery was terminated before the gallbladder could be fully excised due to extensive operation time, and blood/mesentery pooling around the gallbladder. The tools were removed from the SILS port, and the 5 mm port. The camera module was un-deployed by pushing the activation knob into the port cameras cannula housing and rotating the activation knob 180 degrees to align the camera module coaxially with the SILS port cameras channel. It took 1.5 hours to complete peritoneal cavity exploration and gallbladder cystic duct excision.

Many factors contributed to the premature termination of the gallbladder removal. The surgeon noted that the combination of the small 8.9 cm (3.5” diagonal screen size) on-patient LCD screen with a narrow LCD viewing angle made tool navigation and tissue identification difficult. The rigidly fixed on-patient LCD screen, located 90 degrees off the SILS Port Camera’s cannula, made prolonged viewing difficult requiring the surgeon to bend over to bring the LCD into his field of view, see Figure 74. The surgeon would like to see an adjustable screen to allow for a preferred viewing angle to be set.

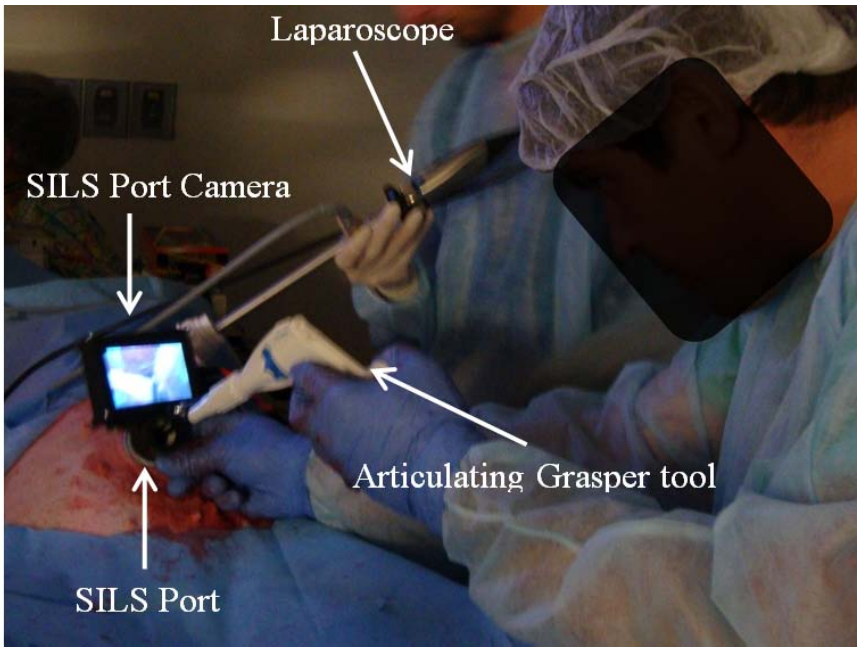

Figure 74: SILS Port Camera Operation.

The lack of zoom offered by the analog camera module made it impossible for the surgeon to obtain up close views of the surgical site to perform delicate surgical tasks such as suturing. The viewing distance is limited by the length of the SILS Port Cameras cannula, meaning the camera module can only be pushed in 130 mm before the device bottoms out in the SILS port, whereas a traditional Laparoscope can translate at a much larger distance into and out of the cannula. Two levels of zoom are needed to provide both a big picture view of the abdominal cavity for tool insertion, allowing the surgeon to focus on the SILS Port Camera distal tip as well as each tools tip to

avoid causing tissue damage, and an up close view once the tools have been deployed and moved to the surgical site. To avoid tool collision and improve tool range of motion the *in vivo* outer diameter of the SILS Port Camera's cannula and the *ex vivo* outer diameter for the Cannula's seal housing needs to be significantly reduced. The surgeon noted that the coupled on-patient LCD provided an upright view of the surgical site regardless of the screen and camera module orientation. This is not the case during traditional laparoscope control, where the surgical assistant must continually orient the laparoscope to keep the video images upright.

4.1.1 Discussion

The porcine study revealed many design issues of the SILS Port Camera device. The range of surgical tool motion was limited due to interference with the Port Cameras cannula. The small fixed on-patient LCD Screen combined with a narrow viewing angle made detailed surgical tasks difficult. The outer diameter of the cannula housing needs to be reduced, to help eliminate competition for space with the other SILS channels tools, while still allowing a variety of different tool sizes to be inserted into the SILS Port Camera. The on-patient LCD screen needs to be optimized to provide the best screen size, orientation, and viewing angle. Improved camera control and zoom is needed to provide detailed views of the surgical site from varying angles.

4.2 SILS Magnet Camera

A gallbladder removal (cholecystectomy) and a liver biopsy were chosen for the MIS procedure to show the SILS Magnet Camera can be used in two common SILS procedures. The animal was placed dorsal recumbently, and under general anesthesia. The SILS Magnet Cameras ring mount was slipped around the base of the SILS Port. A tabbed piece of tape was placed over the camera lens to prevent smudging during insertion, set to be removed by a grasper tool once the SILS device had been mounted to the abdominal wall. The surgeon made a 2.5 cm incision in the umbilicus and the SILS Magnet Camera device and 20.3 cm of service cable (camera and motor power, camera line) followed by the SILS port was inserted into the abdominal cavity.

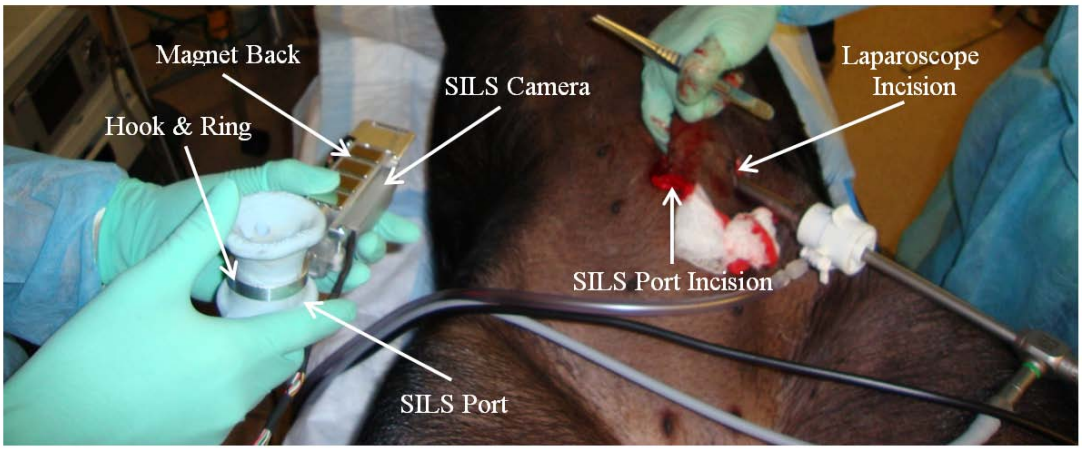

Figure 75: SILS Magnet Camera insertion.

A 5mm incision was introduced to the costal arch on the right side of the animal and the abdominal cavity to allow a laparoscope to be inserted into the abdominal cavity to view the SILS device in action, see Figure 75. Pneumoperitoneum was induced through the dedicated laparoscope port allowing for insufflation of the peritoneal cavity. Due to carbon dioxide leaking out through the SILS port, between the service cable and SILS port, and between the SILS port and the incision point a two sets of sutures were added to tighten the incision around the SILS port, see Figure 76.

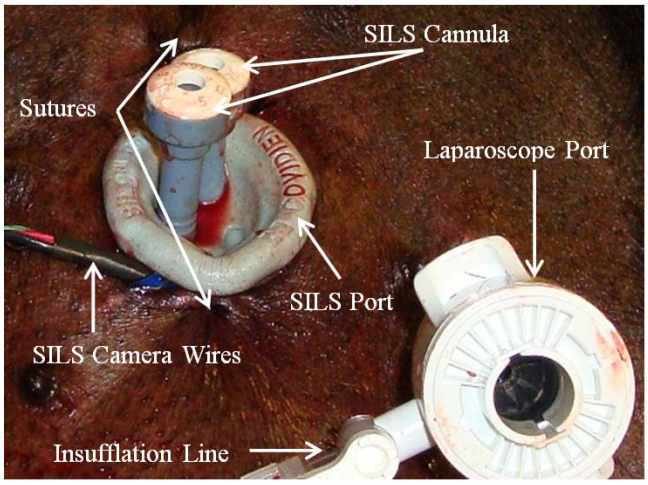

Figure 76: SILS Port and laparoscope port insertion.

The laparoscope video image is displayed on a traditional STORZ operation room LCD, the SILS Device was hooked up to an 18 inch LCD Screen that was placed where the normal off-patient

monitor would be. The swivel feature of the STORZ LCD was used to allow the surgeon an initial view of the abdominal cavity before being rotated away so the SILS Device LCD could be used without distraction, see Figure 77.

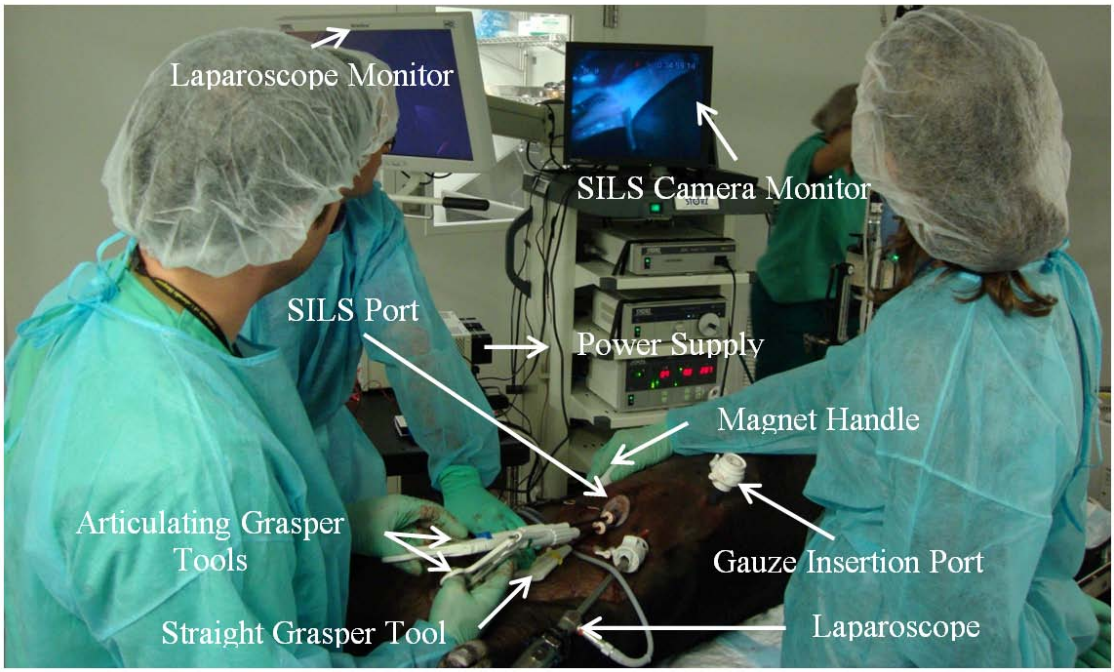

Figure 77: SILS Port Camera surgical setup.

A brief exploration of the abdominal cavity with the laparoscope revealed the SILS Device had been pushed underneath the liver. A grasper tool was inserted into one of the available SILS port channels and was used to push the liver band and away from the SILS device. Simultaneously the magnetic handled was placed (*ex vivo*) onto the abdominal wall to retract the device away from the internal organs and magnetically mount it (*in vivo*) to the abdominal wall. During the insertion of the SILS device the protective tape placed on the camera lens became unattached from the camera mount housing allowing for blood/mesentery to pool into the camera housing. To remove the blood from the camera lens a second 5 mm incision was added 12.7 cm medially and 2.5 cm above. Medical gauze was inserted with a grasper tool and used to wipe the blood off of the camera lens, see Figure 78.

Once the blood was removed the laparoscope lamp and video image were turned off camera and LED were turned on, and the control box was used to explore the abdominal cavity.

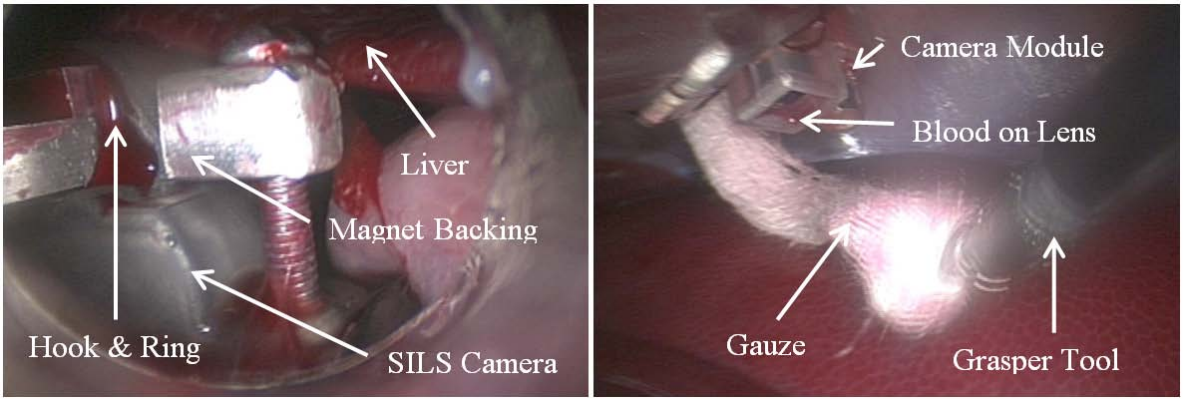

Figure 78: SILS Port Camera underneath the liver (left.) Blood being cleaned off the camera lens (right).

After testing the pant, tilt, and telescoping features of the SILS Device the surgeon used the magnetic handle to successfully rotate the SILS device around the SILS Port incision to provide a wide array of viewing angles. Once the camera module was positioned to view the surgical site (gallbladder), the surgeon attempted to move the liver away from the gallbladder with the grasper tool, see Figure 79.

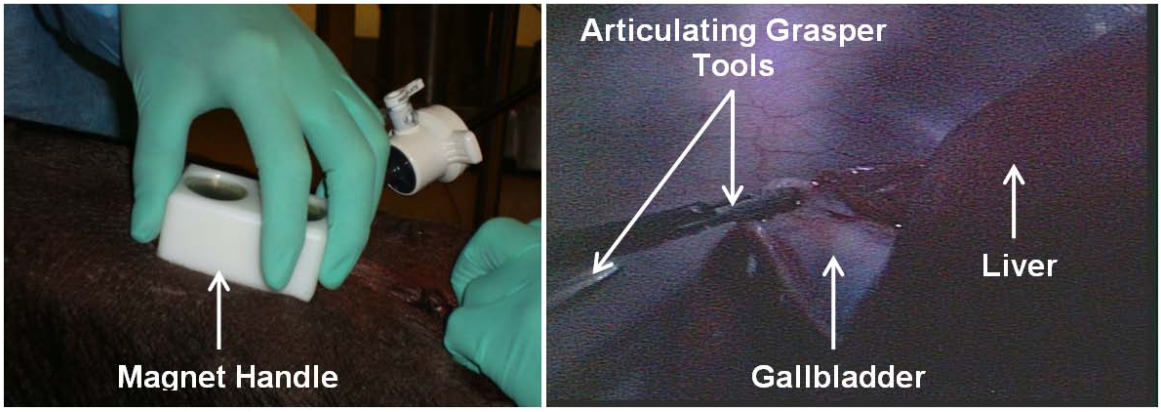

Figure 79: Magnet handle suspending SILS Magnet Camera (left). Initial suspension of the gallbladder (right).

However, during use the grasper tool was kept parallel to the operation table causing it to bind in the ring mount of the SILS Device. To reduce interference between the surgical tools and the mounting ring, the SILS Port was removed from the incision and decoupled from the mounting ring. The SILS Device, now completely suspended by the magnet handle, was then moved away from the incision point and positioned facing the gallbladder, see Figure 80.

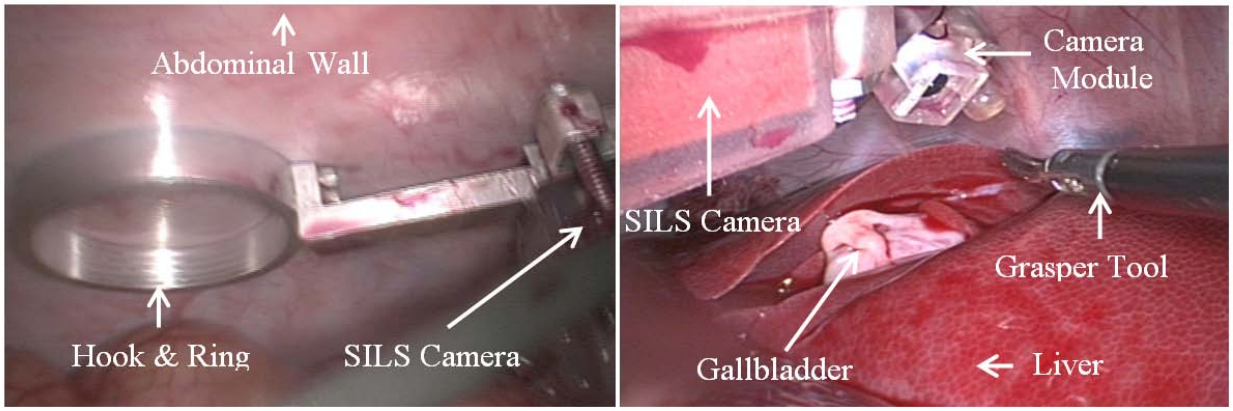

Figure 80: SILS Magnet Camera magnet system (left). Deployed SILS Magnet Camera (right).

Using the articulated grasper (Auto Suture Endo Dissect) to move the liver away from the gallbladder a ratcheting straight grasper (Auto Suture Endo Clinch 2) was inserted through an open channel on the SILS port and positioned to allow the surgeon to grab the gallbladder and move it back to expose the cystic duct. With the gallbladder being suspended the grasper tool holding back the liver was freed and used with a third grasper tool inserted through the last open channel in the SILS Port to triangulate and dissect the tissue surrounding the cystic duct, see Figure 81.

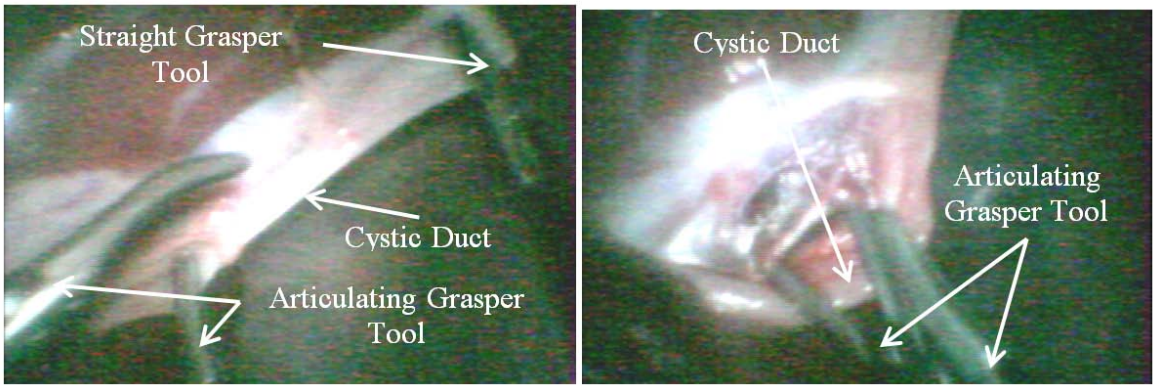

Figure 81: Grasper tool triangulation used to dissect tissue surronding the cystic duct.

Once the cystic duct was exposed the straight grasper tool was removed and a 5 mm clip applier was inserted through the open channel to seal around the excision point. After the clips were applied an articulating cutting tool was inserted through the SILS port to excise the cystic duct and artery. The two ratcheting grasper tools were removed and an articulating cutter was inserted, see Figure 82.

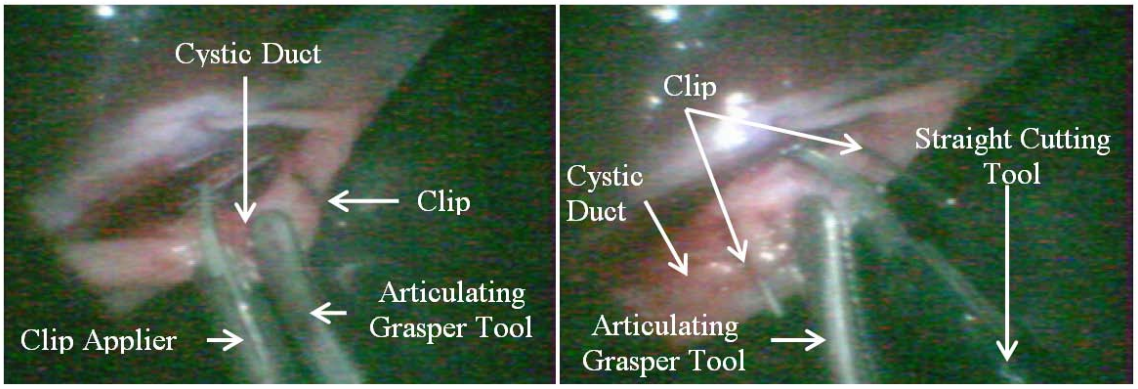

Figure 82: *Clipping the cystic duct of the gallbladder (left).Cutting the cystic duct (right).*

The SILS Magnet Camera Device was used to bring the liver into view; the grasper tool and cutter tool were then used in mock fashion to take a piece of liver. After the mock biopsy the small bowl and stomach were probed to test the flexibility in the tilt, pan, and translation (magnet system) of the camera system and to determine if it could be used for more complicated SILS procedures, see Figure 83.

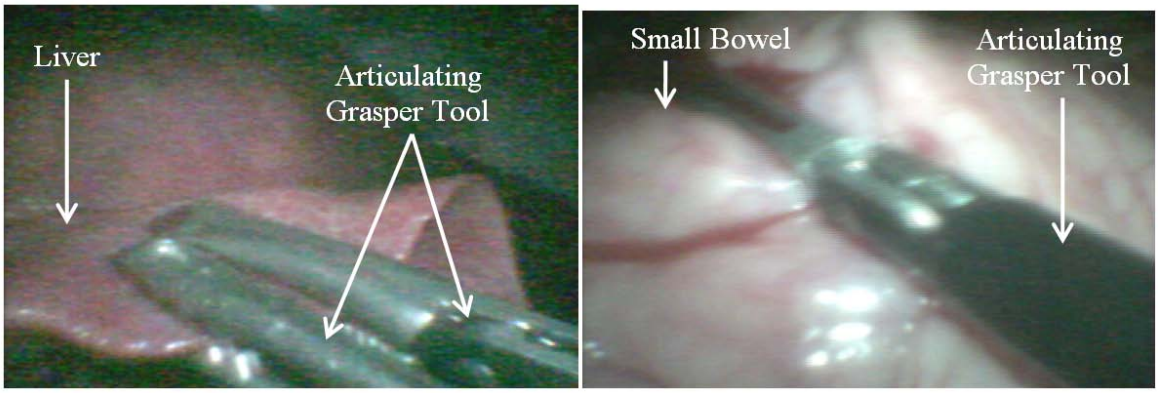

Figure 83: Liver biopsy (left) and small bowel biopsy (right).

The tools were removed from the SILS port, and the 5 mm port. The sutures around the SILS port were removed followed by the SILS port. The magnet handle was removed from the abdominal wall and the SILS Magnet Camera system was removed from the abdominal cavity through the incision in the umbilicus. It took 1.8 hours to complete peritoneal cavity exploration, a cystic duct dissection and division, and mock liver biopsy.

The surgeon noted that the cross sectional size of the device required the incision to be 2.6 cm larger than the typical 2 cm incision size. Running the wires between the SILS port and the abdominal wall created sealing issues requiring extra suturing to tighten the incision around the port. The hook and ring mounting method worked for vertical tool control but caused binding during horizontal tool manipulation.

The magnet handle successfully kept the SILS Magnet Camera device up against the abdominal wall, and provided a means of moving the entire device around the abdominal cavity. The extra mobility offered by the magnet system allowed for many different views of the surgical site to be obtained quickly. The single LED used in the camera mount provided adequate lighting for the procedure; however, the surgeon recommended increasing the brightness three fold in order to enhance the video image.

Smudging of the camera lens was a continual issue during the test. Typically a laparoscope is pulled out several times during a MIS in order to wipe away smearing and condensation. Once inserted the SILS Magnet Camera device is not easily removed, to account for the smearing a built in lens cleaning system needs to be developed to keep the image clear. The surgeon was impressed with the speed and flexibility of the cameras pan and tilt system, allowing him to track tools as they are inserted into the abdominal cavity from the SILS port all the way to their triangulation at the surgical site. The mobility of the camera module combined with orienting the entire system at different locations using the magnet system made up for the analog cameras lacking zoom feature. By removing the dedicated laparoscope the extra channel was used for a third tool during the liver retraction, and space was freed up improving the range and movement for his hands and the surgical tools, see Figure 84.

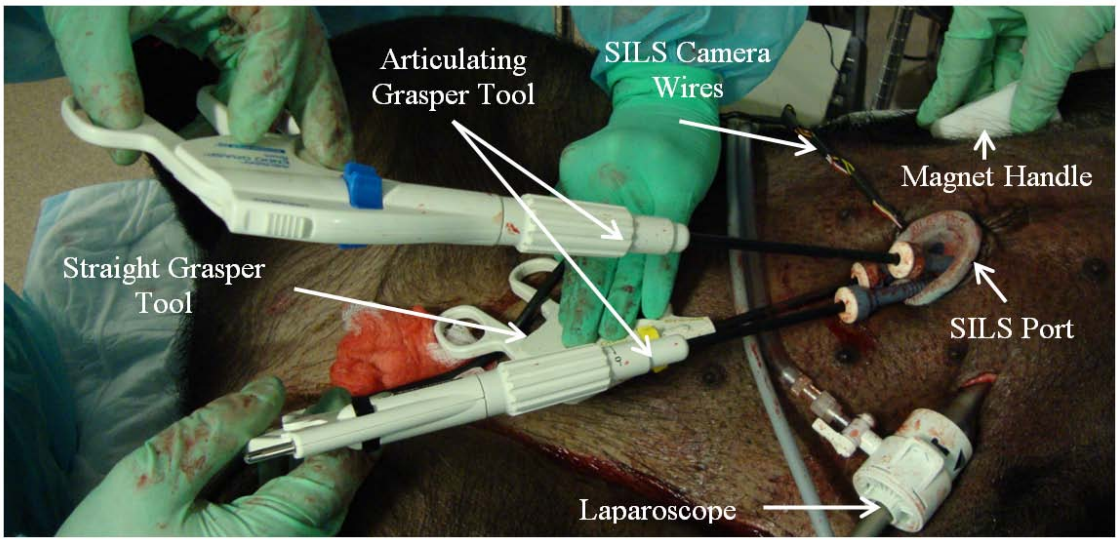

Figure 84: SILS Magnet Camera surgical tool positioning during cholecystectomy.

4.2.1 Discussion

The porcine study revealed many design benefits and issues with the SILS Magnet Camera device. The range of surgical tool motion was increased by mounting the entire camera system away from the SILS port and removing interference caused by a traditional laparoscope. The extra channel

can be left empty or a third tool can be inserted and used. The viewing capacity of the abdominal cavity was significantly increased by enhancing the camera systems mobility with the magnet system, and field of view with the pant/tilt system. The video camera needs to be switched to digital with at least two levels of zoom, and several more LED's need to be added to help illuminate the surgical site. Leaking carbon dioxide around the cable system made maintain a constant insufflation pressure difficult. The camera cable should be run through its own channel in the SILS port to provide adequate sealing. The cross-sectional size of the SILS device needs to be reduced to allow for smaller incisions to be used. A smear and condensation system needs to be developed to keep the camera system clean during use. The housings need to be redesigned to provide tight sealing between the SILS device Electronics and the abdominal cavity.

Chapter 5 - Conclusion

Single incision laparoscopic surgery (SILS) offers many benefits over traditional open surgery, allowing for complex procedures to be performed entirely through the umbilicus by passing multiple tools through a single incision point. SILS offers patient benefits including reduced trauma, risk of infection, post-operative pain, scaring, and a shorter recovery time. However, SILS remains surgically challenging due to limited surgical tool motion and positioning of the traditional laparoscope through the SILS entry incision. Two approaches were taken to develop a SILS specific camera system to eliminate interference caused between the laparoscope and the surgical tools and to improve the field of view of the abdominal cavity.

A prototype for the integrated cannula system (SILS Port Camera) was developed and tested first, followed by a prototype for the removed camera system (SILS Magnet Camera) which improves upon many of the issues associated with the integrated cannula approach. The SILS devices were developed using computer software then rapid prototyped. The SILS Port Camera was built around a cannula adding a separate camera module and LED that could be locked into position, with the video image displayed on an on-patient LCD screen fixed to the outer end of the cannula. The SILS Magnet Camera moved away from this approach focusing on creating a multiple degree of freedom camera system that could be controlled remotely, decoupled from the SILS port, and attached entirely inside the abdominal cavity through the use of a magnet system.

To prove initial feasibility and functionality of the devices were compared to the traditional industry SILS laparoscopic set up and an *ex vivo* participant study was performed. The participants completed a tissue identification task (Ball Drop Task) and a tissue biopsy task (Cut Task) using each device and a traditional laparoscope design. The effects of screen location, camera orientation, and camera system control were compared across the devices. The SILS Port Camera using the on-patient LCD performed similarly to the Laparoscope with no statistical variance in task completion time.

However, the SILS Port Cameras off-patient LCD configuration performed better than the Laparoscope during the Cut task and performed worse than the Laparoscope during the ball drop task. The participants made more errors with the SILS Port Camera versus the laparoscope. From the survey it was found that the participants favored the off-patient LCD SILS Port Camera configuration over the laparoscope and on-patient configurations. Generally, the participants preferred the Port Camera over the Laparoscope in image quality, and functionality.

The SILS Magnet Camera overall task completion time and number of errors per task incurred were significantly lower than the Laparoscope's. From the survey it was found that the participants favored the SILS Magnet Camera over the laparoscope configuration. The participants preferred the SILS Magnet Camera over the laparoscope in image quality, and functionality.

The SILS devices were tested in a live porcine model at the University of Colorado's Hospital in Aurora, Colorado by an experienced laparoscopic surgeon. The SILS devices were successfully inserted through the SILS port and deployed in the abdominal cavity. The surgeon performed an initial cavity exploration followed by a cystic duct division and resection. Then, the surgeon performed an additional mock liver biopsy, small bowel and stomach inspection using the SILS PC2. The SILS devices were then removed and sterilized. The design improvements developed from the porcine studies will be included in future prototypes.

The SILS Magnet Camera device incorporates all of the features of a laparoscopic vision system into a small, portable package that is attached entirely inside the abdominal cavity through the use of an external magnetic handle, thereby avoiding competition for space between the surgical tools. The camera system, allows for three degrees of freedom (pan, tilt, and telescope), and remains separate from the SILS port, thereby removing the need a dedicated laparoscope, and thus allowing for an overall reduction in SILS port size or the use of a third tool through the insertion port regularly reserved for the laparoscope. The SILS Magnet Camera adds increased viewing flexibility over

traditional MIS viewing systems and frees up valuable real-estate allowing for increased tool range of motion and the use of a third tool.

Chapter 6 – Future Work

The SILS Magnet Camera successfully proved initial feasibility of a SILS specific camera system by performing better than a traditional SILS setup during participant testing, completion of a cystic duct division and resection, mock liver biopsy, small bowel inspection, and stomach inspection in a porcine model. The results of these feasibility tests suggest a number of improvements in the design components. The next version of the SILS Magnet Camera will incorporate the following improvements: 1) anti-fog and streak system to keep the visual image clear during operation; once inserted the SILS Magnet Camera cannot be easily removed to clear the lens as is done with a traditional laparoscope; 2) complete containment to prevent leaking of intra-abdominal fluid into the device and to ensure moving components are not put in a bind by being exposed to the abdominal wall; 3) camera conversion to a digital video camera with zoom; 4) overall size reduction of the device to allow it to be inserted through smaller incisions, 5) additional lighting to the camera module, 6) incorporation of an electrical motor stop to control directional tilt and pan limits, 7) battery powered and wireless, and 8) more control of the camera's orientation with the attachment of a small joy stick or directional pad to the surgical tool to allow use of a single thumb during surgery.

Further feasibility tests of the device need to be conducted. A finite element analysis (FEA) will be performed to optimize housing dimensions to ensure the design will not fail at the motor mounts during motor use (excessive torque at motor mounts), fail from forces exerted on the housing from various mounting configurations (magnets, hook & ring), and accidently being dropped. A design for manufacturability (DFM) will be developed to ensure the device and subcomponents can be sterilized between uses, the exposed components are bio-compatible, that the complicated housing pieces can be made through injection molding, and that the overall cost of the device is within reason for its number of uses during its product lifetime. Finally, the new prototype will undergo a risk analysis, a

participant study, and porcine testing in order to obtain feedback on the device, ensure it meets all design specifications, and to compare it to a traditional SILS setup.

Chapter 7 - Bibliography

1. McDougall, M.D., Elspeth M., et al., *A Standardized Guideline for Training Programs*. 2005, American Urological Association Education and Resarch, Inc.
2. Wolf, J.S., Jr. and M.L. Stoller, *The physiology of laparoscopy: basic principles, complications and other considerations.* J Urol, 1994. **152**(2 Pt 1): p. 294-302.
3. Colver, R.M., *Laparoscopy: basic technique, instrumentation, and complications.* Surg Laparosc Endosc, 1992. **2**(1): p. 35-40.
4. Studies, A.C.f.F., *Diagnostic Laparoscop*, in *Arizona Center for Fertility Studies*. 2010.
5. Plus, M., *Laparoscopy*, in *National Library of Medicine* 2009, National Institutes of Health.
6. Ahmed, K., et al., *The role of single-incision laparoscopic surgery in abdominal and pelvic surgery: a systematic review.* Surg Endosc. **25**(2): p. 378-96.
7. Smith, J.F., et al., *Risks and benefits of laparoscopic cholecystectomy in the community hospital setting.* J Laparoendosc Surg, 1991. **1**(6): p. 325-32.
8. Targarona, E.M., et al., *Single-port access: a feasible alternative to conventional laparoscopic splenectomy.* Surg Innov, 2009. **16**(4): p. 348-52.
9. Pnavel Systems, I., *First-in-Man Single Port Reconstructive Urogynecological/Pediatric Urological Operations Performed at Cleveland Clinic* in *Bio Space*. 2007.
10. Center, B.I.D.M., *Single Incision Laparoscopic Kidney Surgery*, in *Beth Israel Deaconess Medical Center*. 2010.
11. Kommu, S.S. and A. Rane, *Devices for laparoendoscopic single-site surgery in urology.* Expert Rev Med Devices, 2009. **6**(1): p. 95-103.
12. Westebring-van der Putten, E.P., et al., *Haptics in minimally invasive surgery--a review.* Minim Invasive Ther Allied Technol, 2008. **17**(1): p. 3-16.
13. Nezhat, C., et al., *Operative Gynecologic Laparoscopy Principles and Techniques*. 2000, McGraww-Hill.
14. Shekhar, R., et al., *Live augmented reality: a new visualization method for laparoscopic surgery using continuous volumetric computed tomography.* Surg Endosc. **24**(8): p. 1976-85.
15. Vilos, G.A., et al., *Laparoscopic entry: a review of techniques, technologies, and complications.* J Obstet Gynaecol Can, 2007. **29**(5): p. 433-65.
16. Lau, H. and F. Lee, *Seroma following endoscopic extraperitoneal inguinal hernioplasty.* Surg Endosc, 2003. **17**(11): p. 1773-7.
17. McKernan, J.B. and J.K. Champion, *Access techniques: Veress needle--initial blind trocar insertion versus open laparoscopy with the Hasson trocar*. Endosc Surg Allied Technol, 1995. **3**(1): p. 35-8.
18. Health, C., *Snowden-Pencer Verres Needles*, in *Cardinal Health*, Snowdn-Pencer.
19. Cakir, T., et al., *Safe Veress needle insertion.* J Hepatobiliary Pancreat Surg, 2006. **13**(3): p. 225-7.
20. Stepanian, A.A., et al., *Comparative analysis of 5-mm trocars: dilating tip versus non-shielded bladed.* J Minim Invasive Gynecol, 2007. **14**(2): p. 176-83.
21. Covidien, *VERSAPORT V2 Conventional Trocars*, in *Syneture*. 2011, Covidien.
22. Chiong, E., et al., *Port-site hernias occurring after the use of bladeless radially expanding trocars.* Urology. **75**(3): p. 574-80.
23. Covidien, *Versaport Plus Bladeless Trocars*, in *Autosuture*. 2011, Covidien.
24. Siqueira, T.M., Jr., et al., *The use of blunt-tipped 12-mm trocars without fascial closure in laparoscopic live donor nephrectomy.* JSLS, 2004. **8**(1): p. 47-50.
25. Hamade, A.M., et al., *Fixity of ports to the abdominal wall during laparoscopic surgery: a randomized comparison of cutting versus blunt trocars.* Surg Endosc, 2007. **21**(6): p. 965-9.
26. Hospital, C.G.M., *Performing a Safe Laparoscopy*, in *Chang Gung Memorial Hospital*, AutoSuture.

27. Choi, J. and L. Milone, *Emerging Technologies—Single-Incision Laparoscopic Surgery: How and Why?*, in *Emerging Technologies*. 2009, Bariatric Times.
28. MacDonald, E.R., E. Brownlee, and I. Ahmed, *New Tools for a New Job-Single Port Laparoscopic Surgery.* 2009. **2**.
29. Page, T. and N.A. Soomro, *Bilateral simultaneous single-port (LESS) laparoscopic nephrectomy (laparoendoscopic single site surgery).* Indian J Urol. **26**(4): p. 590-2.
30. Surgical, C., *SILS Port*, in *AutoSuture*. 2008, Covidien.
31. Covidien, *SILS Port Multiple Instrument Access Port*, in *Covidien*. 2011, Covidien.
32. Rettenmaier, M.A., et al., *A retrospective review of the GelPort system in single-port access pelvic surgery.* J Minim Invasive Gynecol, 2009. **16**(6): p. 743-7.
33. Medical, A., *Gelp Port Laparoscopic System*, in *Milenium Peru*. 2007, AppliedMedical.
34. Romanelli, J.R. and D.B. Earle, *Single-port laparoscopic surgery: an overview.* Surg Endosc, 2009. **23**(7): p. 1419-27.
35. Shussman, N., et al., *Single-incision laparoscopic cholecystectomy: lessons learned.* 2010. **10**(1007).
36. Wong, S.K. and P.W. Chiu, *Laparo-Endoscopic Single-Site Surgery (LESS)*, in *Esurg*, Department of Surgery, Prince of Wales Hospital, The Chinese University of Hong Kong.
37. Micro, *Micro Supplies "Medical Design Excellence Award" Winner*, in *Micro Company*. 2008, Novare SUrgical Systems.
38. Covidien, *Roticulator Articulating Instruments*, in *SILS*. 2008, Covidien.
39. Covidien, *Roticulator Single Use Laparoscopic Hand Instruments Standard Length*, in *Syneture*. 2011, Covidien.
40. Teixeira, J., et al., *Laparoscopic single-site surgery for placement of an adjustable gastric band: initial experience.* Surg Endosc, 2009. **23**(6): p. 1409-14.
41. Palanivelu, C., et al., *Transumbilical flexible endoscopic cholecystectomy in humans: first feasibility study using a hybrid technique.* Endoscopy, 2008. **40**(5): p. 428-431.
42. Inc., O.A., *Deflectable-Tip EndoEYE*, in *General Surgery News*, Olympus.
43. Terry, B.S., et al., *An Integrated Port Camera and Display.* 2010. **57**(5).
44. Ruppert, A., *Design and Experimental Evaluation of an Integrated Canula Visulization System for Laparoscopy*. 2009, The University of Colorado at Boulder: Boulder.
45. Tracy, C.R., et al., *Laparoendoscopic Single-site Surgery in Urology: Instrumentation*, in *Medscape*. 2008, Nat Clin pract Urol.
46. Cadeddu, J., et al., *Novel magnetically guided intra-abdominal camera to facilitate laparoendoscopic single-site surgery: initial human experience.* Surg Endosc, 2009. **23**(8): p. 1894-9.
47. Hu, T., et al., *In vivo pan/tilt endoscope with integrated light source, zoom and auto-focusing.* Stud Health Technol Inform, 2008. **132**: p. 174-9.
48. University, B., *Robotic Surgery*, in *Bio Med Brown*, Brown Univeresity.
49. Surgical, I., *The da Vinci Surgical System*, in *da Vinci Surgery*. 2010, Intuitive Surgical.
50. Terry, B.S., et al., *An integrated port camera and display system for laparoscopy.* IEEE Trans Biomed Eng. **57**(5): p. 1191-7.
51. Limited, B.T.D.C., *OV6920 CMOS Camera Module-Endoscope Camera (RS4018A-55)*, in *Top Free Biz*. 2010, Bangu Technology Development Company Limited.
52. Ibrahim, F.M., *Single Incision Laparoscopic Surgery (SILS) appendicectomy as alternative surgical procedure in diagnosis and treatment of acute appendicitis: Review Article.* 2010.
53. Park, K., et al., *Single-incision Laparoscopic Sleeve Gastrectomy*, in *Bariatric Times*. 2011, Bariatric Times.
54. Online, M.D., *FAULHABER Introduces Family Of 6 mm Motors For New Applications*, in *Medical Design Online*. 2008, Micro-Mo.
55. Ostmo, K., *Two-Axis Gimbal*, in *Wikimedia Commons*. 2006, Wikimedia Commons.

56. Lewotsky, K., *Choosing the Right Linear Actuator* in *Motion Control Online*. 2007, Motion Control Association.
57. Magnetics, K.J., *The Original K&J Magnet Calculator*, in *K&J Magnetics*, K&J Magnetics.
58. Botics, S., *Industrial Circuts Application Note Stepper Motor Basics*, in *Solar Botics*, Solar Botics.
59. Scherz, p., *Practical Electronics for Inventors*. 2007, Nwe York: McGraw-Hill.
60. Jones, D.W., *Stepping Motor Types*, in *Univeristy of Iowa Computer Science*, University of Iowa.
61. Solutions, H.K.M., *21000 Series Size 8 Stepper Motor linear Ctuator*, in *Haydon kerk*, Haydon Kerk.
62. Simulation, -.D.L.T., *Laparoscopic - Minimally Invasive Training System (MITS) TRLCD03 3-Dmed MITS*, in *3-Dmed*, 3-Dmed.
63. Trochim, W.M.K., *The T-Test*, in *Resarch Methods Knowledge Base*. 2006, Social Resarch Methods.

Appendix – Components & Data Sheets

A.1 - RS4018A-55 Analog Camera

Endoscope camera module	
(Model: RS-4018)	
Specification:	
Image Sensor	1/18 OV6920 CMOS
Horizontal Resolution	240TVL
Sensing Area	820μ m× 625μm
Signal System	NTSC
Effective Pixels	320× 240
Scanning frequency	H: 15.7343KHz V: 60Hz
Electronic Shutter	1/60S-5.7μS
S/N Ratio	≥ 42dB
Gray Rating	10th rank
Gamma value	0.45
Low electricity level	0.06 Vp-p
Minimum Illumination	2.0 Lux / F2.0(0 Lux When LED is on)
Video Output	1.0Vp-p 75Ω
Standard layout lens	68° /118°
LED Lamps	1mm-80mm(4 lamps, can be set as you want)
Dimensions of camera board	4mm× 16mm
Power Consumption	DC 3.5V-- 5V camera module: 20mA;
LED: 20mA	
Operation Temperature	-20~40degree RH95% Max

A.2 – BK Precision 1760 A DC Power Supply

Triple Output DC Power Supply
0-60 V/0 – 2 A (2), 4-6.5 V/ 4 A (1)
Model 1762

Model 1762 Triple Output DC Power Supply delivers 0-60 V/0-2 A on 2 outputs and 4-6.5 V/4 A on 1 output. The 4 digit LED display offers 10mV and 1mA resolution, providing the capability to set voltage and current values more accurately and precisely compared to 3 digit displays found in most comparable power supplies. The power supply is fully overload protected and comes with a two year warranty.

Features:

- Continuously monitor voltage and current output on two 4-digit LED displays
- Connect two supplies in parallel to double the current output
- Connect two supplies in series to double the voltage output
- Constant voltage and constant current operation
- Reliable & durable
- Operate continuously at full load without overheating
- Fully overload protected
- Course and fine voltage and current controls
- Excellent regulation
- Very low ripple and noise

Specifications	model 1762
Main Output	
Output Voltage	0-60V (A & B) 4-6.5 V (C)
Output Current	0-2A (A & B) 4A (C)
Constant Voltage Operation	
Voltage Regulation	
Line (120VAC ±10%)	≤ 0.01% +3 mV (A&B) ≤ 10 mV (C)
Load	≤ 0.01% +3 mV (A&B) ≤ 10 mV (C)
Recovery Time	100µs
Ripple & Noise (5Hz to 1MHz)	≤ 1mVrms
Temperature Coefficient	≤ 300 ppm/°C
Constant Current Operation	
Adjustable Current Limit	5% to 100% (A&B)
Current Regulation	
Line (120VAC ±10%)	≤ 0.2% + 3mA
Load	≤ 0.2% + 3 mA
Current Ripple	≤ 3 mA rms
Metering	
Display	2 digital 4 digit LED
Voltmeter Range	0-99.99 V (A & B) 0-99.99 V (C)
Voltmeter Accuracy	± (0.5% rdg + 9 digits)
Ammeter Range	0-9.999 A
General	
Ammeter Accuracy	± (0.5% rdg + 2 digits)
Overload Protection	Current limiting, Reverse polarity, overvoltage, Short circuit
Power Requirements	108-132 VAC 60 Hz, 120/220/230/240/ VAC, ±10%, 50/60 Hz version available
Power Consumption	350 W
Operating Temperature	0° to 40°C ≤ 85% R.H.
Storage Temperature	-15° to 70°C ≤ 85% R.H.
Dimensions (H x W x D)	5.7 x 10.5 x 15" (145 x 267 x 381 mm)
Weight	21 lbs (9.5 kg)
	Two Year Warranty

Accessories
Supplied: User Manual, Spare Fuse, Line Cord

Technical data subject to change
© B&K Precision Corp. 2008
v042109

www.bkprecision.com
Tel.: 714.921.9095

BK PRECISION
ELECTRONIC TEST INSTRUMENTS

A.3 – Accelevision 3.5 Inch LCD

LCD35L

TECHNICAL SPECIFICATIONS

3.5" TFT-LCD COLOR OPEN FRAME MONITOR WITH LED BACKLIGHT

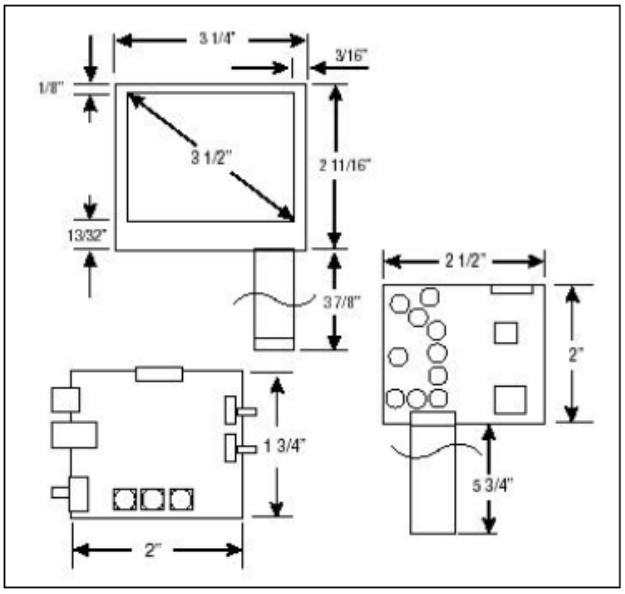

FEATURES

- Flip Image Switch
- Mirror Image Switch
- Anti-glare
- LED Backlight
- NTSC/PAL Auto-switch

SPECIFICATIONS

DISPLAY:	3.5" Color TFT-LCD Active Matrix
INPUT SIGNAL:	Composite, NTSC/PAL (Auto Switch)
DOT FORMAT:	480 x 234
BACKLIGHT:	LED
BRIGHTNESS RATING:	200 NIT
CONTRAST RATIO:	150:1
VIEWING ANGLE (L/R/T/B):	45°/45°/10°/30°
POWER REQUIREMENTS:	12VDC @ 110mA
DIMENSIONS (HxWxD):	2 11/16" x 3 1/4" x 3/16"
DRIVER BOARD (HxWxD):	2" x 2 1/2" x 9/32"
CONTROL BOARD (HxWxD):	1 3/4" x 2" x 1/2"
MONITOR MOUNTING:	Module: None, PC Board: Screw
OPERATING TEMPERATURE:	0° ~ 60°C
STORAGE TEMPERATURE:	-25° ~ 80°C

*Specifications subject to change without notice.

A.4 – Micro-Mo Motor: Series 0615 S

DC-Micromotors

Precious Metal Commutation

0,11 mNm

For combination with
Gearheads:
06/1

Encoders:
PA2-50, HXM3-64

Series 0615 ... S

		0615 N		1,5 S	003 S	4,5 S	
1	Nominal voltage	U_N		1,5	3,0	4,5	Volt
2	Terminal resistance	R		3,9	16,2	37,7	Ω
3	Output power	$P_{2\,max.}$		0,12	0,12	0,11	W
4	Efficiency	$\eta_{max.}$		52	50	48	%
5	No-load speed	n_0		19 100	20 200	20 000	rpm
6	No-load current (with shaft ø 0,8 mm)	I_0		0,030	0,016	0,012	A
7	Stall torque	M_H		0,24	0,22	0,21	mNm
8	Friction torque	M_R		0,02	0,02	0,02	mNm
9	Speed constant	k_n		13 840	7 346	4 872	rpm/V
10	Back-EMF constant	k_E		0,072	0,136	0,205	mV/rpm
11	Torque constant	k_M		0,69	1,30	1,96	mNm/A
12	Current constant	k_I		1,449	0,769	0,510	A/mNm
13	Slope of n-M curve	Δn/ΔM		78 224	91 538	93 713	rpm/mNm
14	Rotor inductance	L		12	39	95	µH
15	Mechanical time constant	τ_m		8	10	10	ms
16	Rotor inertia	J		0,01	0,01	0,01	gcm²
17	Angular acceleration	$\alpha_{max.}$		244	221	213	10^3rad/s²
18	Thermal resistance	R_{th1} / R_{th2}	35 / 76				K/W
19	Thermal time constant	τ_{w1} / τ_{w2}	2,6 / 110				s
20	Operating temperature range:						
	– motor		– 30 ... + 85				°C
	– rotor, max. permissible		+ 85				°C
21	Shaft bearings		sintered bronze sleeves				
22	Shaft load max.:						
	– with shaft diameter		0,8				mm
	– radial at 3 000 rpm (1,5 mm from bearing)		0,5				N
	– axial at 3 000 rpm		0,1				N
	– axial at standstill		20				N
23	Shaft play:						
	– radial	≤	0,03				mm
	– axial	≤	0,15				mm
24	Housing material		steel, black coated				
25	Weight		2				g
26	Direction of rotation		clockwise, viewed from the front face				
Recommended values - mathematically independent of each other							
27	Speed up to	$n_{e\,max.}$		13 000	13 000	13 000	rpm
28	Torque up to	$M_{e\,max.}$		0,11	0,11	0,11	mNm
29	Current up to (thermal limits)	$I_{e\,max.}$		0,341	0,167	0,110	A

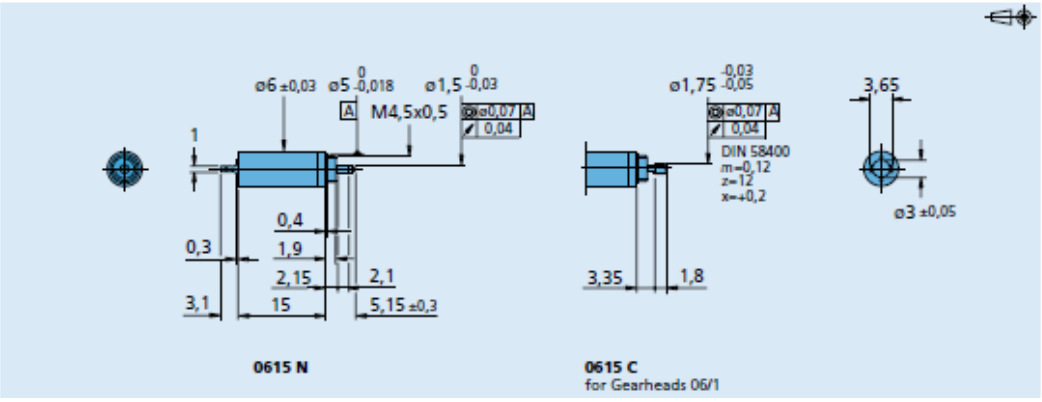

0615 N

0615 C
for Gearheads 06/1

A.5 – Haydon Kerk Series 8 Hybrid Linear Actuator

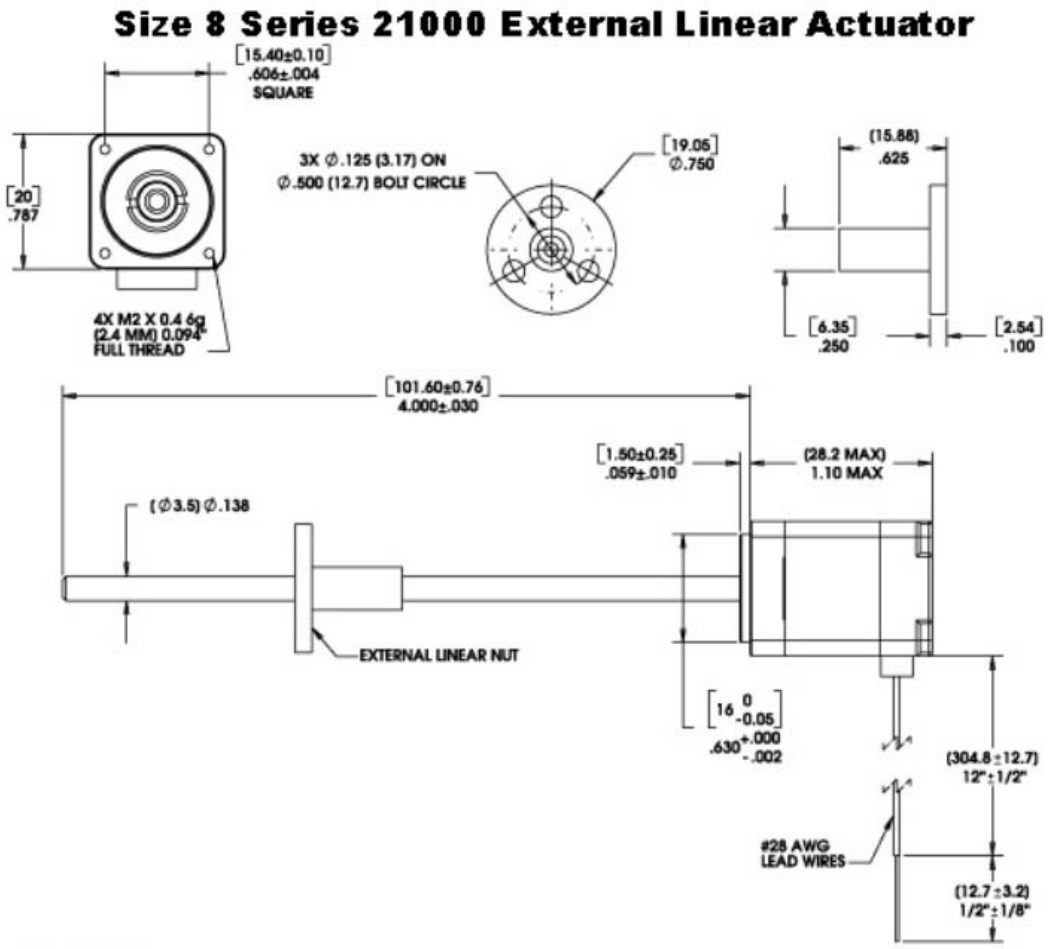

21000 SERIES SIZE 8 STEPPER MOTOR LINEAR ACTUATOR -21mm (0.8") Hybrid Linear Actuator (1.8 Degree step angle)				
Part No.	**Captive**	21H4(X)-V		
	Non-Captive	21F4(X)-V		
	External Lin.	E21H4(X)-V		
Wiring		Bipolar		
Operating voltage		2.5	5	7.5
Current/phase		0.49 A	0.24 A	0.16 A
Resistance/phase		5.1Ω	20.4 Ω	45.9 Ω
Inductance/phase		1.5 mH	5.0 mH	11.7 mH
Power consumption		2.45 W		
Temperature rise		135°F (75°C)		
Weight		1.5 oz (43 g)		
Insulation resistance		20 M Ω		

**Unipolar drive gives approximately 30% less thrust than bipolar drive.

Linear Travel / Step -Screw 0.138" (3.50 mm)		Order Code I.D.
inches	**mm**	
0.00006	0.0015*	**U**
0.000098	0.0025	**AA**
0.00012	0.0030*	**N**
0.00019*	0.005	**AB**
0.00024	0.006*	**K**
0.00039*	0.01	**AC**
0.00048	0.0121*	**J**
0.00078	0.02	**AD**
0.00157*	0.04	**AE**

*Values truncated

Standard motors are Class B rated for maximum temperature of 130°C.

Special drive considerations may be necessary when leaving shaft fully extended or fully retracted.

A.6 – Micro-Mo Planetary Gear Heads

FAULHABER

Planetary Gearheads 25 mNm

For combination with
DC-Micromotors:
0615
Brushless DC-Servomotors:
0620
Stepper Motors:
ADM0620

Series 06/1

	06/1	06/1 K
Housing material	steel	steel
Geartrain material	steel	steel
Recommended max. input speed for:		
– for continuous operation	8 000 rpm	8 000 rpm
Backlash, typical, at no-load	≤ 3°	≤ 3°
Bearings on output shaft	sintered sleeve bearings	ball bearings
Shaft load, max.:		
– radial (3,5 mm from mounting face)	≤ 0,5 N	≤ 5 N
– axial	≤ 0,5 N	≤ 3 N
Shaft press fit force, max.	≤ 3,5 N	≤ 5 N
Shaft play:		
– radial (3,5 mm from mounting face)	≤ 0,04 mm	≤ 0,05 mm
– axial	≤ 0,1 mm	≤ 0,05 mm
Operating temperature range	– 30° ... + 100° C	– 30° ... + 100° C

Specifications

reduction ratio	weight without motor g	length without motor L2 mm	length with motor 0615 C L1 mm	0620 C L1 mm	ADM 0620 L1 mm	output torque continuous operation M max. mNm	output torque intermittent operation M max. mNm	direction of rotation (reversible)	efficiency %
4 :1	2,0	9,2	24,2	29,2	18,6	25	35	=	90
16 :1	2,8	11,9	26,9	31,9	21,3	25	35	=	80
64 :1	3,4	14,6	29,6	34,6	24,0	25	35	=	70
256 :1	4,0	17,3	32,3	37,3	26,7	25	35	=	60
1 024 :1	4,4	20,0	35,0	40,0	29,4	25	35	=	55
4 096 :1	5,0	22,7	37,7	42,7	32,1	25	35	=	48

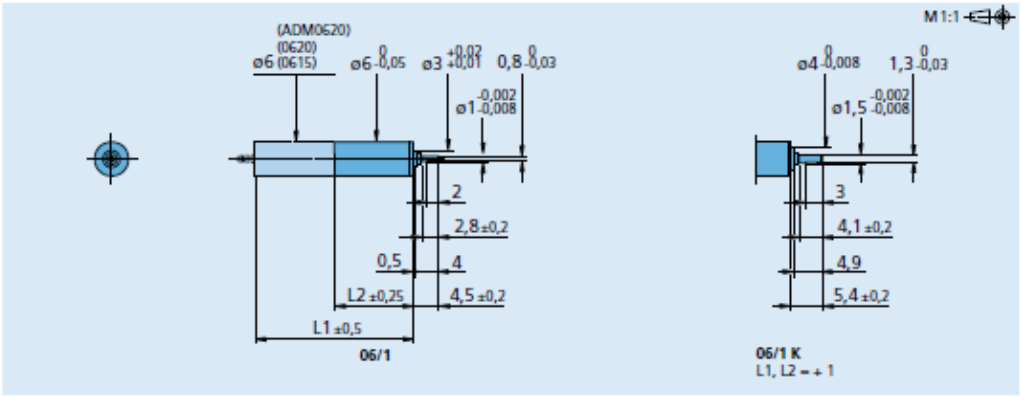

A.7 – EDE 1204

EDE1204 Bi-Polar Stepper Motor IC

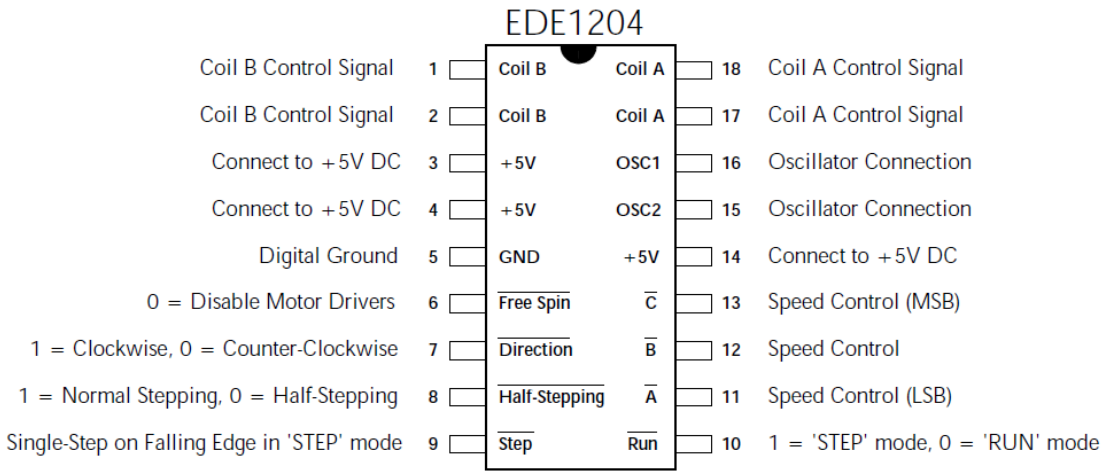

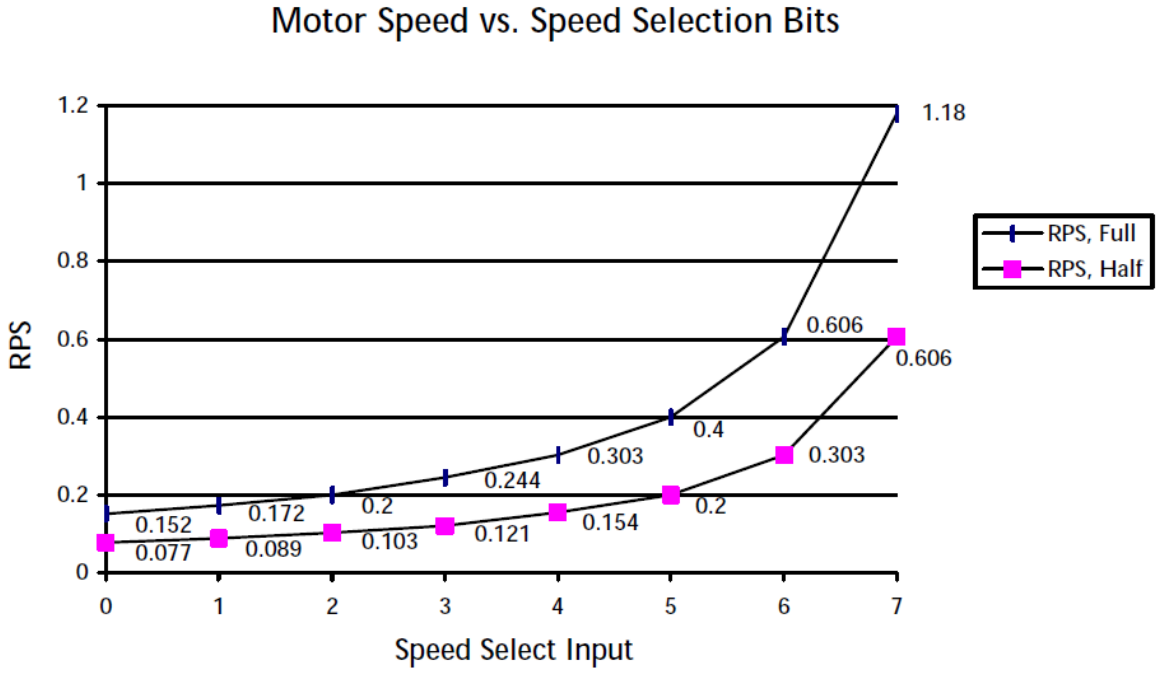

A.7 – L293NE

L293, L293D
QUADRUPLE HALF-H DRIVERS

SLRS009C – SEPTEMBER 1986 – REVISED NOVEMBER 2004

- **Featuring Unitrode L293 and L293D Products Now From Texas Instruments**
- **Wide Supply-Voltage Range: 4.5 V to 36 V**
- **Separate Input-Logic Supply**
- **Internal ESD Protection**
- **Thermal Shutdown**
- **High-Noise-Immunity Inputs**
- **Functionally Similar to SGS L293 and SGS L293D**
- **Output Current 1 A Per Channel (600 mA for L293D)**
- **Peak Output Current 2 A Per Channel (1.2 A for L293D)**
- **Output Clamp Diodes for Inductive Transient Suppression (L293D)**

L293 . . . N OR NE PACKAGE
L293D . . . NE PACKAGE
(TOP VIEW)

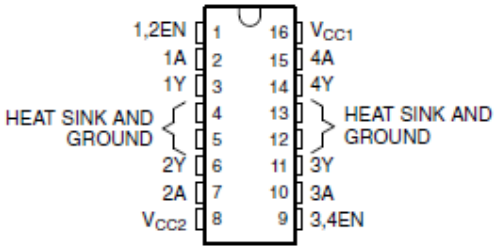

L293 . . . DWP PACKAGE
(TOP VIEW)

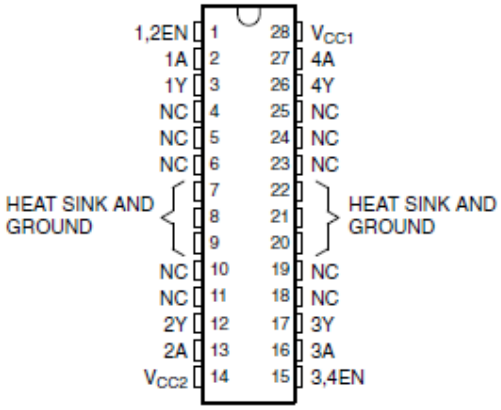

description/ordering information

The L293 and L293D are quadruple high-current half-H drivers. The L293 is designed to provide bidirectional drive currents of up to 1 A at voltages from 4.5 V to 36 V. The L293D is designed to provide bidirectional drive currents of up to 600-mA at voltages from 4.5 V to 36 V. Both devices are designed to drive inductive loads such as relays, solenoids, dc and bipolar stepping motors, as well as other high-current/high-voltage loads in positive-supply applications.

All inputs are TTL compatible. Each output is a complete totem-pole drive circuit, with a Darlington transistor sink and a pseudo-Darlington source. Drivers are enabled in pairs, with drivers 1 and 2 enabled by 1,2EN and drivers 3 and 4 enabled by 3,4EN. When an enable input is high, the associated drivers are enabled, and their outputs are active and in phase with their inputs. When the enable input is low, those drivers are disabled, and their outputs are off and in the high-impedance state. With the proper data inputs, each pair of drivers forms a full-H (or bridge) reversible drive suitable for solenoid or motor applications.

ORDERING INFORMATION

T_A	PACKAGE†		ORDERABLE PART NUMBER	TOP-SIDE MARKING
0°C to 70°C	HSOP (DWP)	Tube of 20	L293DWP	L293DWP
	PDIP (N)	Tube of 25	L293N	L293N
	PDIP (NE)	Tube of 25	L293NE	L293NE
		Tube of 25	L293DNE	L293DNE

† Package drawings, standard packing quantities, thermal data, symbolization, and PCB design guidelines are available at

recommended operating conditions

			MIN	MAX	UNIT
	Supply voltage	V_{CC1}	4.5	7	V
		V_{CC2}	V_{CC1}	36	
V_{IH}	High-level input voltage	$V_{CC1} \le 7$ V	2.3	V_{CC1}	V
		$V_{CC1} \ge 7$ V	2.3	7	V
V_{IL}	Low-level output voltage		−0.3†	1.5	V
T_A	Operating free-air temperature		0	70	°C

† The algebraic convention, in which the least positive (most negative) designated minimum, is used in this data sheet for logic voltage levels.

electrical characteristics, V_{CC1} = 5 V, V_{CC2} = 24 V, T_A = 25°C

PARAMETER			TEST CONDITIONS		MIN	TYP	MAX	UNIT
V_{OH}	High-level output voltage		L293: I_{OH} = −1 A L293D: I_{OH} = −0.6 A		V_{CC2} − 1.8	V_{CC2} − 1.4		V
V_{OL}	Low-level output voltage		L293: I_{OL} = 1 A L293D: I_{OL} = 0.6 A			1.2	1.8	V
V_{OKH}	High-level output clamp voltage		L293D: I_{OK} = −0.6 A			V_{CC2} + 1.3		V
V_{OKL}	Low-level output clamp voltage		L293D: I_{OK} = 0.6 A			1.3		V
I_{IH}	High-level input current	A	V_I = 7 V			0.2	100	µA
		EN				0.2	10	
I_{IL}	Low-level input current	A	V_I = 0			−3	−10	µA
		EN				−2	−100	
I_{CC1}	Logic supply current		I_O = 0	All outputs at high level		13	22	mA
				All outputs at low level		35	60	
				All outputs at high impedance		8	24	
I_{CC2}	Output supply current		I_O = 0	All outputs at high level		14	24	mA
				All outputs at low level		2	6	
				All outputs at high impedance		2	4	

switching characteristics, V_{CC1} = 5 V, V_{CC2} = 24 V, T_A = 25°C

PARAMETER		TEST CONDITIONS	L293NE, L293DNE			UNIT
			MIN	TYP	MAX	
t_{PLH}	Propagation delay time, low-to-high-level output from A input	C_L = 30 pF, See Figure 1		800		ns
t_{PHL}	Propagation delay time, high-to-low-level output from A input			400		ns
t_{TLH}	Transition time, low-to-high-level output			300		ns
t_{THL}	Transition time, high-to-low-level output			300		ns

switching characteristics, V_{CC1} = 5 V, V_{CC2} = 24 V, T_A = 25°C

PARAMETER		TEST CONDITIONS	L293DWP, L293N L293DN			UNIT
			MIN	TYP	MAX	
t_{PLH}	Propagation delay time, low-to-high-level output from A input	C_L = 30 pF, See Figure 1		750		ns
t_{PHL}	Propagation delay time, high-to-low-level output from A input			200		ns
t_{TLH}	Transition time, low-to-high-level output			100		ns
t_{THL}	Transition time, high-to-low-level output			350		ns

A.7 – Bi-Polar Steeper Control Circuit

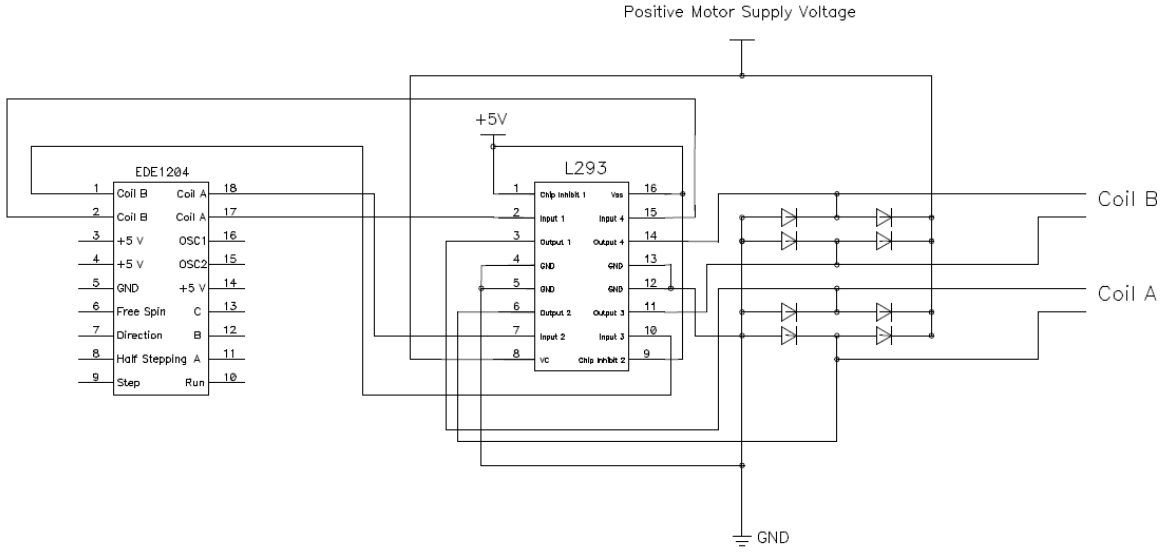

A.8 – Laparoscopic Surgery Trainer

THE 3-Dmed STANDARD TRAINER

Model # TRLCD03

Patent #6659776

Thank you for purchasing the **TRLCD03** Trainer from 3-Dmed. Each unit has been fully tested prior to shipment and is easy to setup and use...

SETUP INSTRUCTIONS

Size & Weight
Length: 17.5"
Width: 12.5"
Height: 7.5"
Weight: 15 lbs.

1. Lift the lid by the black knob to open.

2. The power cord is stored inside the Trainer. Remove the cord by unhooking the black Rip-Tie® strap. The cord can secured back in the retainer for transportation or storage. Warning: Do not transport or ship the trainer without securing the cord tightly in the strap or damage to the screen could result!

3. Attach the cord at the back of the unit (next to the handle). Plug into a standard 110-120v AC outlet.

4. If the screen is not already illuminated, find the button in the lower right corner of the screen bezel labeled "power". Press the button for two seconds and release. The screen will come on in a few seconds. The red LED light indicates that there is power supplied to the monitor. To turn the monitor off: press the "power" button for one second and release.

5. To illuminate the work light use the black switch labeled "💡" that is located on the right side toward the back.

6. If monitor adjustments are needed press the button below the screen labeled "menu". To scroll through the different controls press the "menu" button (repeatedly) until the desired heading is displayed. To make adjustments to that function press (and hold) the "up" or "down" button to change its value. The "mode" setting should always be set to "AV-1".

NOTE: The monitor is a Liquid Crystal Display (LCD) and care must be exercised regarding the surface of the screen. To clean: use a soft cotton cloth lightly dampened with water, vinegar (diluted w/water) or isopropyl alcohol. Do not apply any cleaning solutions directly onto the screen. Never use cleaning products that contain abrasives or strong solvents. To prolong the life of the monitor and light turn them off when not in use.

3-Dmed
255 INDUSTRIAL DR.
FRANKLIN, OHIO 45005
T: 937.746.2901
F: 937.746.5071
E-Mail: Support@3-Dmed.com
Web: 3-Dmed.com

3-Dmed
SURGICAL TRAINING AIDS

THE TRLCD03 STANDARD LAPAROSCOPIC TRAINER

QUICK GUIDE

Your instruments can be inserted into any of the seven ports. They can be used with or without trocars.

The standard grommet has is sized for a 10mm trocar. Grommets with 5mm holes are also available. Both sizes are interchangeable and easily exchanged for any combination.

The trainer has a generous, well lit work area. It will accommodate either artificial anatomical structures or animal tissue. Consider using an absorbent pad under animal tissue or where moisture is present.

Monitor Display Settings:
To make adjustments see the "Setup Instructions".

Brightness - adjusts the light level on the screen.
Contrast - it increases/decreases the separation between light and dark (example: create more shadows).
Color - controls the level of the color (ranging from grey tones to intense yellow)
Tint - controls the color balance (from green to magenta).

Camera Positioning and focus:
The camera is mounted inside the body with Velcro® strips. This allows for some adjustment. Extra strips can be added to relocate the camera more to the right for an offset camera view. The focus can be adjusted by loosening the lens set screw on the side of the camera body with a .050" hex wrench. Twist lens left or right. Re-tighten set screw. For more information visit the F.A.Q. Page on our web site: www.3-Dmed.com.

Using Alternate Displays:
The camera image can be displayed on any monitor that has an RCA video input. Simply remove the black RCA elbow from the gold RCA receptacle on the screen bezel and attach an RCA female/male extension cord (not supplied) between the black elbow and the alternate monitor. This works great for lectures or demonstrations.

Recording:
Activity can be recorded digitally by connecting the 3-Dmed SSVI07 Video Interface between the trainer and a digital storage device (computer/network). Analog recording can be done as well. Additionally, the SSVI07 can split the input signal providing outputs for up to four monitors. For more information please visit our web site.

3-Dmed
255 INDUSTRIAL DRIVE
FRANKLIN, OHIO 45005 USA
T: 937.746.2901
F: 937.746.5071
Web: www.3-Dmed.com
E-Mail: Support@3-Dmed.com

3-Dmed
SURGICAL TRAINING AIDS

A.9 – Sony GV-HD700 Recorder

Digital HD Videocassette Recorder

Operating Guide

GV-HD700/HD700E

HDV 1080i

Getting Started 11

Basic Operations 20

Dubbing/Editing 38

Using a "Memory Stick Duo" 44

Customizing your VCR 53

Troubleshooting 65

Additional Information 75

Quick Reference 87

Spanish Quick Guide/ Guía rápida en español 95

A.9 – AS-400 Polymer

ABS
FDM Material Properties

STRATASYS®

A true industrial thermoplastic, ABS is widely used throughout industry. When combined with the Fused Deposition Modeling (FDM) systems by Stratasys, this material is ideal for the rapid production of prototypes, tooling and the direct manufacturing (tool-less) of production parts.

MECHANICAL PROPERTIES[1]

	Test Method	Imperial	Metric
Tensile Strength, Type 1, 0.125	ASTM D638	3,200 psi	22 MPa
Tensile Modulus, Type 1, 0.125	ASTM D638	236,000 psi	1,627 MPa
Tensile Elongation, Type 1, 0.125	ASTM D638	6 %	6 %
Flexural Strength	ASTM D790	6,000 psi	41 MPa
Flexural Modulus	ASTM D790	268,000 psi	1,834 MPa
IZOD Impact, un-notched	ASTM D256	4 ft-lb/in	
IZOD Impact, notched	ASTM D256	2 ft-lb/in	

THERMAL PROPERTIES

Heat Deflection (HDT)	ASTM D648	205 °F	96 °C
Glass Transition (Tg)	DMA (SSYS)	219 °F	104 °C
Melt Point		Not Applicable[2]	Not Applicable[2]

OTHER

Specific Gravity	1.05
Vertical Burning Test	HB, UL94
Coefficient of Thermal Expansion	5.60E-05 in/in/F
Rockwell Hardness	R105
Dielectric S (kV/mm)	32
Dielectric C (60Hz)	2.4

APPEARANCE

- White available on all FDM systems
- Colors available on the FDM Maxum include:
  - Black, Blue, Green, Grey (light), Grey (steel), Red and Yellow
  - Custom color program available
- Colors available on FDM Prodigy Plus
  - Black, Blue, Green, Red and Yellow
  - Custom color program available

SYSTEM AVAILABILITY

- FDM Maxum
- FDM Titan TI
- FDM Vantage *SE*
- FDM Vantage *S*
- FDM Vantage *i* (when configured with ABS)
- FDM Prodigy Plus

Stratasys, Inc.
14950 Martin Drive
Eden Prairie, MN USA 55344
Ph: 952.937.3000
Fax: 952.937.0070
www.stratasys.com

The information presented are typical values intended for reference and comparison purposes only. They should not be used for design specifications or quality control purposes. End-use material performance can be impacted (+/-) by, but not limited to, part design, end-use conditions, test conditions, etc. Actual values will vary with build conditions.

Product specifications are subject to change without notice.

[1] Build orientation is on side edge
[2] Due to amorphous nature, material does not display a melting point

A.10 – Somos 10120

Samples available by request — Last Updated: 03 December, 2010

Resin	WaterClear 10120	9120	RenShape SL-5260	WaterShed XC 11122	Somos NeXt	O-XT 18420	Accura 55
Color	Clear	Amber	Opaque White	Clear	White	White	White
Manufacturer	DSM Somos	DSM Somos	Huntsman	DSM Somos	DSM Somos	DSM Somos	3D Systems
Description	ABS-Like	Polypropylene-Like	ABS-Like	ABS-Like	ABS-Like	ABS-Like	ABS-Like
Machine	500, 5000, 350	Viper si2	250	Viper si2	Viper si2	350, 5000, Viper si2	IPro 9000
Build Envelope (In.)	20 x 20 x 24	10 x 10 x 10	10 x 10 x 10	10 x 10 x 10	10 x 10 x 10	13.8 x13.8x11.5, 20x 20x 24, & 10x10x10	29.5 x 25.6 x 21.6
Build Layer Thickness	.006" or .004"	.002" or .004"	.006"	.002" or .004"	.004"	.002" .004" or .006"	.004"
Typical Properties : Cured Resin							
Density g/cc	1.12	1.13	1.22	1.12	1.17	1.13	1.2
Tensile Strength ASTM D638 psi (Mpa)	3,736 (35 Mpa)	4400 - 4700 (30 - 32 Mpa)	8,300 (58 Mpa)	6831 - 7774 (47.1 - 53.6 Mpa)	5900 - 6300 (41.1 - 43.3 Mpa)	6100 - 6400 (42.2 - 43.8 Mpa)	8410 - 9860 (58 - 68 Mpa)
with additional thermal post cure			8600 (60 Mpa)			9600 - 9900 (66.1 - 68.1 Mpa)	
Tensile Modulus ASTM D638 psi (Mpa)	250,000 - 280,000 (1,722 - 1,929 Mpa)	178000 - 212000 (1227 - 1462 Mpa)	360,000 (2,500 Mpa)	(2650 - 2880 Mpa)	343000 - 361000 (2370 - 2490 Mpa)	313000 - 336000 (2180 - 2310 Mpa)	460000 - 490000 (3200 - 3380 Mpa)
with additional thermal post cure			350,000 (2400 Mpa)			417000 - 430000 (2880 - 2960 Mpa)	
Elongation at Break ASTM D638	23%	15 - 25%	12%	11 - 20%	8 - 10%	8 - 16%	5 - 8%
with additional thermal post cure			14%			6-9%	
Flexural Strength ASTM D790 psi (Mpa)	5,276 (36.5 Mpa)	6000 - 6700 (41 - 46 Mpa)	11,000 (81 Mpa)	9152 - 10756 (63.1 - 74.2 Mpa)	9800 - 10300 (67.8 - 70.8 Mpa)	9700 - 10200 (66.7 - 70.5 Mpa)	12830 - 15920 (88 - 110 Mpa)
with additional thermal post cure			11,000 (81)			123000 - 127000 (84.9 - 87.7)	
Flexural Modulus ASTM D790 psi (Mpa)	326,334 (2,250 Mpa)	190000 - 211000 (1310 - 1455 Mpa)	350,000 (2,400 Mpa)	310,381 (2,140 Mpa)	350000 - 366000 (2415 - 2525 Mpa)	289000 - 309000 (1990 - 2130 Mpa)	390000 - 470000 (2690 - 3240 Mpa)
with additional thermal post cure			330,000 (2300 Mpa)			331000 - 339000 (2280 - 2340 Mpa)	
Notched Izod Impact Strength ASTM D256 ft-lb/in (J/m)	0.9 (48 J/m)	.9 - 1.0 (48 - 53 J/m)	0.7 (40 J/m)	0.362 (19.3 J/m)	.88 - .97 (47 - 52 J/m)	.37 - .41 (20 - 22 J/m)	.2 - .4 (12 - 22 J/m)
with additional thermal post cure			0.7 (40 J/m)			.17 - .39 (9 - 21 J/m)	
Hardness Shore D Scale	81	80 - 82	85	n/a	82	87 - 88	85
with additional thermal post cure			86			86 - 87	
Glass Transition Temperature	82.4°F (28°C)	n/a	163°F (73°C)	106°F (41°C)	n/a	135 - 138°F (57 - 59°C)	132°F (56°C)
with additional thermal post cure			203° (95°C)			136 - 147°F (98 - 111°C)	
Heat Deflection Temperature ASTM D648 @ 66psi	127°F (52.9°C)	126 - 142°F (52 - 61°C)	136°F (58°C)	121°F (49.6°C)	131 - 134°F (55 - 57°C)	131 - 136°F (53 - 58°C)	131 - 136°F (55 - 58°C)
with additional thermal post cure			207°F (97°C)			199 - 208°F (93 - 98°C)	
Heat Deflection Temperature ASTM D648 @ 264psi	114°F (45.7°C)	n/a	124°F (51°C)	115°F (46.2°C)	118 - 124°F (48 - 51°C)	114 - 116°F (46 - 47°C)	123 - 127°F (51 - 53°C)
with additional thermal post cure			172°F (78°C)			166 - 172°F (74 - 78°C)	
Dielectric Constant 60 Hz	4.2	n/a	n/a	3.9 - 4.1	4.65	3.5 - 3.6	n/a
Dielectric Constant 1 KHz	4.0	n/a	n/a	3.7 - 3.9	3.97	3.4 - 3.5	n/a
Dielectric Constant 1MHz	3.5	n/a	n/a	3.4 - 3.5	3.62	3.1 - 3.3	n/a